SF 298 MASTER COPY KEEP THIS COPY FOR REPRODUCTION PURPOSES

REPORT DOCUMENTATION PAGE

Form Approved
OMB NO. 0704-0188

1. AGENCY USE ONLY *(Leave blank)*	2. REPORT DATE	3. REPORT TYPE AND DATES COVERED
	9/14/97	Technical Report

4. TITLE AND SUBTITLE

Heat Transfer in Microchannels

5. FUNDING NUMBERS

DAAH04-94-G-0348

6. AUTHOR(S)

Xianming Wang
Timothy A. Ameel
Robert O. Warrington

7. PERFORMING ORGANIZATION NAME(S) AND ADDRESS(ES)

Louisiana Tech University
P.O. Box 7923 T.S.
Ruston, LA 71272

8. PERFORMING ORGANIZATION REPORT NUMBER

9. SPONSORING / MONITORING AGENCY NAME(S) AND ADDRESS(ES)

U.S. ARMY RESEARCH OFFICE
P.O. BOX 12211
RESEARCH TRIANGLE PARK, NC 27709-2211

10. SPONSORING / MONITORING AGENCY REPORT NUMBER

ARO 33844.2-PH-DPS

11. SUPPLEMENTARY NOTES

The views, opinions and/or findings contained in this report are those of the author(s) and should not be construed as an official Department of the Army position, policy, or decision, unless so designated by other documentation.

12a. DISTRIBUTION / AVAILABILITY STATEMENT

Approved for public release; distribution unlimited.

12b. DISTRIBUTION CODE

13. ABSTRACT *(Maximum 200 words)*

The objective of this research was to develop an analytical solution to the heat transfer problem in microchannels with slip-flow and an isothermal wall, a heat transfer problem for gases at low pressures or in extremely small geometries, and to verify this solution experimentally. In this investigation, an analytical expression for the velocity distribution with slip-flow was obtained which involved the Knudsen number *Kn* in an infinite series form. *Kn* for extremely small channels may become large enough to significantly affect the velocity distribution and consequently affect the heat transfer properties. A mathematical model of temperature distribution was established by combining the energy and momentum equations.

A new technique for evaluation of eigenvalues for the solution of the heat transfer problem in microchannels was developed from the method of Frobenius. The computational results show that the method is effective. The local and average Nusselt numbers were found for $0.005 \leq Kn < 0.30$ with aspect ratio a = 1, 2/3, 1/2, 1/4, and 1/8. Experiments for helium flow in a rectangular microchannel of dimension 117 μm x 24 μm x 63.5 μm and a microtube with inside diameter of 52 μm were conducted.

14. SUBJECT TERMS

CONVECTION HEAT TRANSFER, RECTANGULAR MICRO CHANNELS

15. NUMBER OF PAGES

123

16. PRICE CODE

17. SECURITY CLASSIFICATION OR REPORT	18. SECURITY CLASSIFICATION OF THIS PAGE	19. SECURITY CLASSIFICATION OF ABSTRACT	20. LIMITATION OF ABSTRACT
UNCLASSIFIED	UNCLASSIFIED	UNCLASSIFIED	UL

HEAT TRANSFER IN MICROCHANNELS

TECHNICAL REPORT

XIANMING WANG
TIMOTHY A. AMEEL

SEPTEMBER, 1996

U.S ARMY RESEARCH OFFICE

CONTRACT/GRANT NUMBER
DAAH04-94-G-0348

LOUISIANA TECH UNIVERSITY
P.O. BOX 7923 T.S.
RUSTON, LA 71272

ABSTRACT

The objective of this research was to develop an analytical solution to the heat transfer problem in microchannels with slip–flow — a heat transfer problem for gases at low pressures or in extremely small geometries, and to verify this solution experimentally. In this investigation, an analytical expression for the velocity distribution with slip–flow was obtained which involved the Knudsen (Kn) number in an infinite series form. The result showed that the velocity always increased as the Knudsen number was increased. The Knudsen number for extremely small channels may become large enough to affect significantly the velocity distribution and consequently affect the heat transfer properties. A mathematical model of temperature distribution was established by combining the energy and momentum equations. A series solution was obtained. Also, expressions for the local and overall Nusselt numbers were derived in terms of the Knudsen number and Graetz number.

A new technique for evaluation of eigenvalues for the solution of the heat transfer problem in microchannels was developed. This method was based on the construction of a matrix. The computational results showed that the method was effective. The local values and average Nusselt number were found for Kn from 0.005 to 0.3 with aspect ratio a = 1, 2/3, 1/2, 1/4 and 1/8. Experiments for helium through a microchannel with dimensions of 117 μm x 24 μm x 63.5 mm and a microtube with inside diameter of 52 μm were conducted.

TABLE OF CONTENTS

LIST OF TABLES

LIST OF FIGURES

NOMENCLATURE

A_w	tube surface area [m^2]
a	aspect ratio h/b
$a_{p,q}$, $a_{p,q}$	coefficient in Eq. (4.2)
$b_{p,q}(m,n)$	coefficient in Eq. (4.6)
C_n	coefficient in Eq. (3.5)
$d_{i,j}$	coefficient in Eq. (4.11)
D_H	hydraulic diameter[m]
$e_{m,n}$	$\delta_{m,n}\Lambda_{m,n}$ in Eq. (4.13)
F	specular reflection coefficient $(u_r - u_i) / (U_w - u_i)$
G	$G(x,y)$ in Eq. (3.3)
G_v	volume flow rate
Gz	Graetz number, (RePr(D/L))
h_x	local convective heat transfer coefficient [W/m^2–K]
$\bar{h}_c$	average convective heat transfer coefficient [W/m^2–K]
H	characteristic dimension
k	thermal conductivity [W/m–K]; ratio of $Nu_\infty(Kn)/Nu_\infty(0)$
Kn	Knudsen number, (λ/D)
L	length of ducts[m]
M	Mach number; molecular weight
Nu_∞	fully–developed Nusselt number coefficient, (h_cD/k)
$\overline{Nu}$	Nusselt number, ($\bar{h}_cD/k$)
Nu_x	local Nusselt number, (h_cD/k)
p	fluid pressure [Pa]
q	heat flux per unit wall area [W/m^2]
Q	heat transfer rate [W]
r	w/w_0
Re	Reynolds number, ($\rho uD/\mu$)
R_g	ideal gas constant [J/kg–K]
Pr	Prandtl number, (ν/α)
T	T(r,x), temperature [K]
T_B	bulk temperature [K]
T_L	temperature at ς=L [K]
$(\Delta T)_{LN}$,	log–mean–temperature difference (LMTD) [K]
u	velocity in ξ or x direction [m/s]
u_i	average streamwise velocity of the incident molecules [m/s]

u_r	average streamwise velocity of the reflected molecules [m/s]
U_w	average streamwise velocity of the surface [m/s]
v	velocity in η or y direction [m/s]
w	velocity in ς or z direction [m/s]
w_0	average velocity [m/s]
x	dimensionless width, (ξ/D_H)
x*	dimensionless length, (x/L)
y	dimensionless width, (η/D_H)
z	dimensionless distance, (ς/D_H)

Greek Symbols

α	fluid thermal diffusivity, ($k/\varrho c$) [m^2/s]
α_i	velocity eigenvalues
β	$(1+a)/2$
β'	$(1+1/a)/2$
γ	ratio of specific heats
$\delta_{p,q}$	coefficient in Eq. (4.6)
$\Delta(\lambda)$	eigenfunction Eq. (5.8)
ξ	width
η	width
ς	distance along duct
ϕ	function in Eq. (4.1)
Λ	coefficient in Eq. (4.1)
λ	eigenvalue
λ_m	mean free path [m]
μ	dynamic viscosity[kg/m s]
ν	kinematic viscosity [m^2/s]
ϱ	density[kg/m^3]
π	3.141592654
θ	$(T-T_w)/(T_0-T_w)$ dimensionless temperature
θ_B	$(T_B-T_w)/(T_0-T_w)$ dimension–less bulk temperature
$\theta_{B,L}$	dimensionless fluid bulk temperature at ς=L
θ_{LN}	dimensionless LMTD
$\Theta(x,y)$	function expressed as Eq. (4.2)

Subscripts

0	at $z = 0$
B	bulk
m	average
s	slip–flow
w	wall

ACKNOWLEDGEMENTS

I would like to record my sincerest indebtedness to all the people who have offered encouragement and help during this research.

I am deeply grateful first of all to the Chairmen of my advisory committee, Dr. Randall F. Barron and Dr. Robert O. Warrington, who delivered excellent instruction and quality advising and supplied many useful reference materials and software throughout my research and the development of the dissertation.

My further thanks are due Dr. Timonthy A. Ameel, who offered much valuable advising on the research, the conduct to the experiments and on my dissertation.

I would also like to express my sincere appreciation to Dr. Huaijin Gu for his kindly being a member of the advisory committee, for his careful review of this dissertation, and for his many valuable suggestions and comments on the dissertation.

Special thanks are due Dr. Duli Yu, Mr. Roger Stanley, and Mr. Ji Fang for their kindly helping me with the experimental work.

I would like also to publicly acknowledge and thank the Lord God, as I do privately, as it is He who has given me whatever gifts and compassion I possess.

And finally, my profound and continuous thanks to my family, especially my wife, Li Ma, my son, Sean Wang, for all their real love, moral encouragement, and financial support, without which it would have been impossible for me to study at Louisiana Tech University.

CHAPTER 1

INTRODUCTION

The objective of this research is to develop an analytical solution of the heat transfer problem in microchannels with slip–flow — a heat transfer problem for gases at low pressures or in extremely small ducts, and to verify the analytical model experimentally. To do this, the velocity profile with slip–flow must be found first. A mathematical model of the temperature distribution in slip flow should be established by combining the energy and momentum equations. And finally, an effective technique for evaluation of the eigenvalues for the series solution should be developed and heat transfer experiments with microchannel/microtube should be conducted.

1.1 Heat Transfer Problem in Ducts

By the end of the last century, the problem of forced convection heat transfer in a circular tube in laminar flow gained interest because of its fundamental importance in physical problems such as the analysis and design of heat exchangers.

The Graetz problem is a simplified case of the problem of forced convection heat transfer in a circular tube in laminar flow. With the assumptions of steady and incompressible flow, constant fluid properties, no "swirl" component of velocity, fully developed velocity profile, and negligible energy dissipation effects, Graetz (1883) originally solved this problem analytically. The solution by Graetz involved an infinite number of eigenvalues, and in his paper, only the first two eigenvalues were evaluated.

Since the accuracy of the Graetz solution mainly depends on the number of eigenvalues, it is extremely important to obtain more eigenvalues, as Tribus and Klein (1953) pointed out. For seventy years, the research on this problem focused mainly on finding more eigenvalues. Abramowitz (1953) employed a fairly rapidly converging series solution of the Graetz equation in making the calculation and found the lowest five values with much more accuracy. Sellars et al. (1956) extended the problem to include a more effective approximation technique for evaluation of the eigenvalues of the problem; they could get any number of eigenvalues as needed. This work solved the Graetz problem completely.

Dennis et al. (1959) studied the case in rectangular ducts. By employing homogeneous linear algebraic equations and Rayleigh quotient, they devoloped a technique for evaluation of the eigenvalues for the analytical solution of the problem of forced convection heat transfer in rectangular ducts with different aspect ratios. The same results were obtained by other researchers numerically (Shah and London, 1978).

1.2 Heat Transfer Problem in Ducts in Slip–Flow

Applications of microstructures such as micro heat exchangers have led to increased interest in convection heat transfer in micro–geometries. Some experimental work has been done , such as the experimental investigations in microtubes (Choi et al., 1991), in microchannels (Pfahler et al., 1991), and in micro heat pipes (Petersen et al., 1993). Appropriate models are needed to explain the significant departures in the micro–scale experimental results from the thermofluid correlations used for conventional–sized geometries. For example, Choi et al. (1991) conducted heat transfer experiments using essentially smooth tubes with a relative roughness of 0.0003 and a diameter ranging from 3 μm to 81 μm. As shown in Fig. 1.1, the measured heat transfer coefficients in laminar

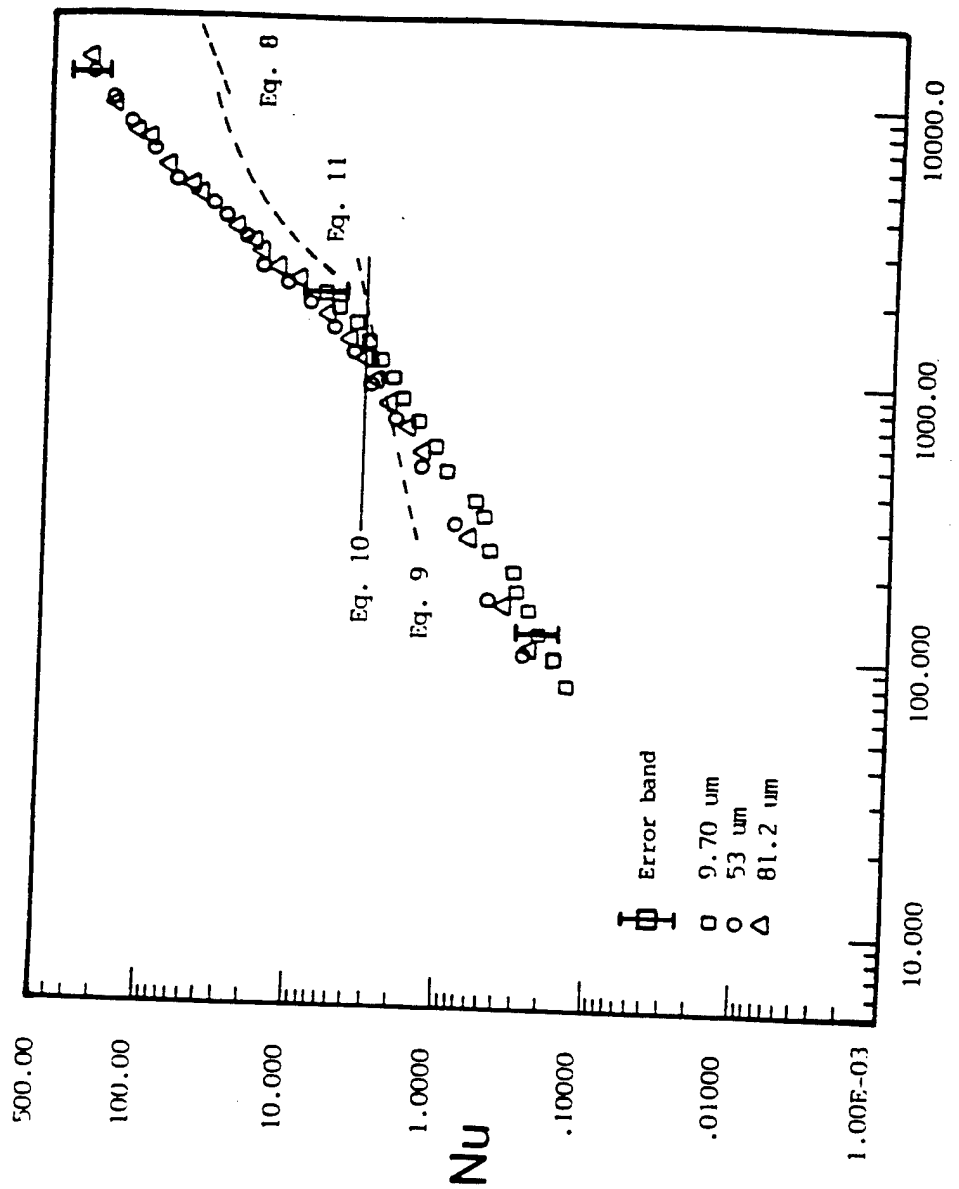

Fig. 1.1 Nu as a function of Re in microtubes [Choi et al.]

flow in small tubes exhibited a Reynolds number dependence, in contrast to the conventional prediction for fully established laminar flow, in which the Nusselt number is constant. Also, an experimental investigation of fluid flow in extremely small channels showed that there are deviations between the Navier–Stokes predictions and the experimental observations (Pfahler et al., 1991).

Therefore, some effects and conditions that are normally neglected when considering macro–scale flow must be taken into consideration in micro–scale convection. One of these conditions is slip–flow (Flik et al., 1992, Beskok and Karniadakis, 1992). It has been found that the analytical model combined with slip–flow conditions can fit the experimental data in microchannels with a uniform cross–sectional area (Arkilic et al., 1994) and with a non–uniform cross–sectional area (Liu et al., 1995).

Slip–flow occurs when gases are at low pressures or for flow in extremely small passages. At low pressures, with correspondingly low densities, the molecular mean free path, which can be expressed as Eq. (1.1), becomes comparable with the body dimensions, and then the effect of molecular structure becomes a factor in flow and heat transfer mechanisms (Eckert and Drake,1972).

$$\lambda_m = \frac{\mu}{p}\sqrt{\frac{\pi R_u T}{2 g_c M}} \tag{1.1}$$

The relative importance of effects due to the rarefaction of a gas can be indicated by the Knudsen number, a ratio of the magnitude of the mean free molecular path in the gas to the characteristic dimension in the flow field. The effects of rarefaction phenomena on flow and heat transfer becomes important when the Knudsen number can no longer be neglected. The Knudsen number may be defined as

$$Kn = \frac{\lambda_m}{D_H} = \frac{\mu}{p D_H}\sqrt{\frac{\pi R_u T}{2 g_c M}} \tag{1.2}$$

In defining when slip–flow occurs, Beskok and Karniadakis (1992) have proposed to classify four flow regimes for gases, as follows:

Continuum flow:	$Kn < 10^{-3}$
Slip–flow:	$10^{-3} < Kn < 0.1$
Transition flow:	$0.1 < Kn < 10$
Free molecular flow	$10 \leq Kn$

When slip–flow occurs, the gas adjacent to the surface, in contrast to its behavior in continuum flow, no longer reaches the velocity or temperature of the surface. In continuum flow, intermolecular collisions dominate the flow field, and a usual boundary condition (continuous boundary) at the interface between a fluid and a solid surface is that the fluid adjacent to the surface assumes both the velocity and temperature of the surface. In the case of slip–flow, the molecular mean free path λ_m is rather larger than any significant body dimension so that most of the gas molecules striking and leaving the body surface do not collide with free–stream molecules until very far from the surface. Thus, the gas at the surface has a tangential velocity, and it appears to slip along the surface.

The slip velocity can be expressed as follows as a function of the velocity gradient near the wall:

$$u_s = -\lambda_m \left(\frac{du}{dy} \right)_{y=0} \tag{1.3}$$

and Arkilic et al. (1994) give the expression as follows:

$$\frac{u_s}{c} = \frac{2-F}{F} Kn \left(\frac{du/c}{dy/H} \right)_{y=0} \tag{1.4a}$$

or

$$u_s = \frac{2-F}{F} \lambda_m \left(\frac{du}{dy} \right)_{y=0} \tag{1.4b}$$

which includes the consideration of three accommodation coefficients represented by the speculation reflection coefficient F, which has values that typically lie between 0.9 and 1 (Ebert et al., 1965). In the case of F having the value one, Eq. (1.4) becomes Eq. (1.3). For simplicity in this investigation, Eq. (1.3) was applied to evaluate the velocity.

The temperature boundary condition can be regarded as discontinuous; that is, there is a jump in temperature at the wall. Actually, the temperature of the gas near the solid surface changes continuously to the temperature of the surface but only in a very thin layer on a microscale so that on the macroscale there appears to be a jump in temperature between the surface and the adjacent gas. Eckert and Drake (1972) give expressions for the temperature jump condition:

$$T_s - T_w = -\left(\frac{2\gamma}{1+\gamma}\right)\frac{\lambda_m}{Pr}\left(\frac{\partial T}{\partial y}\right)_{y=0} \qquad (1.5)$$

where λ_m represents the mean free path for collisions between a moving molecule and the fixed molecules (or λ_m^{-1} is the average number of collisions per unit distance) (Present, 1958), and $\partial T/\partial y$ is the temperature gradient at the wall. As shown in Eq. (1.5), the temperature jump is proportional to λ_m: a small value of λ_m means that a great numbers of molecules are involved in energy transport so that the temperature jump is small, while a large value of λ_m means that fewer molecules are involved in energy transport so that the temperature jump is relatively larger. When λ_m is small enough, as in a conventional case, the temperature jump may be neglected.

With the introduction of the slip–flow condition into the Graetz problem, it becomes more difficult to solve such problems. The classical Graetz problem is governed by a partial differential equation with a continuous temperature boundary condition; while in the Graetz problem combined with slip–flow condition, the temperature boundary condition is no longer continuous, which makes the solution as well as the corresponding eigenvalues much more complicated and difficult.

In the case of circular tubes in slip–flow, that is, gases at low pressures or in extremely small tubes, the heat transfer coefficient depends not only on the Reynolds number and Prandtl number, but also on the Knudsen number. Barron et al. (1995) developed a technique and evaluated the eigenvalues of the analytical solution for this problem in the case of a constant wall temperature. Wang et al. (1995) solved this problem completely. Their studies shows that the Nusselt number increases significantly with the increase of the Knudsen number, as shown in Fig. 1.2. Ameel et al. (1996) studied the case with

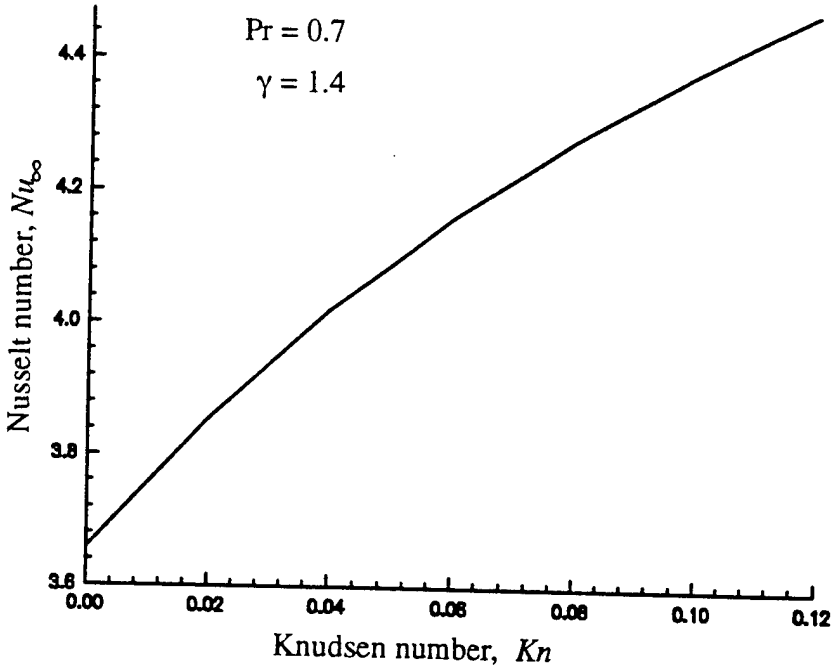

Fig. 1.2 Fully developed *Nu* as a function of *Kn* [Barron et al.]
(constant wall temperature)

constant heat flux, and the results indicate that the fully–developed Nusselt number decreases with the increase of the Knudsen number, as shown in Fig. 1.3. Therefore, some research is needed to analyze this type of problem in the case of rectangular ducts in slip–flow.

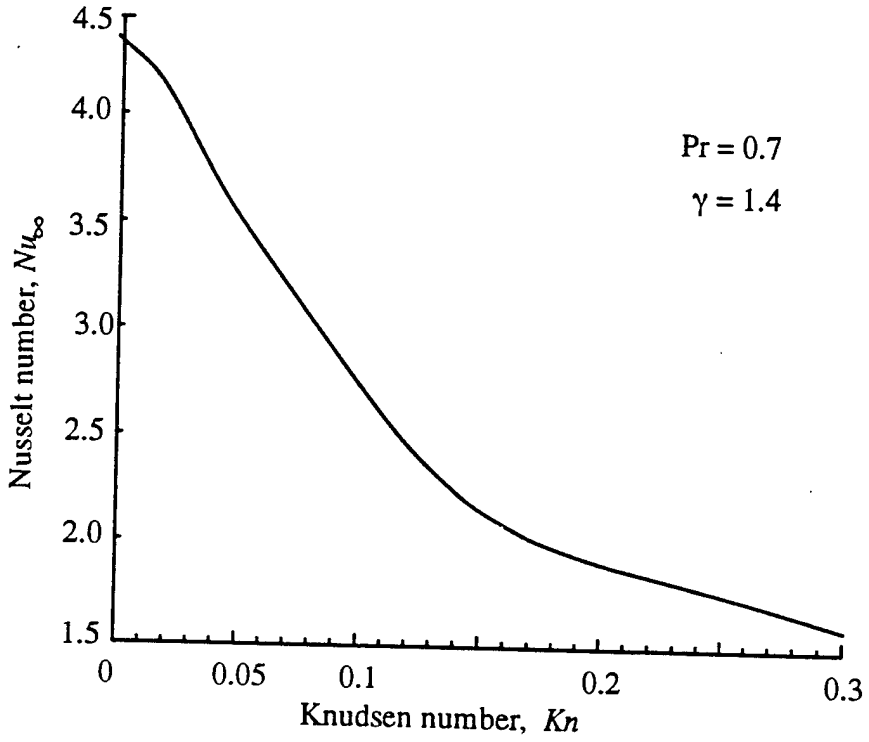

Fig. 1.3 Fully developed *Nu* as a function of *Kn* [Ameel et al.]
(constant heat flux)

1.3 Related Research

Ebert and Sparrow (1965) have found the fluid velocity distribution for slip–flow in microchannels. Their results can be summarized as follows:

The momentum equation can be written as follows in the coordinate system shown in Fig. 1.4:

$$\frac{\partial^2 w}{\partial \xi^2} + \frac{\partial^2 w}{\partial \eta^2} = \frac{1}{\mu}\frac{dp}{d\zeta} \tag{1.6}$$

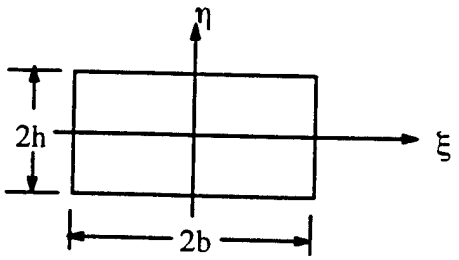

$a = h/b$

$$D_H = \frac{4h}{1+a}$$

Fig. 1.4 Coordinate system

with the slip–flow boundary condition

$$w = -\frac{2-F}{F}\lambda\frac{\partial w}{\partial \eta} \quad at\ \eta = h,\quad 0 \le \xi < b \tag{1.7a}$$

$$w = -\frac{2-F}{F}\lambda\frac{\partial w}{\partial \xi} \quad at\ \xi = b,\quad 0 \le \eta < h \tag{1.7b}$$

$$\frac{\partial w}{\partial \eta} = 0 \quad at\ \eta = 0,\quad 0 \le \xi \le b \tag{1.7c}$$

$$\frac{\partial w}{\partial \xi} = 0 \quad at\ \xi = 0,\quad 0 \le \eta \le h \tag{1.7d}$$

The velocity can expressed as

$$\frac{w}{\frac{D_H}{\mu}\frac{dp}{dz}} = -2\sum_{i=1}^{\infty} \frac{\cos \alpha_i \eta}{\alpha_i^3}\left(\frac{\sin \alpha_i}{1 + 2\,Kn \sin^2 \alpha_i}\right)\left(1-\frac{\cosh \frac{\alpha_i}{a}\xi}{\cosh \frac{\alpha_i}{a} + 2\,Kn\,\alpha_i \sin \frac{\alpha_i}{a}}\right) \tag{1.8}$$

and the mean velocity can be determined by

$$\frac{w_0}{\frac{D_H}{\mu}\frac{dp}{dz}} = -2\sum_{i=1}^{\infty} \frac{a}{\alpha_i^5}\left(\frac{\sin^2 \alpha_i}{1 + 2\,Kn \sin^2 \alpha_i}\right)\left(\frac{\alpha_i}{a}-\frac{\sinh \frac{\alpha_i}{a}}{\cosh \frac{\alpha_i}{a} + 2\,Kn\,\alpha_i \sin \frac{\alpha_i}{a}}\right) \tag{1.9}$$

where the eigenvalues a_i satisfy

$$\alpha_i \tan \alpha_i = \frac{1}{2\,Kn} \tag{1.10}$$

Dennis et al. (1959) solved the problem of forced heat convection in laminar flow through rectangular ducts with non–slip–flow. Their results may be summarized as follows:

The energy equation can be written as follows in the coordinate system shown in Fig. 1.5:

$$k\left(\frac{\partial^2 T}{\partial \xi^2} + \frac{\partial^2 T}{\partial \eta^2} + \frac{\partial^2 T}{\partial \varsigma^2}\right) = \varrho c w \frac{\partial T}{\partial \varsigma} \tag{1.11}$$

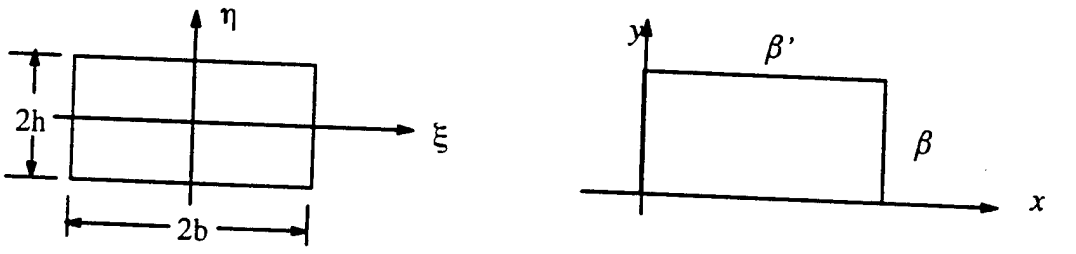

$a = h/b \qquad D_H = \frac{4h}{1 + a} \qquad \beta = \frac{2h}{D_H} = \frac{1 + a}{2} \qquad \beta' = \frac{2b}{D_H} = \frac{1 + 1/a}{2}$

Fig. 1.5 New coordinate system for dimensionless variables

with the boundary condition

$$T_w = T_1 \qquad \varsigma > 0 \tag{1.12a}$$

$$T = T_0 \qquad \varsigma < 0 \tag{1.12b}$$

Introducing dimensionless variables

$$x = \frac{\xi}{D_H} \quad y = \frac{\eta}{D_H} \quad z = \frac{\varsigma}{D_H} \quad \theta = \frac{T-T_1}{T_0-T_1}$$

where the hydraulic diameter $D_H = 4A/S$, and the aspect ratio a and Knudsen number

$$a = \frac{h}{b} \qquad \text{Kn} = \frac{2-F}{F}\frac{\lambda_m}{2h}$$

When the aforementioned change of variables is carried out and neglecting the axial conduction $k\partial^2T/\partial\varsigma^2$ for large enough Peclet number, since it is of order $(1/\text{Pe})^2$ compared to the axial convection term $w\partial T/\partial\varsigma$, the governing equations and the boundary conditions become

$$\frac{\partial^2 w}{\partial x^2} + \frac{\partial^2 w}{\partial y^2} = \frac{D_H}{\mu}\frac{dp}{dz} \qquad \text{or} \qquad \nabla_1{}^2 w = \frac{D_H}{\mu}\frac{dp}{dz} \tag{1.13}$$

$$k\left(\frac{\partial^2 T}{\partial x^2} + \frac{\partial^2 T}{\partial y^2}\right) = wD_H\frac{\partial T}{\partial z} \qquad \text{or} \qquad \nabla_1{}^2\theta = \frac{w}{w_0}\frac{\partial\theta}{dz} \tag{1.14}$$

where $\nabla_1{}^2 \equiv \partial^2/\partial x^2 + \partial^2/\partial y^2$, w_0 is the mean velocity, and

$$w = -\text{Kn}\,\beta\frac{\partial w}{\partial y} \quad at \quad y = 0 \text{ and } \beta, \quad 0 < x < \beta' \tag{1.15a}$$

$$w = -\text{Kn}\,\beta'\frac{\partial w}{\partial \xi} \quad at \quad x = 0 \text{ and } \beta', \quad 0 < y < \beta \tag{1.15b}$$

$$\frac{\partial w}{\partial y} = 0 \quad at\ y = \frac{\beta}{2}, \quad 0 \le x \le \beta' \tag{1.15c}$$

$$\frac{\partial w}{\partial x} = 0 \quad at\ x = \frac{\beta'}{2}, \quad 0 \le y \le \beta \tag{1.15d}$$

and

$$\theta_w = \theta_1 \neq 0 \qquad z > 0 \tag{1.16a}$$

$$\theta = 1 \qquad z \leq 0 \tag{1.16b}$$

The solution of Eq. (1.16) can be written as

$$\theta = \sum_{n=1}^{\infty} C_n G_n(x,y) e^{-\lambda_n z} + \theta_1 \tag{1.17}$$

where G_n and λ_n are eigenfunctions and eigenvalues required to make the solution to the following membrane equation:

$$\nabla_1^2 G + \frac{\lambda w(x,y)}{w_0} G = 0 \tag{1.18}$$

subject to the boundary condition deduced from Eqs. (1.14) $G_n = 0$ on the boundary C'.

Coefficients C_n can be determined by

$$C_n = \frac{\iint_{D'} w\ G_n\ dx\ dy}{\iint_{D'} w\ dx\ dy} \tag{1.19}$$

The Nusselt number can be determined by

$$Nu(z) = \frac{1}{4\theta_B} \sum_{n=1}^{\infty} \lambda_n C_n^2 e^{-\lambda_n z}$$

where

$$\theta_B = \frac{\int\int_{D'} w\ \theta\ dx\ dy}{\int\int_{D'} w\ dx\ dy} \qquad (1.20)$$

$$= \sum_{n=1}^{\infty} C_n^2 e^{-\lambda_n z}$$

and $\mathrm{Nu}_\infty = \lambda_1 / 4$.

Eigenvalues λ_n can be determined by the following infinite set of homogeneous linear algebraic equations

$$\sum_{p=0}^{\infty} \sum_{q=0}^{\infty} \{\delta_{p,q}(m,n)\, \Lambda_{m,n} - \lambda\ b_{p,q}(m,n)\}\ a_{p,q} = 0 \quad (\ m,n = 0,1,2,\ \dots\ ) \qquad (1.21)$$

where

$$\delta_{p,q}(m,n) = \int\int_{D'} \phi_{m,n} \phi_{p,q}\ \ dx\ dy \qquad (1.22)$$

$$\delta_{m,n}(m,n) \Lambda_{m,n} = (\pi^2 / 4a)\,(m^2 + a^2 n^2), \qquad (1.23)$$

$$b_{p,q}(m,n) = \frac{1}{4}\{\ d_{|m-p|,|n-q|} - d_{|m-p|,n+q} + d_{m+p,n+q} - d_{m+p,|n-q|}\ \} \qquad (1.24)$$

$$d_{i,j} = \int_0^{\beta}\int_0^{\beta'} \frac{w}{w_0}\ cos\ (\frac{i\pi x}{\beta})\ cos\ (\frac{i\pi y}{\beta'})\ dx\ dy \qquad (i,j=0,1,2,\ \dots\ ) \qquad (1.25)$$

$$b_{p,q}(m,n)\ \begin{cases} \neq 0 & \text{for all } p,q,m,n \neq 0 \\ = 0 & \text{for any } p,q,m,n = 0 \end{cases} \qquad (1.26)$$

Dennis et al. (1959) estimated the eigenvalues for different aspect ratios for nonslip–flow by employing the Rayleigh quotient

$$\lambda_n = -\int_0^{\beta}\int_0^{\beta'} \theta_n \nabla_1^2 \theta_n dx\ dy \Big/ \int_0^{\beta}\int_0^{\beta'} r\theta_n^2 dx\ dy$$

$$= \sum_{p=0}^{\infty}\sum_{q=0}^{\infty} \delta_{p,q}(p,q)(\beta_p^2 + \gamma_q)[A_{p,q}(n)]^2 \Big/ \sum_{i=1}^{\infty}\sum_{j=1}^{\infty}\sum_{p=1}^{\infty}\sum_{q=1}^{\infty} b_{p,q}(i,j)A_{i,j}(n)A_{p,q}(n) \tag{1.27}$$

for example, for aspect ratio $a = 1$, $\lambda_1 = 11.91$ and $\mathrm{Nu}_\infty = 2.98$.

Therefore, based on those research, a model for the case of rectangular channel in slip–flow can be established and a technique of evaluation of the corresponding eigenvalues for the analytical solution of the model should be developed.

CHAPTER 2

VELOCITY AND TEMPERATURE DISTRIBUTIONS

In order to build the mathematical model for the problem in slip–flow, the velocity profile must be found first in the new coordinate system. In this chapter, based on some assumptions, the expression for velocity will be derived from the continuity equation and momentum equation. The slip condition will be used to evaluate the slip velocity, and the velocity will be expressed in terms of a Knudsen number. A mathematical model of temperature distribution in slip–flow will be established by combining the energy and momentum equations.

2.1 Velocity Distribution

Consider the flow of a fluid in a rectangular duct, as shown in Figure 2.1:

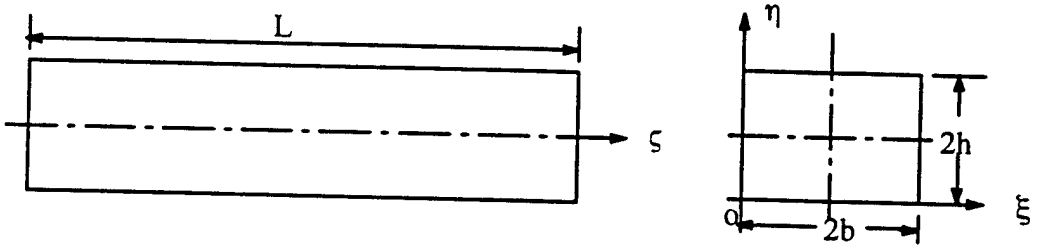

Fig. 2.1 Coordinate system for the problem

For this model, the following conditions have been assumed (Barron, 1996):

(1) The flow is steady. This means that the properties of the flow are time independent.

(2) The fluid is incompressible (or, if a gas is considered, the Mach number is less than 0.30). In this case, the density may be assumed constant.

(3) The flow is fully established. In this case, the axial velocity, w, is a function of the coordinates η and ξ only, and not a function of the axial coordinate ς. In addition, the radial velocity is zero.

(4) The "swirl" component of velocity is identically zero. This means that both $u = 0$ and $v = 0$.

(5) Fluid properties are constant.

(6) Energy dissipation effects are negligible.

(7) The tube wall temperature is constant.

2.1.1 Continuity Equation

The general continuity equation can be written in the cartesian coordinates as follows:

$$\frac{\partial \varrho}{\partial t} + \frac{\partial}{\partial \xi}(\varrho u) + \frac{\partial}{\partial \eta}(\varrho v) + \frac{\partial}{\partial \zeta}(\varrho w) = 0 \tag{2.1}$$

For steady flow of an incompressible fluid, the equation above reduces to:

$$\frac{\partial u}{\partial \xi} + \frac{\partial v}{\partial \eta} + \frac{\partial w}{\partial \zeta} = 0 \tag{2.2}$$

For fully developed flow,

$$\frac{\partial w}{\partial \zeta} = 0$$

Therefore,

$$\frac{\partial u}{\partial \xi} + \frac{\partial v}{\partial \eta} = 0$$

Since the normal velocity is zero at the walls (the wall is impermeable), we must conclude that:

$u = 0$ (identically).

and

$v = 0$ (identically).

2.1.2 Velocity Distribution with Slip Condition

The Momentum Equation can be written in the coordinates shown in Fig. 2.2 as follows (Kays et al., 1993) for fully–developed (hydrodynamic) flow:

$$\frac{\partial^2 w}{\partial \xi^2} + \frac{\partial^2 w}{\partial \eta^2} = \frac{1}{\mu}\frac{dp}{d\varsigma} \tag{2.3}$$

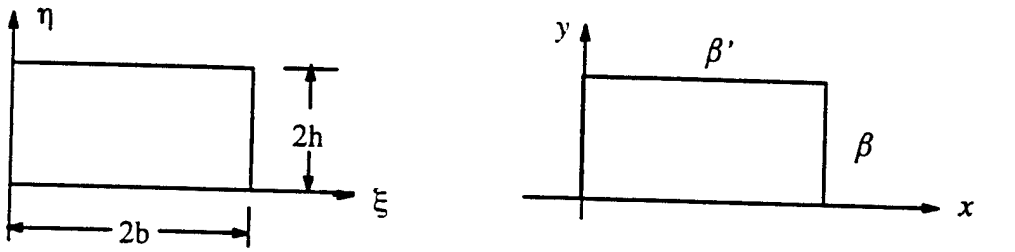

a = h/b $\quad D_H = \frac{4h}{1+a} \quad \beta = \frac{2h}{D_H} = \frac{1+a}{2} \quad \beta' = \frac{2b}{D_H} = \frac{1+1/a}{2}$

Fig. 2.2 New coordinate system for dimensionless variables

with the slip–flow boundary condition

$$w = -\frac{2-F}{F}\lambda_m \frac{\partial w}{\partial \eta} \quad at\ \eta = 0, 2h, \quad 0 < \xi < 2b \tag{2.4a}$$

$$w = -\frac{2-F}{F}\lambda_m \frac{\partial w}{\partial \xi} \quad at\ \xi = 0, 2b, \quad 0 < \eta < 2h \tag{2.4b}$$

$$\frac{\partial w}{\partial \eta} = 0 \quad at\ \eta = h, \quad 0 \le \xi \le 2b \tag{2.4c}$$

$$\frac{\partial w}{\partial \xi} = 0 \quad at\ \xi = b, \quad 0 \le \eta \le 2h \tag{2.4d}$$

Introducing dimensionless variables

$$x = \frac{\xi}{D_H} \quad y = \frac{\eta}{D_H} \quad z = \frac{\varsigma}{D_H}$$

where the hydraulic diameter $D_H = 4A/S$, and the aspect ratio a and Knudsen number

$$a = \frac{h}{b} \qquad \text{Kn} = \frac{2-F}{F}\frac{\lambda_m}{2h}$$

The governing equations and the boundary conditions become

$$\frac{\partial^2 w}{\partial x^2} + \frac{\partial^2 w}{\partial y^2} = \frac{D_H}{\mu}\frac{dp}{dz} \qquad \text{or} \qquad \nabla_1{}^2 w = \frac{D_H}{\mu}\frac{dp}{dz} \tag{2.5}$$

$$w = -\text{Kn}\,\beta\,\frac{\partial w}{\partial y} \quad at \quad y = 0 \text{ and } \beta, \quad 0 < x < \beta' \tag{2.6a}$$

$$w = -\text{Kn}\,\beta'\frac{\partial w}{\partial x} \quad at \quad x = 0 \text{ and } \beta', \quad 0 < y < \beta \tag{2.6b}$$

$$\frac{\partial w}{\partial y} = 0 \quad at\ y = \frac{\beta}{2}, \quad 0 \le x \le \beta' \tag{2.6c}$$

$$\frac{\partial w}{\partial x} = 0 \quad at\ x = \frac{\beta'}{2}, \quad 0 \le y \le \beta \tag{2.6d}$$

The solution may be proposed as

$$\frac{w}{\frac{D_H}{\mu}\frac{dp}{dz}} = \sum_{i=1}^{\infty} \Psi_i(x)\ cos\ (\frac{2y}{\beta}-1)\alpha_i \tag{2.7}$$

where α_i are a set of eigenvalues, and the $\Psi_i(x)$ are a set of x – dependent functions. Eq. (2.7) identically satisfies boundary condition (2.6c), that is

$$\frac{\frac{\partial w}{\partial y}}{\frac{D_H}{\mu}\frac{dp}{dz}} = -\frac{2}{\beta}\alpha_i\sum_{i=1}^{\infty}\Psi_i(x)\ sin\ (\frac{2y}{\beta}-1)\alpha_i = 0 \quad at\ y = \beta/2$$

By substituting Eq. (2.7) into the boundary condition (2.6a), we have

$$\frac{w}{\frac{D_H}{\mu}\frac{dp}{dz}} = \sum_{i=1}^{\infty} \Psi_i\,(x)\ cos\ (\frac{2y}{\beta}-1)\alpha_i$$

$$-\mathrm{Kn}\ \beta\ \frac{\partial w}{\partial y} = -Kn\ \beta[-\frac{2}{\beta}\alpha_i \sum_{i=1}^{\infty} \Psi_i\,(x)\ sin\ (\frac{2y}{\beta}-1)\alpha_i\ ]$$

so

$$\sum_{i=1}^{\infty} \Psi_i\,(x)\ [cos\ (\frac{2y}{\beta}-1)\alpha_i - 2Kn\ \alpha_i\ sin\ (\frac{2y}{\beta}-1)\alpha_i\ ] = 0 \tag{2.8}$$

For a non–trivial velocity solution, it is necessary that

$$\alpha_i\ tan\ \alpha_i = \frac{1}{2\ Kn} \tag{2.9}$$

This is the condition from which the eigenvalues are determined.

Now, we find the function $\Psi_i\,(x)$. To do this, Eq. (2.5) can be rewritten as

$$\frac{\partial^2 w}{\partial x^2} + \frac{\partial^2 w}{\partial y^2} = \frac{D_H}{\mu}\frac{dp}{dz} \sum_{i=1}^{\infty} \Omega_i\,(x)\ cos\ (\frac{2y}{\beta}-1)\alpha_i \tag{2.10}$$

From Eq. (2.7), we have

$$\frac{\partial^2 w}{\partial x^2} = -\frac{D_H}{\mu}\frac{dp}{dz} \sum_{i=1}^{\infty} \frac{d^2\Psi_i}{dx^2}\ cos\ (\frac{2y}{\beta}-1)\alpha_i$$

$$\frac{\partial^2 w}{\partial y^2} = -\frac{D_H}{\mu}\frac{dp}{dz}\frac{4\alpha_i^2}{\beta^2} \sum_{i=1}^{\infty} \Psi_i\ cos\ (\frac{2y}{\beta}-1)\alpha_i \tag{2.11}$$

so we derive a differential equation

$$\frac{d^2\Psi_i}{dx^2} - (\frac{2\alpha_i}{\beta})^2\ \Psi_i - \Omega_i\ = 0 \tag{2.12}$$

We can obtain the homogeneous solution from

$$\lambda^2 - (\frac{2a_i}{\beta})^2 = 0 \tag{2.13}$$

that is,

$$\lambda = \pm (\frac{2a_i}{\beta}) \tag{2.14}$$

Therefore, let

$$\Psi_i^* = C_1 e^{\frac{2a_i}{\beta}x} + C_2 e^{-\frac{2a_i}{\beta}x} + C_3 \tag{2.15}$$

substituting Eq. (2.15) into Eq. (2.12), we have

$$-(\frac{2a_i}{\beta})^2 C_3 - \Omega_i = 0$$

or

$$C_3 = -\frac{\beta^2 \Omega_i}{4a_i^2} \tag{2.16}$$

From boundary condition (2.6d), that is,

$$\frac{d\Psi_i}{dx} = (\frac{2a_i}{\beta})^2 [C_1 e^{\frac{2a_i}{\beta}x} - C_2 e^{-\frac{2a_i}{\beta}x}]_{x=\beta'/2} = 0 \tag{2.17}$$

Therefore, we obtain

$$C_2 = C_1 e^{\frac{2a_i}{\beta}}$$

so

$$\Psi_i^* = C_1 e^{\frac{a_i}{\beta}} [\, e^{\frac{a_i}{\beta}(2x-\beta')} + e^{-\frac{a_i}{\beta}(2x-\beta')} \,] + C_3$$

$$= D_1 \cosh \frac{a_i}{\beta}(2x-\beta') + C_3 \tag{2.18}$$

And from boundary condition (2.6b), we have

$$\frac{w}{\frac{D_H}{\mu}\frac{dp}{dz}} = \sum_{i=1}^{\infty} \Psi_i\,(x)\ cos\ (\frac{2y}{\beta}-1)\alpha_i = -\mathrm{Kn}\ \beta\ \frac{\partial w}{\partial x}$$

$$= -Kn\ \beta'[\sum_{i=1}^{\infty} \frac{\partial \Psi_i\,(x)}{\partial x}\ sin\ (\frac{2y}{\beta}-1)\alpha_i\ ]_{x=\beta'}$$

or

$$\Psi_i\,(x) + Kn\ \beta'[\frac{\partial \Psi_i\,(x)}{\partial x}\ ]_{x=\beta'} = 0 \tag{2.19}$$

Substituting Eq. (2.18) into Eq. (2.19), we have

$$C_1[e^{\frac{2\alpha_i}{a}} + e^{\frac{2\alpha_i}{a}-\frac{2\alpha_i}{a}}] + C_3 + C_1\ Kn\ \beta'\frac{2\alpha_i}{\beta}[[e^{\frac{2\alpha_i}{a}} - e^{\frac{2\alpha_i}{a}-\frac{2\alpha_i}{a}}] = 0$$

$$C_1 = C_3/[(e^{\frac{2\alpha_i}{a}} + 1\ ) + 2\ Kn\ \frac{\alpha_i}{a}(e^{\frac{2\alpha_i}{a}} - 1)]$$

$$= -\frac{\frac{\beta^2\Omega_i}{4\alpha_i^{\,2}}e^{-\frac{2\alpha_i}{a}}}{[\ cosh\frac{\alpha_i}{a} + 2\ Kn\ \frac{\alpha_i}{a}sinh\frac{\alpha_i}{a}\ ]} \tag{2.20}$$

Evaluation of $\Omega_i(x)$ can be made from the assumption

$$\sum_{i=1}^{\infty} \Omega_i\,(x)\ cos\ (\frac{2y}{\beta}-1)\alpha_i = 1 \tag{2.21}$$

and the property of orthogonality

$$\Omega_i \int_{\beta/2}^{\beta} [cos\ \alpha_i\ (\frac{2y}{\beta}-1)]^2\ d(\frac{2y}{\beta}-1) = \int_{\beta/2}^{\beta} cos\ \alpha_i\ (\frac{2y}{\beta}-1)\ d(\frac{2y}{\beta}-1) \tag{2.22}$$

Let $\sigma = (2y/\beta - 1)$, we have

$$\sum_{i=1}^{\infty} \Omega_i (x) \cos \alpha_i \sigma = 1 \tag{2.23}$$

From the orthogonality we have

$$\Omega_j \int_0^1 \cos \alpha_i \sigma \cos \alpha_j \sigma \, d\sigma = \int_0^1 \cos \alpha_j \sigma \, d\sigma \tag{2.24}$$

Carrying out the integration for $\alpha_i = \alpha_j$, we obtain:

$$\Omega_i [\frac{\alpha_i + \sin\alpha_i \cos\alpha_i}{2\alpha_i}] = \frac{\sin\alpha_i}{\alpha_i}$$

or

$$\Omega_i = \frac{2\sin\alpha_i}{\alpha_i + \sin\alpha_i \cos\alpha_i} = \frac{2}{\alpha_i} (\frac{\sin\alpha_i}{1 + 2\, Kn \sin^2\alpha_i}) \tag{2.25}$$

Now, the velocity can be expressed as

$$w/C = -2\sum_{i=1}^{\infty} \frac{\cos \alpha_i (2y/\beta - 1)}{\alpha_i^3} (\frac{\sin \alpha_i}{1 + 2\, Kn \sin^2 \alpha_i})(1 - \frac{\cosh \frac{\alpha_i}{a}(2x/\beta' - 1)}{\cosh \frac{\alpha_i}{a} + 2\, Kn\, \alpha_i \sin \frac{\alpha_i}{a}}) \tag{2.26}$$

where $C = (D_H/\mu)(dp/dz)$ and the mean velocity is found by integration of Eq. (2.26) across the section of the channel: thus,

$$w_0 = \frac{1}{A} \int_A w \, dA \tag{2.27}$$

Upon carrying out the indicated operation, we obtain:

$$w_0/C = -2\sum_{i=1}^{\infty} \frac{a}{\alpha_i^5}\left(\frac{\sin^2 \alpha_i}{1 + 2\ Kn\ \sin^2 \alpha_i}\right)\left(\frac{\alpha_i}{a} - \frac{\sinh \frac{\alpha_i}{a}}{\cosh \frac{\alpha_i}{a} + 2\ Kn\ \alpha_i \sin \frac{\alpha_i}{a}}\right) \qquad (2.28)$$

2.2 Temperature Distribution

The general temperature field equation for flow of an incompressible fluid with zero swirl or angular components, zero energy generation, and negligible frictional energy dissipation is:

$$k\left(\frac{\partial^2 T}{\partial \xi^2} + \frac{\partial^2 T}{\partial \eta^2} + \frac{\partial^2 T}{\partial \varsigma^2}\right) = \varrho cw \frac{\partial T}{\partial \varsigma} \qquad (2.30)$$

with the boundary condition

$$T_w = T_1 \qquad \varsigma > 0 \qquad (2.31a)$$

$$T = T_0 \qquad \varsigma < 0 \qquad (2.31b)$$

introducing dimensionless variables

$$x = \frac{\xi}{D_H} \quad y = \frac{\eta}{D_H} \quad z = \frac{\varsigma}{D_H} \quad \theta = \frac{T - T_1}{T_0 - T_1}$$

When the aforementioned change of variables is carried out and the axial conduction $k\partial^2 T/\partial \varsigma^2$ can be neglected for a large enough Peclet number, the governing equations and the boundary conditions become

$$k\left(\frac{\partial^2 T}{\partial x^2} + \frac{\partial^2 T}{\partial y^2}\right) = \varrho cw D_H \frac{\partial T}{\partial z} \qquad \text{or} \qquad \nabla_1^{\,2}\theta = \frac{w}{w_0}\frac{\partial \theta}{dz} \qquad (2.32)$$

where $\nabla_1^{\,2} \equiv \partial^2/\partial x^2 + \partial^2/\partial y^2$, with the boundary condition

$$\theta_w = \theta_1 = 0 \qquad z > 0 \tag{2.33a}$$

$$\theta = 1 \qquad z \leq 0 \tag{2.33b}$$

2.3 Summary

In this chapter, the velocity distribution with slip–flow has been obtained which can be expressed simply in terms of the Knudsen number. From the relationship of Kn in terms of pressure and dimension, we can see that Kn in microtubes may become large enough to significantly affect the velocity distribution and consequently affect the heat transfer for this problem. Also, a mathematical model of temperature distribution in slip–flow has been established by combining the energy and momentum equations.

CHAPTER 3

ANALYTICAL SOLUTION

In the last chapter, the velocity distribution was expressed in terms of mean velocity and Knudsen number, and a mathematical model of temperature distribution in slip–flow was established by combining the energy and momentum equations. In this chapter, a series solution will be obtained by the method of Frobenius. Considering the boundary condition, a temperature distribution in terms of a generalized Fourier series will be derived. Also, expressions for the local and overall Nusselt numbers will be obtained.

3.1 Graetz Solution

3.1.1 Separation of Variables Solution

The governing equation

$$\nabla_1^2\theta = \frac{w}{w_0}\frac{\partial\theta}{\partial z} \tag{3.1}$$

where $\nabla_1^2 \equiv \partial^2/\partial x^2 + \partial^2/\partial y^2$, with the boundary condition

$$\theta_w = 0 \qquad z > 0 \tag{3.2a}$$

$$\theta = 1 \qquad z \leq 0 \tag{3.2b}$$

Eq. (3.1) can be solved by a separation–of–variables technique. Suppose we let:

$$\theta(x,y,z) = G(x,y)\,Z(z)$$

Making this substitution into Eq. (3.1) and rearranging results in the following:

$$\left(\frac{\partial^2 G}{\partial x^2} + \frac{\partial^2 G}{\partial y^2} \right) \frac{w_0}{Gw} = \frac{dZ}{Zdz} = -\lambda \tag{3.3}$$

where λ is an arbitrary constant. The ordinary differential equations which result are:

$$\frac{dZ}{dz} + \lambda Z = 0 \tag{3.4}$$

and

$$\nabla_1^{\,2} G + \frac{\lambda w(x,y)}{w_0} G = 0 \tag{3.5}$$

with boundary conditions:

$$G(0,0) = 0$$

$$G(0,l) = 0$$

$$G(l',0) = 0$$

$$G(l',l) = 0.$$

The solution of Eq. (3.4) is:

$$Z(z) = C \, exp[-\lambda z] \tag{3.6}$$

The constant C in Eq. (3.6) will be evaluated below and λ will be evaluated later.

3.1.2 Determination of Constants C_n

We can write the solution for the temperature distribution in terms of a generalized Fourier series, as follows:

$$\theta = \sum_{n=1}^{\infty} C_n G_n(x,y) e^{-\lambda_n z} \tag{3.5}$$

where G_n and λ_n are eigenfunctions and eigenvalues required to make the solution to the Eq. (3.3) subject to the boundary conditions deduced from the boundary condition Eq. (3.2a)

$$G(0,0) = G(0,l) = G(l',0) = G(l',l) = 0.$$

The constants C_n can be found from the entrance condition, Eq. (3.2b)

$$\text{at } z = 0\,,\ q\,(\,x,y,0\,) = 1$$

Making this substitution into Eq. (3.5), we obtain:

$$\sum_{j=0}^{\infty} C_n \ G_n(x,y) \ = \ 1 \tag{3.6}$$

The governing differential equation, along with the boundary conditions, is a Sturm–Liouville problem, with a weight function,

$$w = w(x,y)$$

where $w(x,y)$ is the z–component of velocity and from orthogonality,

$$\int\int_{D'} w(x,y) G_n G_m \ dx \ dy \ = \ 0 \qquad\qquad for \ m \neq n \tag{3.7}$$

The constants may be evaluated by multiplying Eq. (3.6) on both sides by

$$w(x,y) G_m$$

and integrating between on the domain D' bounded by C'. Only the term in which m = n is the result non–zero, and we find:

$$C_n \int\int_{D'} w(x,y)(G_n)^2 dx\ dy = \int\int_{D'} w(x,y)\ G_n\ dx\ dy \tag{3.8}$$

therefore,

$$C_n = \frac{\int\int_{D'} w(x,y)\ G_n\ dx\ dy}{\int\int_{D'} w(x,y)\ (G_n)^2 dx\ dy} \tag{3.9}$$

Each G_n has arbitrary amplitude which we choose for convenience, so that

$$C_n = \frac{\int\int_{D'} w(x,y)\ G_n\ dx\ dy}{\int\int_{D'} w(x,y)\ dx\ dy} \tag{3.10}$$

The temperature $\theta(x, y, z)$ is therefore known to any desired accuracy once sufficient G_n have been found. Two further thermal quantities are of interest. Experimental measurements are made on the basis of a mean mixed temperature of the fluid, that is, $\theta(x, y, z)$ averaged with respect to the local fluid velocity over any section of the channel. This temperature is a function of z only and its difference between any two sections gives a measure of the heat transferred across the wall between them.

From these expressions, we can see that the coefficients G_n and C_n must be predetermined in order to calculate the temperature.

3.2 Heat Transfer Coefficient Correlation

3.2.1 Bulk Temperature

The bulk or average temperature can be determined from:

$$\theta_B = \frac{\int\int_{D'} w(x,y)\ \theta\ dx\ dy}{\int\int_{D'} w(x,y)\ dx\ dy}$$

or

$$\theta_B(z) = \sum_{n=1}^{\infty} C_n^2\ e^{-\lambda_n z} \tag{3.11}$$

where:

$$\theta_B = \frac{T_B - T_w}{T_0 - T_w}$$

3.2.2 Local Heat Transfer Coefficient

The local or "point" convective heat transfer coefficient can be defined by:

$$Q/A_w = h_x\ (\ T_B - T_w\ ) \tag{3.12}$$

The heat flux can also be written, as follows:

$$q = \frac{Q}{A_w} = -k\ d\varsigma \int_C \frac{\partial T}{\partial \nu}\ ds\ = -k\ (\ T_0 - T_w\ ) \cdot d\varsigma \int_C \frac{\partial \theta}{\partial \nu}\ ds \tag{3.13}$$

where s is the distance measured along the perimeter of the boundary curve C in an anti–clockwise direction and ν is the outward–drawn coordinate normal to the channel wall: $\nu'=\nu/D_H, s'=s/D_H$. Equating the heat flux from Eqs. (3.12) and (3.13) and making the substitutions from Eq. (3.11) for the temperature gradient at the wall and for the local bulk temperature, the following expression is obtained for the local or "point" Nusselt number.

$$Nu(z) = -D_H \int_C \frac{\partial \theta}{\partial \nu'} \, ds' / S\theta_B \tag{3.14}$$

We now eliminate q in term of the G_n by Eq. (3.5) and apply Green's theorem to Eq. (3.3), so that

$$\int_C \frac{\partial G_n \theta}{\partial \nu'} \, ds' = -\frac{\lambda_n}{w_0} \int\int_{D'} w(x,y) \; G_n \; dx \; dy \tag{3.15}$$

Using Eq. (3.10) and since $\int\int_{D'} w \, dx \, dy = A' w_0$, where A' is the dimensionless area within C', we finally obtain

$$Nu(z) = \frac{1}{4\theta_B} \sum_{n=1}^{\infty} \lambda_n C_n^2 \; e^{-\lambda_n z} \tag{3.16}$$

At large distances down the channel, $Nu(z)$ approaches a limiting minimum value. If λ_1 is the smallest of the λ' we have, as $z \to \infty$, that $4\theta_B \, Nu(z) \sim \lambda_1 \, C_1^2 \exp(-\lambda_1 z)$ and $\theta_B(z) \sim C_1^2 \exp(-\lambda_1 z)$ so that

$$Nu(\infty) = \frac{\lambda_1}{4} \tag{3.17}$$

3.2.3 Overall Convective Heat Transfer Coefficient

The average or overall convective heat transfer coefficient is defined through the following expression:

$$Q = \bar{h}_c \, (4 \, h \, b \, L) \, (\Delta \, T)_{LN} = \int_0^L h_z \, (T_0 - T_w) \, (4 \, h \, b \, d\varsigma) \tag{3.18}$$

where $(\Delta T)_{LN}$ = log–mean–temperature difference (LMTD).

The LMTD may be written in terms of the inlet temperature T_0 and the exit bulk temperature T_L , as follows:

$$(\Delta \, T)_{LN} = \frac{(T_0 - T_w) - (T_L - T_w)}{ln \, [(T_0 - T_w) / (T_L - T_w)]} = \frac{(\theta_{B,L} - 1) (T_0 - T_w)}{ln \, (\theta_{B,L})} \tag{3.19}$$

Let us define the dimensionless LMTD, as follows:

$$\theta_{LN} = \frac{(\Delta \, T)_{LN}}{T_0 - T_w} \tag{3.20}$$

Then,

$$\theta_{LN} = \frac{(\theta_{B,L} - 1)}{ln \, (\theta_{B,L})} \tag{3.21}$$

The expression for the average convective heat transfer coefficient can then be written, from Eq. (3.18):

$$\bar{h}_c = \frac{1}{\theta_{LN}} \int_0^1 h_z \, \theta_B \, dz \tag{3.22}$$

In the fundamental equation, we have $q = h_{LN} \, S \, \varsigma \, \Delta T_{LN}$. Now q can either be obtained by integrating Eq. (3.13) from zero to ς or, alternatively, it is the heat given up by the fluid

in cooling from T_0 to T_m, so that $q = Aw_0\varrho c_p(T_0 - T_m)$. Equating these two and introducing dimensionless quantities, we have the mean logarithmic Nusselt number, $h_{LN}D_H/k$, given by:

$$\overline{Nu} = \frac{(1 - \theta_{B,L})}{4\ \theta_{LN}} = -\frac{1}{4}\ ln\ (\theta_{B,L}) \tag{3.23}$$

3.3 Summary

In this chapter, a series solution for the mathematical model of temperature distribution in slip flow in microchannels has been obtained. Considering the given boundary condition, a temperature distribution in terms of a generalized Fourier series has been derived. Also, expressions for the local and overall Nusselt numbers have been obtained. All these expressions can be taken as functions of the Knudsen number and the Graetz number. In order to calculate either the temperature or the Nusselt numbers, the coefficient C_n and λ_n must be predetermined.

CHAPTER 4

EVALUATION OF EIGENVALUES

In the last chapter, we obtained a series solution for the temperature distribution. Also, expressions for the local and overall Nusselt numbers have been obtained as functions of the Knudsen number and aspect ratio. In this chapter, we present a technique for evaluation of eigenvalues for the solution of the heat transfer problem in slip–flow, since eigenvalues λ_n must be predetermined for the calculation of either the temperature distribution or the Nusselt numbers. A matrix will be constructed and a formulation described to find the coefficients $b_{p,q}$(m,n). Based on these $b_{p,q}$(m,n) the eigenvalues λ_n can be calculated numerically.

4.1. Introduction

We consider the general domain D'. Based on the principle of the method of Galerkin, let $\{\phi_{m,n}\}$ be the complete set of eigenfunctions of the equation

$$\nabla^2\phi + \Lambda\phi = 0 \tag{4.1}$$

with $\partial\phi/\partial\nu' = -N\phi$ on C'. Any arbitrary function $\Theta(x,y)$ which satisfies these boundary conditions and which possesses continuous partial derivatives up to the second order can be expanded in an absolutely and uniformly convergent series in the form

$$\Theta(x,y) = \sum_{m=0}^{\infty} \sum_{n=0}^{\infty} a_{m,n}\, \phi_{m,n}(x,y) \tag{4.2}$$

where

$$a_{m,n} = \frac{1}{\delta_{p,q}(m,n)} \int\int_{D'} \Theta \phi_{m,n} \, dx \, dy \tag{4.3}$$

and

$$\delta_{p,q}(m,n) = \int\int_{D'} \phi_{m,n} \phi_{p,q} \, dx \, dy \tag{4.4}$$

$\delta_{p,q}(m,n) = 0$ unless $m = p$ *and* $n = q$. We can make Θ the solution of Eq. (3.5) so that multiplying this equation by $\phi_{m,n}$ and integrating over D' we have, by Eqs. (4.1) and (4.3),

$$\delta_{m,n}(m,n) \, \Lambda_{m,n} \, a_{m,n} = \lambda \int\int_{D'} r(x,y) \Theta \phi_{m,n} \, dx \, dy \tag{4.5}$$

where $r(x,y) = w(x,y) / w_0$. If we substitute for Θ by Eq. (4.2), then Eq. (4.5) is reduced to an infinite set of homogeneous linear algebraic equations

$$\sum_{p=0}^{\infty} \sum_{q=0}^{\infty} \{\delta_{p,q}(m,n) \, \Lambda_{m,n} - \lambda \, b_{p,q}(m,n)\} \, a_{p,q} = 0 \quad (m,n = 0, 1, 2, \ \ldots) \tag{4.6}$$

where

$$b_{p,q}(m,n) = \int\int_{D'} r \, \phi_{m,n} \phi_{p,q} \, dx \, dy \tag{4.7}$$

The matrix associated with Eqs. (4.6) is symmetrical since $b_{p,q}(m,n) = b_{m,n}(p,q)$ and the eliminant for a non–trivial solution gives an infinite determinantal equation $\Delta(\lambda) = 0$ whose latent roots are the eigenvalues of Eq. (3.5). Dividing each row of $\Delta(\lambda)$ by its leading diagonal elements, the resulting determinant converges if the off–diagonal sum is absolutely convergent and λ has no value which makes a leading diagonal element zero.

If this condition is satisfied, then the convergence of sum $\sum_{p=0}\sum_{q=0} \mid a_{p,q} \mid$ and, moreover, of sum $\sum_{p=0}\sum_{q=0} \delta_{p,q}(p,q)\Lambda_{p,q,} \mid a_{p,q} \mid$ follows. The eigenvectors $\{a_{p,q}{}^{(n)}\}$ corresponding to a given root $\lambda = \lambda_1$ can then be obtained, theoretically, in terms of any arbitrary coefficient; in practice, the determination of a given eigensolution is a problem in numerical analysis.

Eigenvalues λ_n can determined by the following infinite set of homogeneous linear algebraic equations

$$\sum_{p=0}^{\infty} \sum_{q=0}^{\infty} \{\delta_{p,q}(m,n)\, \Lambda_{m,n} - \lambda\, b_{p,q}(m,n)\}\, a_{p,q} = 0 \quad (m,n = 0,1,2, \ldots) \tag{4.6}$$

where

$$\delta_{p,q}(m,n) = \int\int_{D'} \phi_{m,n}\phi_{p,q}\, dx\, dy \tag{4.8}$$

$$\delta_{m,n}(m,n)\Lambda_{m,n} = (\pi^2/4a)\,(m^2 + a^2n^2), \tag{4.9}$$

$$b_{p,q}(m,n) = \frac{1}{4}\{\, d_{|m-p|,|n-q|} - d_{|m-p|,n+q} + d_{m+p,n+q} - d_{m+p,|n-q|}\,\} \tag{4.10}$$

$$d_{i,j} = \int_0^{l}\int_0^{l'} \frac{w'}{w_0} \cos\left(\frac{i\pi}{\beta}x\right) \cos\left(\frac{i\pi}{\beta'}y\right) dx\, dy \qquad (i,j=0,1,2, \ldots) \tag{4.11}$$

with

$$b_{p,q}(m,n) \begin{cases} \neq 0 & \text{for all } p,q,m,n \neq 0 \\ = 0 & \text{for any } p,q,m,n = 0 \end{cases} \tag{4.12}$$

4.2 Expansion of Eq. (4.6)

Considering the condition Eqs. (4.8) and (4.12) and underlining the only one with both p = m and q = n, we have the following expansion:

1) m = 0, n = 0

$$\underline{(\delta_{0,0}\Lambda_{0,0}}-\lambda b_{0,0})a_{0,0}+(\delta_{0,1}\Lambda_{0,0}-\lambda b_{0,1})a_{0,1}+(\delta_{0,2}\Lambda_{0,0}-\lambda b_{0,2})a_{0,2}+(\delta_{0,3}\Lambda_{0,0}-\lambda b_{0,3})a_{0,3}+\ldots$$
$$(\delta_{1,0}\Lambda_{0,0}-\lambda b_{1,0})a_{1,0}+(\delta_{1,1}\Lambda_{0,0}-\lambda b_{1,1})a_{1,1}+(\delta_{1,2}\Lambda_{0,0}-\lambda b_{1,2})a_{1,2}+(\delta_{1,3}\Lambda_{0,0}-\lambda b_{1,3})a_{1,3}+\ldots$$
$$(\delta_{2,0}\Lambda_{0,0}-\lambda b_{2,0})a_{2,0}+(\delta_{2,1}\Lambda_{0,0}-\lambda b_{2,1})a_{2,1}+(\delta_{2,2}\Lambda_{0,0}-\lambda b_{2,2})a_{2,2}+(\delta_{2,3}\Lambda_{0,0}-\lambda b_{2,3})a_{2,3}+\ldots$$
$$(\delta_{3,0}\Lambda_{0,0}-\lambda b_{3,0})a_{3,0}+(\delta_{3,1}\Lambda_{0,0}-\lambda b_{3,1})a_{3,1}+(\delta_{3,2}\Lambda_{0,0}-\lambda b_{3,2})a_{3,2}+(\delta_{3,3}\Lambda_{0,0}-\lambda b_{3,3})a_{3,3}+\ldots$$
$$= 0$$

the underlined term may not be equal to zero. All terms of $\delta_{p,q}\Lambda_{0,0}$ and coefficients of λ, $b_{p,q}$ but $\underline{\delta_{0,0}\Lambda_{0,0}}$ are zeros according to the condition Eqs. (4.8) and (4.12); therefore,

$$(\delta_{0,0}\Lambda_{0,0})a_{0,0} = 0$$

2) m = 0, n = 1

$$(\delta_{0,0}\Lambda_{0,1}-\lambda b_{0,0})a_{0,0}+(\underline{\delta_{0,1}\Lambda_{0,1}}-\lambda b_{0,1})a_{0,1}+(\delta_{0,2}\Lambda_{0,1}-\lambda b_{0,2})a_{0,2}+(\delta_{0,3}\Lambda_{0,1}-\lambda b_{0,3})a_{0,3}+\ldots$$
$$(\delta_{1,0}\Lambda_{0,1}-\lambda b_{1,0})a_{1,0}+(\delta_{1,1}\Lambda_{0,1}-\lambda b_{1,1})a_{1,1}+(\delta_{1,2}\Lambda_{0,1}-\lambda b_{1,2})a_{1,2}+(\delta_{1,3}\Lambda_{0,1}-\lambda b_{1,3})a_{1,3}+\ldots$$
$$(\delta_{2,0}\Lambda_{0,1}-\lambda b_{2,0})a_{2,0}+(\delta_{2,1}\Lambda_{0,1}-\lambda b_{2,1})a_{2,1}+(\delta_{2,2}\Lambda_{0,1}-\lambda b_{2,2})a_{2,2}+(\delta_{2,3}\Lambda_{0,1}-\lambda b_{2,3})a_{2,3}+\ldots$$
$$(\delta_{3,0}\Lambda_{0,1}-\lambda b_{3,0})a_{3,0}+(\delta_{3,1}\Lambda_{0,1}-\lambda b_{3,1})a_{3,1}+(\delta_{3,2}\Lambda_{0,1}-\lambda b_{3,2})a_{3,2}+(\delta_{3,3}\Lambda_{0,1}-\lambda b_{3,3})a_{3,3}+\ldots$$
$$= 0$$

therefore,

$$(\delta_{0,1}\Lambda_{0,1})a_{0,1} = 0$$

Similarly,

3) m = 0, n = 2

$$(\delta_{0,2}\Lambda_{0,2})a_{0,2} = 0$$

4) m = 0, n = 3

$$(\delta_{0,3}\Lambda_{0,3})a_{0,3} = 0$$

.....

5) m = 1, n = 0

$(\delta_{0,0}\Lambda_{1,0}-\lambda b_{0,0})a_{0,0}+(\delta_{0,1}\Lambda_{1,0}-\lambda b_{0,1})a_{0,1}+(\delta_{0,2}\Lambda_{1,0}-\lambda b_{0,2})a_{0,2}+(\delta_{0,3}\Lambda_{1,0}-\lambda b_{0,3})a_{0,3}+...$

$(\underline{\delta_{1,0}\Lambda_{1,0}}-\lambda b_{1,0})a_{1,0}+(\delta_{1,1}\Lambda_{1,0}-\lambda b_{1,1})a_{1,1}+(\delta_{1,2}\Lambda_{1,0}-\lambda b_{1,2})a_{1,2}+(\delta_{1,3}\Lambda_{1,0}-\lambda b_{1,3})a_{1,3}+...$

$(\delta_{2,0}\Lambda_{1,0}-\lambda b_{2,0})a_{2,0}+(\delta_{2,1}\Lambda_{1,0}-\lambda b_{2,1})a_{2,1}+(\delta_{2,2}\Lambda_{1,0}-\lambda b_{2,2})a_{2,2}+(\delta_{2,3}\Lambda_{1,0}-\lambda b_{2,3})a_{2,3}+...$

$(\delta_{3,0}\Lambda_{1,0}-\lambda b_{3,0})a_{3,0}+(\delta_{3,1}\Lambda_{1,0}-\lambda b_{3,1})a_{3,1}+(\delta_{3,2}\Lambda_{1,0}-\lambda b_{3,2})a_{3,2}+(\delta_{3,3}\Lambda_{1,0}-\lambda b_{3,3})a_{3,3}+...$

$= 0$

therefore,

$(\underline{\delta_{1,0}\Lambda_{1,0}})a_{1,0}= 0$

6) m = 1, n = 1

$(\delta_{0,0}\Lambda_{1,1}-\lambda b_{0,0})a_{0,0}+(\delta_{0,1}\Lambda_{1,1}-\lambda b_{0,1})a_{0,1}+(\delta_{0,2}\Lambda_{1,1}-\lambda b_{0,2})a_{0,2}+(\delta_{0,3}\Lambda_{1,1}-\lambda b_{0,3})a_{0,3}+...$

$(\delta_{1,0}\Lambda_{1,1}-\lambda b_{1,0})a_{1,0}+(\underline{\delta_{1,1}\Lambda_{1,1}}-\lambda b_{1,1})a_{1,1}+(\delta_{1,2}\Lambda_{1,1}-\lambda b_{1,2})a_{1,2}+(\delta_{1,3}\Lambda_{1,1}-\lambda b_{1,3})a_{1,3}+...$

$(\delta_{2,0}\Lambda_{1,1}-\lambda b_{2,0})a_{2,0}+(\delta_{2,1}\Lambda_{1,1}-\lambda b_{2,1})a_{2,1}+(\delta_{2,2}\Lambda_{1,1}-\lambda b_{2,2})a_{2,2}+(\delta_{2,3}\Lambda_{1,1}-\lambda b_{2,3})a_{2,3}+...$

$(\delta_{3,0}\Lambda_{1,1}-\lambda b_{3,0})a_{3,0}+(\delta_{3,1}\Lambda_{1,1}-\lambda b_{3,1})a_{3,1}+(\delta_{3,2}\Lambda_{1,1}-\lambda b_{3,2})a_{3,2}+(\delta_{3,3}\Lambda_{1,1}-\lambda b_{3,3})a_{3,3}+...$

$= 0$

therefore,

$(\underline{\delta_{1,1}\Lambda_{1,1}}-\lambda b_{1,1})a_{1,1}+(-\lambda b_{1,2})a_{1,2}+(-\lambda b_{1,3})a_{1,3}+...$

$+(-\lambda b_{2,1})a_{2,1}+(-\lambda b_{2,2})a_{2,2}+(-\lambda b_{2,3})a_{2,3}+ ...$

$+(-\lambda b_{3,1})a_{3,1}+(-\lambda b_{3,2})a_{3,2}+(-\lambda b_{3,3})a_{3,3}+ ... = 0$

or,

$(\underline{\delta_{1,1}\Lambda_{1,1}} -\lambda b11_{1,1})a_{1,1}+(-\lambda b11_{1,2})a_{1,2}+(-\lambda b11_{1,3})a_{1,3}+ ...$

$+(-\lambda b11_{2,1})a_{2,1}+(-\lambda b11_{2,2})a_{2,2}+(-\lambda b11_{2,3})a_{2,3}+ ...$

$+(-\lambda b11_{3,1})a_{3,1}+(-\lambda b11_{3,2})a_{3,2}+(-\lambda b11_{3,3})a_{3,3}+ ... = 0$

7) m = 1, n = 2

$(\delta_{0,0}\Lambda_{1,2}-\lambda b_{0,0})a_{0,0}+(\delta_{0,1}\Lambda_{1,2}-\lambda b_{0,1})a_{0,1}+(\delta_{0,2}\Lambda_{1,2}-\lambda b_{0,2})a_{0,2}+(\delta_{0,3}\Lambda_{1,2}-\lambda b_{0,3})a_{0,3}+...$

$(\delta_{1,0}\Lambda_{1,2}-\lambda b_{1,0})a_{1,0}+(\delta_{1,1}\Lambda_{1,2}-\lambda b_{1,1})a_{1,1}+(\underline{\delta_{1,2}\Lambda_{1,2}}-\lambda b_{1,2})a_{1,2}+(\delta_{1,3}\Lambda_{1,2}-\lambda b_{1,3})a_{1,3}+...$

$(\delta_{2,0}\Lambda_{1,2}-\lambda b_{2,0})a_{2,0}+(\delta_{2,1}\Lambda_{1,2}-\lambda b_{2,1})a_{2,1}+(\delta_{2,2}\Lambda_{1,2}-\lambda b_{2,2})a_{2,2}+(\delta_{2,3}\Lambda_{1,2}-\lambda b_{2,3})a_{2,3}+...$

$(\delta_{3,0}\Lambda_{1,2}-\lambda b_{3,0})a_{3,0}+(\delta_{3,1}\Lambda_{1,2}-\lambda b_{3,1})a_{3,1}+(\delta_{3,2}\Lambda_{1,2}-\lambda b_{3,2})a_{3,2}+(\delta_{3,3}\Lambda_{1,2}-\lambda b_{3,3})a_{3,3}+...$

$= 0$

therefore,

$(-\lambda b_{1,1})a_{1,1}+(\underline{\delta_{1,2}\Lambda_{1,2}}-\lambda b_{1,2})a_{1,2}+(-\lambda b_{1,3})a_{1,3}+...$

$+(-\lambda b_{2,1})a_{2,1}+(-\lambda b_{2,2})a_{2,2}+(-\lambda b_{2,3})a_{2,3}+ ...$

$+(-\lambda b_{3,1})a_{3,1}+(-\lambda b_{3,2})a_{3,2}+(-\lambda b_{3,3})a_{3,3}+ ... = 0$

or,

$(-\lambda b12_{1,1})a_{1,1}+(\underline{\delta_{1,2}\Lambda_{1,2}}-\lambda b12_{1,2})a_{1,2}+(-\lambda b12_{1,3})a_{1,3}+ ...$

$+(-\lambda b12_{2,1})a_{2,1}+(-\lambda b12_{2,2})a_{2,2}+(-\lambda b12_{2,3})a_{2,3}+ ...$

$+(-\lambda b12_{3,1})a_{3,1}+(-\lambda b12_{3,2})a_{3,2}+(-\lambda b12_{3,3})a_{3,3}+ ... = 0$

8) m = 1, n = 3

$(\delta_{0,0}\Lambda_{1,3}-\lambda b_{0,0})a_{0,0}+(\delta_{0,1}\Lambda_{1,3}-\lambda b_{0,1})a_{0,1}+(\delta_{0,2}\Lambda_{1,3}-\lambda b_{0,2})a_{0,2}+(\delta_{0,3}\Lambda_{1,3}-\lambda b_{0,3})a_{0,3}+...$

$(\delta_{1,0}\Lambda_{1,3}-\lambda b_{1,0})a_{1,0}+(\delta_{1,1}\Lambda_{1,3}-\lambda b_{1,1})a_{1,1}+(\delta_{1,2}\Lambda_{1,3}-\lambda b_{1,2})a_{1,2}+(\underline{\delta_{1,3}\Lambda_{1,3}}-\lambda b_{1,3})a_{1,3}+...$

$(\delta_{2,0}\Lambda_{1,3}-\lambda b_{2,0})a_{2,0}+(\delta_{2,1}\Lambda_{1,3}-\lambda b_{2,1})a_{2,1}+(\delta_{2,2}\Lambda_{1,3}-\lambda b_{2,2})a_{2,2}+(\delta_{2,3}\Lambda_{1,3}-\lambda b_{2,3})a_{2,3}+...$

$(\delta_{3,0}\Lambda_{1,3}-\lambda b_{3,0})a_{3,0}+(\delta_{3,1}\Lambda_{1,3}-\lambda b_{3,1})a_{3,1}+(\delta_{3,2}\Lambda_{1,3}-\lambda b_{3,2})a_{3,2}+(\delta_{3,3}\Lambda_{1,3}-\lambda b_{3,3})a_{3,3}+...$

$= 0$

therefore,

$(-\lambda b_{1,1})a_{1,1}+(-\lambda b_{1,2})a_{1,2}+(\underline{\delta_{1,3}\Lambda_{1,3}}-\lambda b_{1,3})a_{1,3}+...$

$+(-\lambda b_{2,1})a_{2,1}+(-\lambda b_{2,2})a_{2,2}+(-\lambda b_{2,3})a_{2,3}+ ...$

$+(-\lambda b_{3,1})a_{3,1}+(-\lambda b_{3,2})a_{3,2}+(-\lambda b_{3,3})a_{3,3}+ ... = 0$

or

$(-\lambda b13_{1,1})a_{1,1}+(\underline{\delta_{1,2}\Lambda_{1,2}}-\lambda b13_{1,2})a_{1,2}+(-\lambda b13_{1,3})a_{1,3}+ ...$

$+(-\lambda b13_{2,1})a_{2,1}+(-\lambda b32_{2,2})a_{2,2}+(-\lambda b13_{2,3})a_{2,3}+ ...$

$+(-\lambda b13_{3,1})a_{3,1}+(-\lambda b13_{3,2})a_{3,2}+(-\lambda b13_{3,3})a_{3,3}+ ... = 0$

.....

Similarly,

9) m = 2, n = 0

$$(\underline{\delta_{2,0}\Lambda_{2,0}})a_{2,0}= 0$$

10) m = 2, n = 1

$$(-\lambda b21_{1,1})a_{1,1}+(-\lambda b21_{1,2})a_{1,2}+(-\lambda b21_{1,3})a_{1,3}+ \ldots$$
$$+(\underline{\delta_{2,1}\Lambda_{2,1}} -\lambda b21_{2,1})a_{2,1}+(-\lambda b21_{2,2})a_{2,2}+(-\lambda b21_{2,3})a_{2,3}+ \ldots$$
$$+(-\lambda b21_{3,1})a_{3,1}+(-\lambda b21_{3,2})a_{3,2}+(-\lambda b21_{3,3})a_{3,3}+ \ldots = 0$$

11) m = 2, n = 2

$$(-\lambda b22_{1,1})a_{1,1}+(-\lambda b22_{1,2})a_{1,2}+(-\lambda b22_{1,3})a_{1,3}+ \ldots$$
$$+(-\lambda b12_{2,1})a_{2,1}+(\underline{\delta_{2,2}\Lambda_{2,2}} -\lambda b12_{2,2})a_{2,2}+(-\lambda b12_{2,3})a_{2,3}+ \ldots$$
$$+(-\lambda b22_{3,1})a_{3,1}+(-\lambda b22_{3,2})a_{3,2}+(-\lambda b22_{3,3})a_{3,3}+ \ldots = 0$$

12) m = 2, n = 3

$$(-\lambda b23_{1,1})a_{1,1}+(-\lambda b23_{1,2})a_{1,2}+(-\lambda b23_{1,3})a_{1,3}+ \ldots$$
$$+(-\lambda b23_{2,1})a_{2,1}+(-\lambda b23_{2,2})a_{2,2}+(\underline{\delta_{2,3}\Lambda_{2,3}} -\lambda b23_{2,3})a_{2,3}+ \ldots$$
$$+(-\lambda b23_{3,1})a_{3,1}+(-\lambda b23_{3,2})a_{3,2}+(-\lambda b23_{3,3})a_{3,3}+ \ldots = 0$$

.....

13) 3 = 2, n = 0

$$(\underline{\delta_{3,0}\Lambda_{3,0}})a_{3,0}= 0$$

14) m = 3, n = 1

$$(-\lambda b31_{1,1})a_{1,1}+(-\lambda b31_{1,2})a_{1,2}+(-\lambda b31_{1,3})a_{1,3}+ \ldots$$
$$+(-\lambda b31_{2,1})a_{2,1}+(-\lambda b31_{2,2})a_{2,2}+(-\lambda b31_{2,3})a_{2,3}+ \ldots$$
$$+(\underline{\delta_{3,1}\Lambda_{3,1}} -\lambda b31_{3,1})a_{3,1}+(-\lambda b31_{3,2})a_{3,2}+(-\lambda b31_{3,3})a_{3,3}+ \ldots = 0$$

15) m = 3, n = 2

$$(-\lambda b32_{1,1})a_{1,1}+(-\lambda b32_{1,2})a_{1,2}+(-\lambda b32_{1,3})a_{1,3}+ \ldots$$
$$+(-\lambda b32_{2,1})a_{2,1}+(-\lambda b32_{2,2})a_{2,2}+(-\lambda b32_{2,3})a_{2,3}+ \ldots$$
$$+(-\lambda b32_{3,1})a_{3,1}+(\underline{\delta_{3,2}\Lambda_{3,2}} -\lambda b32_{3,2})a_{3,2}+(-\lambda b32_{3,3})a_{3,3}+ \ldots = 0$$

16) m = 3, n = 3

$$(-\lambda b33_{1,1})a_{1,1}+(-\lambda b33_{1,2})a_{1,2}+(-\lambda b33_{1,3})a_{1,3}+ \ldots$$
$$+(-\lambda b33_{2,1})a_{2,1}+(-\lambda b33_{2,2})a_{2,2}+(-\lambda b33_{2,3})a_{2,3}+ \ldots$$
$$+(-\lambda b33_{3,1})a_{3,1}+(-\lambda b33_{3,2})a_{3,2}+(\underline{\delta_{3,3}\Lambda_{3,3}} -\lambda b33_{3,3})a_{3,3}+ \ldots = 0$$

.....

From all these expansions, we can obtain

$$(\underline{\delta_{i,0}\Lambda_{i,0}})a_{i,0}= 0$$

and, in matrix form and introducing $e_{m,n} = \delta_{m,n}\Lambda_{m,n}$, Eq. (4.6) becomes

$$\begin{bmatrix} e_{1,1}-\lambda b11_{1,1} & -\lambda b11_{1,2} & -\lambda b11_{1,3} & \ldots & -\lambda b11_{2,1} & -\lambda b11_{2,2} & -\lambda b11_{2,3} & \ldots \\ -\lambda b12_{1,1} & e_{1,2}-\lambda b12_{1,2} & -\lambda b12_{1,3} & \ldots & -\lambda b12_{2,1} & -\lambda b12_{2,2} & -\lambda b12_{2,3} & \ldots \\ -\lambda b13_{1,1} & -\lambda b13_{1,2} & e_{1,3}-\lambda b13_{1,3} & \ldots & -\lambda b13_{2,1} & -\lambda b13_{2,2} & -\lambda b13_{2,3} & \ldots \\ \ldots & \ldots & \ldots & \ldots & \ldots & \ldots & \ldots & \ldots \\ -\lambda b21_{1,1} & -\lambda b21_{1,2} & -\lambda b21_{1,3} & \ldots & e_{2,1}-\lambda b21_{2,1} & -\lambda b21_{2,2} & -\lambda b21_{2,3} & \ldots \\ -\lambda b22_{1,1} & -\lambda b22_{1,2} & -\lambda b22_{1,3} & \ldots & -\lambda b22_{2,1} & e_{2,2}-\lambda b22_{2,2} & -\lambda b22_{2,3} & \ldots \\ -\lambda b23_{1,1} & -\lambda b23_{1,2} & -\lambda b23_{1,3} & \ldots & -\lambda b23_{2,1} & -\lambda b23_{2,2} & e_{2,3}-\lambda b23_{2,3} & \ldots \\ \ldots & \ldots & \ldots & & \ldots & \ldots & \ldots & \ldots \end{bmatrix} \begin{bmatrix} a_{1,1} \\ a_{1,2} \\ a_{1,3} \\ \ldots \\ a_{2,1} \\ a_{2,2} \\ a_{2,3} \\ \ldots \end{bmatrix} = 0$$

(4.13)

In the next section, we will deal with Eq. (4.13).

4.3 Simplification of Eq. (4.13)

From condition (4.12) and $bmn_{p,q}$ being non–zero only if $m+p$ and $n+q$ are both even, Eq. (4.13) can be further simplified as

$$\begin{bmatrix} e_{1,1}-\lambda b11_{1,1} & 0 & -\lambda b11_{1,3} & \dots & 0 & 0 & 0 & \dots \\ 0 & e_{1,2}-\lambda b12_{1,2} & 0 & \dots & 0 & 0 & 0 & \dots \\ -\lambda b13_{1,1} & 0 & e_{1,3}-\lambda b13_{1,3} & \dots & 0 & 0 & 0 & \dots \\ \dots & \dots & \dots & \dots & \dots & \dots & \dots & \dots \\ 0 & 0 & 0 & \dots & e_{2,1}-\lambda b21_{2,1} & 0 & -\lambda b21_{2,3} & \dots \\ 0 & 0 & 0 & \dots & 0 & e_{2,2}-\lambda b22_{2,2} & 0 & \dots \\ 0 & 0 & 0 & \dots & -\lambda b23_{2,1} & 0 & e_{2,3}-\lambda b23_{2,3} & \dots \\ \dots & \dots & \dots & & \dots & \dots & \dots & \dots \end{bmatrix} \begin{bmatrix} a_{1,1} \\ a_{1,2} \\ a_{1,3} \\ \dots \\ a_{2,1} \\ a_{2,2} \\ a_{2,3} \\ \dots \end{bmatrix} = 0 \tag{4.14}$$

or generalized as

$$\begin{bmatrix} x & 0 & x & 0 & \dots & 0 & 0 & 0 & 0 & \dots & x & 0 & x & 0 & \dots \\ 0 & x & 0 & x & \dots & 0 & 0 & 0 & 0 & \dots & 0 & x & 0 & x & \dots \\ x & 0 & x & 0 & \dots & 0 & 0 & 0 & 0 & \dots & x & 0 & x & 0 & \dots \\ 0 & x & 0 & x & \dots & 0 & 0 & 0 & 0 & \dots & 0 & x & 0 & x & \dots \\ \dots & \dots & \dots & \dots & \dots & \dots & \dots & \dots & \dots & \dots & \dots & \dots & \dots & \dots & \dots \\ 0 & 0 & 0 & 0 & \dots & x & 0 & x & 0 & \dots & 0 & 0 & 0 & 0 & \dots \\ 0 & 0 & 0 & 0 & \dots & 0 & x & 0 & x & \dots & 0 & 0 & 0 & 0 & \dots \\ 0 & 0 & 0 & 0 & \dots & 0 & 0 & x & 0 & \dots & 0 & 0 & 0 & 0 & \dots \\ 0 & 0 & 0 & 0 & \dots & 0 & x & 0 & x & \dots & 0 & 0 & 0 & 0 & \dots \\ \dots & \dots & \dots & \dots & \dots & \dots & \dots & \dots & \dots & \dots & \dots & \dots & \dots & \dots & \dots \\ x & 0 & x & 0 & \dots & 0 & 0 & 0 & 0 & \dots & x & 0 & x & 0 & \dots \\ 0 & x & 0 & x & \dots & 0 & 0 & 0 & 0 & \dots & 0 & x & 0 & x & \dots \\ x & 0 & x & 0 & \dots & 0 & 0 & 0 & 0 & \dots & x & 0 & x & 0 & \dots \\ 0 & x & 0 & x & .. & 0 & 0 & 0 & 0 & \dots & 0 & x & 0 & x & \dots \\ \dots & \dots & \dots & & \dots & \dots & \dots & \dots & \dots & \dots & \dots & \dots & \dots & \dots & \dots \end{bmatrix} \begin{bmatrix} a_{1,1} \\ a_{1,2} \\ a_{1,3} \\ a_{1,4} \\ \dots \\ a_{2,1} \\ a_{2,2} \\ a_{2,3} \\ a_{2,4} \\ \dots \\ a_{3,1} \\ a_{3,2} \\ a_{3,3} \\ a_{3,4} \\ \dots \end{bmatrix} = 0$$

where x are $(e_{p,q} - \lambda bpq_{p,q})$ and x are $- \lambda bmn_{p,q}$.

Employing block matrices, Eq. (4.14) can be further rewritten as

$$\begin{matrix} \\ p \end{matrix}\begin{matrix} \begin{bmatrix} X_1 & \mathbf{0} & \mathbf{x}_{13} & \mathbf{0} & \mathbf{x}_{15} & \cdots \\ \mathbf{0} & X_2 & \mathbf{0} & \mathbf{x}_{24} & \mathbf{0} & \cdots \\ \mathbf{x}_{31} & \mathbf{0} & X_3 & \mathbf{0} & \mathbf{x}_{35} & \cdots \\ \mathbf{0} & \mathbf{x}_{42} & \mathbf{0} & X_4 & \mathbf{0} & \cdots \\ \mathbf{x}_{51} & \mathbf{0} & \mathbf{x}_{53} & \mathbf{0} & X_5 & \cdots \\ \cdots & \cdots & \cdots & \cdots & \cdots & \cdots \end{bmatrix} \\ q \end{matrix} \begin{bmatrix} A_1 \\ A_2 \\ A_3 \\ A_4 \\ A_5 \\ \cdots \end{bmatrix} = 0 \qquad (4.15)$$

where

$$X_p = \begin{matrix} \\ m \end{matrix}\begin{matrix} \begin{bmatrix} x_1 & 0 & \mathrm{x} & 0 & \cdots \\ 0 & x_2 & 0 & \mathrm{x} & \cdots \\ \mathrm{x} & 0 & x_3 & 0 & \cdots \\ 0 & \mathrm{x} & 0 & x_4 & \cdots \\ \cdots & \cdots & \cdots & \cdots & \cdots \end{bmatrix} \\ n \end{matrix} \qquad \mathbf{x}_{pq} = \begin{matrix} \\ m \end{matrix}\begin{matrix} \begin{bmatrix} \mathrm{x} & 0 & \mathrm{x} & 0 & \cdots \\ 0 & \mathrm{x} & 0 & \mathrm{x} & \cdots \\ \mathrm{x} & 0 & \mathrm{x} & 0 & \cdots \\ 0 & \mathrm{x} & 0 & \mathrm{x} & \cdots \\ \cdots & \cdots & \cdots & \cdots & \cdots \end{bmatrix} \\ n \end{matrix} \qquad A_p = \begin{bmatrix} a_{p,1} \\ a_{p,2} \\ a_{p,3} \\ a_{p,4} \\ \cdots \\ a_{p,q} \\ \cdots \end{bmatrix}$$

4.4. Summary

In this chapter, a technique for calculation of the eigenvalues occurring in the heat transfer problem in slip–flow has been derived by constructing a matrix. With this formulation, any number of eigenvalues can be theoretically determined. The next chapter will deal with the algorithms and the computational procedure, and the calculation of the eigenvalues will be carried out.

CHAPTER 5

COMPUTATIONAL RESULTS

In the previous chapter, the formulation for the calculation of the coefficients occurring in the eigenfunction was determined. In this chapter, we will discuss the procedures for the evaluation of eigenvalues for the heat transfer problem in slip–flow. We will calculate the eigenvalues and discuss the computational results.

5.1 Procedures of Computation

The procedures of computation are as following:

1) Calculate a_i for certain Knudsen number Kn by Eq. (2.10) in Chapter 2

$$a_i \tan a_i = \frac{1}{2\ Kn} \tag{5.1}$$

2) Calculate coefficients $d_{i,j}$ for certain Knudsen number Kn and aspect ratio a by Eq. (4.11) in Chapter 4

$$d_{i,j} = \int_0^{\beta} \int_0^{\beta'} \frac{w}{w_0} \cos\left(\frac{i\pi}{\beta}x\right) \cos\left(\frac{i\pi}{\beta'}y\right) dx\, dy \qquad (i,j=0,1,2,\ldots) \tag{5.2}$$

where

$$w/C = -2\sum_{i=1}^{\infty} \frac{\cos a_i \left(\frac{2}{\beta}y - 1\right)}{a_i^3} \left(\frac{\sin a_i}{1 + 2\ Kn \sin^2 a_i}\right)\left(1 - \frac{\cosh \frac{a_i}{a}\left(\frac{2}{\beta'}x - 1\right)}{\cosh \frac{a_i}{a} + 2\ Kn\ a_i \sin \frac{a_i}{a}}\right) \tag{5.3}$$

and

$$w_0/C = -2\sum_{i=1}^{\infty} \frac{a}{\alpha_i^5}\left(\frac{\sin^2 \alpha_i}{1 + 2\ Kn\ \sin^2 \alpha_i}\right)\left(\frac{\alpha_i}{a} - \frac{\sinh \frac{\alpha_i}{a}}{\cosh \frac{\alpha_i}{a} + 2\ Kn\ \alpha_i\ \sin \frac{\alpha_i}{a}}\right) \qquad (5.4)$$

3) Determine $b_{p,q}(m, n)$ (or $bmn_{p,q}$) by Eq. (4.10) in Chapter 4

$$b_{p,q}(m,n) = \frac{1}{4}\{\ d_{|m-p|,|n-q|} - d_{|m-p|,n+q} + d_{m+p,n+q} - d_{m+p,|n-q|}\ \} \qquad (5.5)$$

4) Calculate $e_{p,q} = \delta_{p,q}\Lambda_{p,q}$ for certain m and n by Eq. (4.9)

$$\delta_{p,q}(m,n)\Lambda_{p,q} = (\pi^2/4a)\,(m^2 + a^2n^2), \qquad (5.6)$$

5) Determine truncation eigenfunction for certain m and n by Eq. (4.15) in Chapter 4

$$\begin{bmatrix} X_1 & 0 & x_{13} & 0 & x_{15} & \cdots \\ 0 & X_2 & 0 & x_{24} & 0 & \cdots \\ x_{31} & 0 & X_3 & 0 & x_{35} & \cdots \\ 0 & x_{42} & 0 & X_4 & 0 & \cdots \\ x_{51} & 0 & x_{53} & 0 & X_5 & \cdots \\ \cdots & \cdots & \cdots & \cdots & \cdots & \cdots \end{bmatrix} \begin{bmatrix} A_1 \\ A_2 \\ A_3 \\ A_4 \\ A_5 \\ \cdots \end{bmatrix} = 0 \qquad (5.7)$$

where

$$X_m = \begin{bmatrix} x & 0 & x & 0 & \cdots \\ 0 & x & 0 & x & \cdots \\ x & 0 & x & 0 & \cdots \\ 0 & x & 0 & x & \cdots \\ \cdots & \cdots & \cdots & \cdots & \cdots \end{bmatrix} \quad x_{mn} = \begin{bmatrix} x & 0 & x & 0 & \cdots \\ 0 & x & 0 & x & \cdots \\ x & 0 & x & 0 & \cdots \\ 0 & x & 0 & x & \cdots \\ \cdots & \cdots & \cdots & \cdots & \cdots \end{bmatrix} \quad A_m = \begin{bmatrix} a_{m,1} \\ a_{m,2} \\ a_{m,3} \\ a_{m,4} \\ \cdots \\ a_{m,n} \\ \cdots \end{bmatrix}$$

where x are ($e_{p,q} - \lambda bmn_{p,q}$) and x are $-\lambda bmn_{p,q}$ and $e_{p,q} = \delta_{p,q}\Lambda_{p,q}$ for certain m and n.

For example, the truncated eigenfunction for m, n = 0,1 and for m, n = 0,1,2,3 are respectively

$$\Delta_1(\lambda) = |X_1| = 0 \tag{5.8a}$$

$$\Delta_3(\lambda) = |X_1|\,|X_2|\,|X_3| - |x_{31}|\,|X_2|\,|x_{13}| = 0 \tag{5.8b}$$

and $\Delta(\lambda) = \lim \Delta_p(\lambda)$ when $p \to \infty$.

6) Evaluate the eigenvalue λ by the known truncated eigenfunction such as Eq. (5.8)

7) Determine the fully–developed Nusselt number by Eq. (3.17) in Chapter 3

$$Nu_\infty = \frac{\lambda_1}{4} \tag{5.9}$$

5.2 Calculation of α_i

Table 5.1 lists the first eight values of each α_i for Kn from 0.005 to 0.3 by Eq.(5.1). Fig.5.1 shows that α_i vary as functions of Kn. From Fig.5.1, we can see that the difference of the adjacent α_i and α_{i+1} becomes smaller as Kn increases but goes to a constant π as both Kn and i increase.

Table 5.1 The first eight values of α_i

Kn	α_1	α_2	α_3	α_4	α_5	α_6	α_7	α_8
0.005	1.5552	4.6658	7.7764	10.887	13.998	17.109	20.221	23.333
0.01	1.5400	4.6202	7.7012	10.783	13.867	16.952	20.039	23.128
0.02	1.5105	4.5330	7.5603	10.595	13.638	16.690	19.752	22.822
0.04	1.4549	4.3757	7.3240	10.306	13.320	16.360	19.421	22.498
0.06	1.4039	4.2416	7.1452	10.114	13.132	16.183	19.258	22.348
0.08	1.3570	4.1286	7.0112	9.9841	13.014	16.079	19.165	22.265
0.10	1.3138	4.0336	6.9096	9.8928	12.935	16.011	19.106	22.213
0.20	1.1422	3.7318	6.6431	9.6776	12.760	15.864	18.981	22.104
0.30	1.0211	3.5776	6.5330	9.5967	12.697	15.813	18.937	22.067

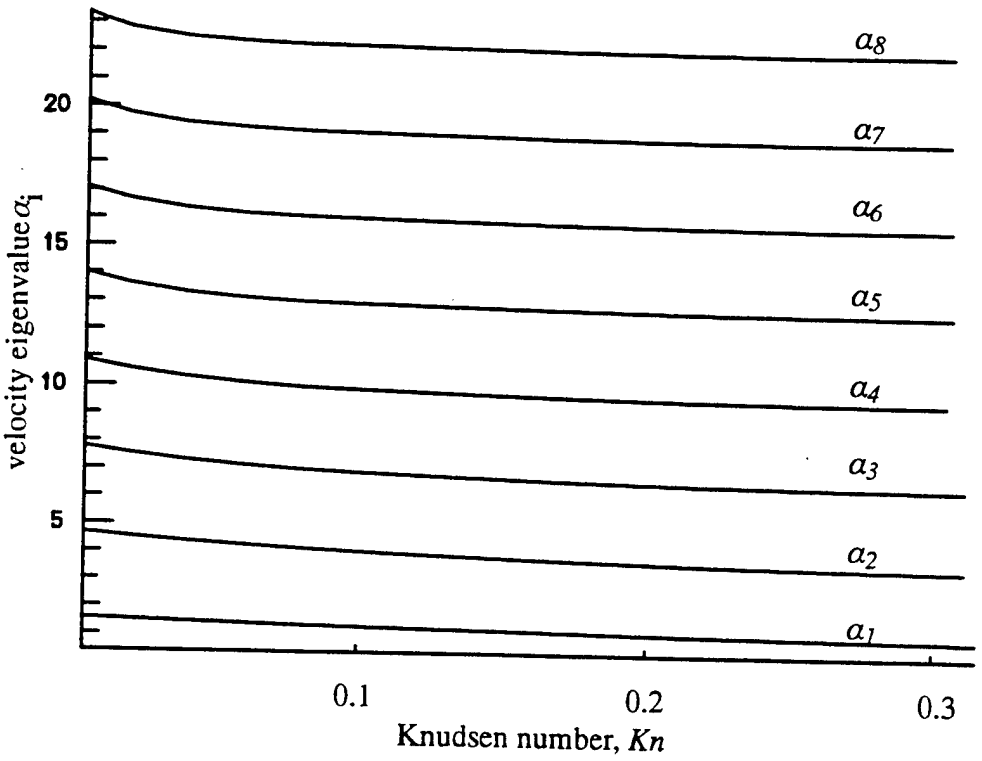

Fig. 5.1 Velocity eigenvalues α_i as functions of Kn

5.3 Calculation of $d_{i,j}$

For $Kn = 0.00$ and $a = 1$ (for $Kn = 0.00$ and $a = 1$ see Appendix B), and i,j = 0,1,2, ... , 10, the $d_{i,j}$ are as following:

$$d_{i,j} = \begin{bmatrix} 1.0015 & 0 & -0.27819 & 0 & -0.08309 & 0 & -0.03854 & 0 & -0.02209 & 0 & -0.01431 \\ 0 & 0 & 0 & 0 & 0 & 0 & 0 & 0 & 0 & 0 & 0 \\ -0.27809 & 0 & 0.08285 & 0 & 0.02237 & 0 & 0.00979 & 0 & 0.00542 & 0 & 0.00342 \\ 0 & 0 & 0 & 0 & 0 & 0 & 0 & 0 & 0 & 0 & 0 \\ -0.08299 & 0 & 0.02237 & 0 & 0.00725 & 0 & 0.00338 & 0 & 0.0192 & 0 & 0.00122 \\ 0 & 0 & 0 & 0 & 0 & 0 & 0 & 0 & 0 & 0 & 0 \\ -0.03844 & 0 & 0.00979 & 0 & 0.00338 & 0 & 0.01670 & 0 & 9.73e{-4} & 0 & 6.31e{-4} \\ 0 & 0 & 0 & 0 & 0 & 0 & 0 & 0 & 0 & 0 & 0 \\ -0.02198 & 0 & 0.00542 & 0 & 0.00191 & 0 & 9.73e{-4} & 0 & 5.82e{-4} & 0 & 3.84e{-4} \\ 0 & 0 & 0 & 0 & 0 & 0 & 0 & 0 & 0 & 0 & 0 \\ -0.01418 & 0 & 0.00343 & 0 & 0.00122 & 0 & 6.30e{-4} & 0 & 3.94e{-4} & 0 & 2.63e{-4} \end{bmatrix}$$

5.4 Determination of $b_{p,q}(m, n)$ (or $bmn_{p,q}$)

$b_{p,q}(m, n)$ (or $bmn_{p,q}$) for $m,n = 1,2,3$ and $p,q = 0,1,2, \ldots , 5$ are as following:

$$b11_{p,q} = \begin{bmatrix} 0 & 0 & 0 & 0 & 0 & 0 \\ 0 & 0.41015 & 0 & -0.06390 & 0 & -0.01428 \\ 0 & 0 & 0 & 0 & 0 & 0 \\ 0 & -0.06390 & 0 & 0.01134 & 0 & 0.002178 \\ 0 & 0 & 0 & 0 & 0 & 0 \\ 0 & -0.01428 & 0 & 0.002178 & 0 & 5.340\ e{-4} \end{bmatrix}$$

$$b12_{p,q} = \begin{bmatrix} 0 & 0 & 0 & 0 & 0 & 0 \\ 0 & 0 & 0.3463 & 0 & -0.07818 & 0 \\ 0 & 0 & 0 & 0 & 0 & 0 \\ 0 & 0 & -0.05256 & 0 & 0.01352 & 0 \\ 0 & 0 & 0 & 0 & 0 & 0 \\ 0 & 0 & -0.01211 & 0 & 0.002718 & 0 \end{bmatrix}$$

$$b13_{p,q} = \begin{bmatrix} 0 & 0 & 0 & 0 & 0 & 0 \\ 0 & -0.06390 & 0 & 0.3320 & 0 & -0.08338 \\ 0 & 0 & 0 & 0 & 0 & 0 \\ 0 & 0.01134 & 0 & -0.05040 & 0 & 0.01425 \\ 0 & 0 & 0 & 0 & 0 & 0 \\ 0 & 0.002178 & 0 & -0.01157 & 0 & 0.002908 \end{bmatrix}$$

$$b14_{p,q} = \begin{bmatrix} 0 & 0 & 0 & 0 & 0 & 0 \\ 0 & 0 & -0.07818 & 0 & 0.3268 & 0 \\ 0 & 0 & 0 & 0 & 0 & 0 \\ 0 & 0 & 0.01352 & 0 & -0.04965 & 0 \\ 0 & 0 & 0 & 0 & 0 & 0 \\ 0 & 0 & 0.002718 & 0 & -0.01137 & 0 \end{bmatrix}$$

$$b15_{p,q} = \begin{bmatrix} 0 & 0 & 0 & 0 & 0 & 0 \\ 0 & -0.01428 & 0 & -0.08338 & 0 & 0.3243 \\ 0 & 0 & 0 & 0 & 0 & 0 \\ 0 & 0.00218 & 0 & 0.01425 & 0 & -0.04933 \\ 0 & 0 & 0 & 0 & 0 & 0 \\ 0 & 5.4\ e\text{–}4 & 0 & 0.00291 & 0 & -0.01128 \end{bmatrix}$$

$$b21_{p,q} = \begin{bmatrix} 0 & 0 & 0 & 0 & 0 & 0 \\ 0 & 0 & 0 & 0 & 0 & 0 \\ 0 & 0.3463 & 0 & -0.05256 & 0 & -0.01211 \\ 0 & 0 & 0 & 0 & 0 & 0 \\ 0 & -0.07818 & 0 & 0.01352 & 0 & 0.002718 \\ 0 & 0 & 0 & 0 & 0 & 0 \end{bmatrix}$$

$$b22_{p,q} = \begin{bmatrix} 0 & 0 & 0 & 0 & 0 & 0 \\ 0 & 0 & 0 & 0 & 0 & 0 \\ 0 & 0 & 0.2937 & 0 & -0.06466 & 0 \\ 0 & 0 & 0 & 0 & 0 & 0 \\ 0 & 0 & -0.06466 & 0 & 0.01624 & 0 \\ 0 & 0 & 0 & 0 & 0 & 0 \end{bmatrix}$$

$$b23_{p,q} = \begin{bmatrix} 0 & 0 & 0 & 0 & 0 & 0 \\ 0 & 0 & 0 & 0 & 0 & 0 \\ 0 & -0.05256 & 0 & 0.2816 & 0 & -0.06914 \\ 0 & 0 & 0 & 0 & 0 & 0 \\ 0 & 0.01352 & 0 & -0.6194 & 0 & 0.01715 \\ 0 & 0 & 0 & 0 & 0 & 0 \end{bmatrix}$$

$$b24_{p,q} = \begin{bmatrix} 0 & 0 & 0 & 0 & 0 & 0 \\ 0 & 0 & 0 & 0 & 0 & 0 \\ 0 & 0 & -0.06466 & 0 & 0.2771 & 0 \\ 0 & 0 & 0 & 0 & 0 & 0 \\ 0 & 0 & 0.01624 & 0 & -0.061024 & 0 \\ 0 & 0 & 0 & 0 & 0 & 0 \end{bmatrix}$$

$$b25_{p,q} = \begin{bmatrix} 0 & 0 & 0 & 0 & 0 & 0 \\ 0 & 0 & 0 & 0 & 0 & 0 \\ 0 & -0.01207 & 0 & -0.06984 & 0 & 0.3126 \\ 0 & 0 & 0 & 0 & 0 & 0 \\ 0 & 0.02460 & 0 & 0.01568 & 0 & -0.06173 \\ 0 & 0 & 0 & 0 & 0 & 0 \end{bmatrix}$$

$$b31_{p,q} = \begin{bmatrix} 0 & 0 & 0 & 0 & 0 & 0 \\ 0 & -0.06373 & 0 & 0.01040 & 0 & 0.001988 \\ 0 & 0 & 0 & 0 & 0 & 0 \\ 0 & 0.3705 & 0 & -0.05134 & 0 & -0.01595 \\ 0 & 0 & 0 & 0 & 0 & 0 \\ 0 & -0.08289 & 0 & 0.01306 & 0 & 0.002629 \end{bmatrix}$$

$$b32_{p,q} = \begin{bmatrix} 0 & 0 & 0 & 0 & 0 & 0 \\ 0 & 0 & -0.05333 & 0 & 0.012390 & 0 \\ 0 & 0 & 0 & 0 & 0 & 0 \\ 0 & 0 & 0.31922 & 0 & -0.6294 & 0 \\ 0 & 0 & 0 & 0 & 0 & 0 \\ 0 & 0 & -0.06984 & 0 & 0.01568 & 0 \end{bmatrix}$$

$$b33_{p,q} = \begin{bmatrix} 0 & 0 & 0 & 0 & 0 & 0 \\ 0 & 0.01040 & 0 & -0.5134 & 0 & 0.01306 \\ 0 & 0 & 0 & 0 & 0 & 0 \\ 0 & -0.05134 & 0 & 0.3076 & 0 & -0.06721 \\ 0 & 0 & 0 & 0 & 0 & 0 \\ 0 & 0.01306 & 0 & -0.06721 & 0 & 0.01658 \end{bmatrix}$$

$$b34_{p,q} = \begin{bmatrix} 0 & 0 & 0 & 0 & 0 & 0 \\ 0 & 0 & 0.01239 & 0 & -0.05068 & 0 \\ 0 & 0 & 0 & 0 & 0 & 0 \\ 0 & 0 & -0.06294 & 0 & 0.3033 & 0 \\ 0 & 0 & 0 & 0 & 0 & 0 \\ 0 & 0 & 0.01568 & 0 & -0.06631 & 0 \end{bmatrix}$$

$$b35_{p,q} = \begin{bmatrix} 0 & 0 & 0 & 0 & 0 & 0 \\ 0 & 0.001988 & 0 & 0.01306 & 0 & -0.05038 \\ 0 & 0 & 0 & 0 & 0 & 0 \\ 0 & -0.01160 & 0 & -0.06721 & 0 & 0.3013 \\ 0 & 0 & 0 & 0 & 0 & 0 \\ 0 & 0.002629 & 0 & 0.01658 & 0 & -0.06591 \end{bmatrix}$$

$bmn_{p,q}$ should be equal to $bnm_{p,q}$ or the matrices bmn should be equal to bnm^{T}. Using these properties, we can check the computational errors. For example, from $b11_{3,1} = -0.06390$ and $b31_{1,1} = -0.06373$, we know the third digit in these values maybe not be correct.

5.5 Determination of Truncation Eigenfunction

$$X_1 = \begin{bmatrix} 4.9348-\lambda 0.41015 & 0 & \lambda 0.06390 & \cdots \\ 0 & 12.33701-\lambda 0.3463 & 0 & \cdots \\ \lambda 0.06390 & 0 & 24.67401-\lambda 0.3320 & \cdots \\ \cdots & \cdots & \cdots & \cdots \end{bmatrix}$$

$$X_2 = \begin{bmatrix} 12.33701-\lambda 0.3463 & 0 & \lambda 0.05256 & \dots \\ 0 & 19.73921-\lambda 0.3294 & 0 & \dots \\ \lambda 0.05256 & 0 & 32.07621-\lambda 0.3705 & \dots \\ \dots & \dots & \dots & \dots \end{bmatrix}$$

$$X_3 = \begin{bmatrix} 24.67401-\lambda 0.3320 & 0 & \lambda 0.05134 & \dots \\ 0 & 32.07621-\lambda 0.3705 & 0 & \dots \\ \lambda 0.05134 & 0 & 44.41322-\lambda 0.3076 & \dots \\ \dots & \dots & \dots & \dots \end{bmatrix}$$

$$x_{13} = x_{31} = \begin{bmatrix} \lambda 0.06373 & 0 & -\lambda 0.01040 & \dots \\ 0 & \lambda 0.05333 & 0 & \dots \\ -\lambda 0.01040 & 0 & \lambda 0.05134 & \dots \\ \dots & \dots & \dots & \dots \end{bmatrix}$$

If we take the first 3x3 elements of each matrices only, we have then

$|X_1| = (12.33701-\lambda 0.3463)[(4.9348-\lambda 0.41015)(24.67401-\lambda 0.3320)-\lambda^2 0.06390^2]$

$|X_2| = (19.73921-\lambda 0.3294)[(12.33701-\lambda 0.3463)(32.07621-\lambda 0.3705)-\lambda^2 0.05256^2]$

$|X_3| = (32.07621-\lambda 0.3705)[(24.67401-\lambda 0.3320)(44.41322-\lambda 0.3076)-\lambda^2 0.05134^2]$

$|x_{31}| = |x_{13}| = \lambda^3[(0.06373)(0.05333)(0.05134) - (0.0104)^2(0.05333)]$

Therefore,

$\Delta_1(\lambda) = |X_1|$

$= (12.33701-\lambda 0.3463)[(4.9348-\lambda 0.41015)(24.67401-\lambda 0.3320)-\lambda^2 0.06390^2] = 0$

and

$$\Delta_3(\lambda) = |X_1|\,|X_2|\,|X_3| - |x_{31}|\,|X_2|\,|x_{13}|$$

$$= \{(12.33701-\lambda 0.3463)[(4.9348-\lambda 0.41015)(24.67401-\lambda 0.3320)-\lambda^2 0.06390^2]-$$

$$(19.73921-\lambda 0.3294)[(12.33701-\lambda 0.3463)(32.07621-\lambda 0.3705)-\lambda^2 0.05256^2]-$$

$$(32.07621-\lambda 0.3705)[(24.67401-\lambda 0.3320)(44.41322-\lambda 0.3076)-\lambda^2 0.05134^2]\}-$$

$$\{(19.73921-\lambda 0.3294)\lambda^6[(12.33701-\lambda 0.3463)(32.07621-\lambda 0.3705)-\lambda^2 0.05265^2]$$

$$[(0.06390)(0.05333)(0.05134) - (0.0104)^2(0.05333)]^2\} = 0$$

In the first order approximation of eigenfunction $\Delta_1(\lambda)$, the value of λ_1 can be calculated approximately by the first term $(4.9348-\lambda 0.41015)$, because the value of the term $(\lambda^2 0.06373^2)$ can be neglected. It will be discussed in the following section.

5.6 Evaluation of Eigenvalue λ and Fully–Developed Nusselt Number

From the above approximation of eigenfunctions, we can evaluate the eigenvalues. Table 5.2 shows the comparison of $\lambda_1(a=1)$ for $Kn = 0.00$ with previously known values (see Appendix C). From this comparison, we know that the first eigenvalues calculated by the first term are sufficiently accurate.

Table 5.2 Comparison of $\lambda_1(a=1)$ calculated by different approximation

	Dennis et al.	First term	$\Delta_1(\lambda)$	$\Delta_3(\lambda)$
λ_1	11.91	12.030528	11.96289311	11.962888035
difference %	0	1.012	0.44410672	0.44406406

Table 5.3 gives the computational results of $\lambda_1(a)$ by the first term for different aspect ratios. Table 5.4 lists the comparison of $\lambda_1(a)$ for $Kn = 0.00$ with previously known values

Table 5.3 Eigenvalue $\lambda_1(a)$ for different aspect ratios

Kn	$\lambda_1(1)$	$\lambda_1(2/3)$	$\lambda_1(1/2)$	$\lambda_1(1/4)$	$\lambda_1(1/8)$
0	12.0305	12.6418	13.7316	17.9174	22.487
0.005	12.219	12.7896	13.873	18.0654	22.653
0.01	12.380	12.9928	14.071	18.2681	22.839
0.02	12.680	13.1959	14.266	18.4708	23.025
0.04	13.204	13.5795	14.638	18.8488	23.465
0.06	13.646	13.9631	15.011	19.2153	23.905
0.08	14.027	14.3466	15.383	19.5876	24.344
0.10	14.359	14.7302	15.755	19.9829	24.784
0.20	15.549	15.8749	17.281	20.8838	25.467
0.30	16.295	16.6361	17.618	21.7846	26.151
0.50	17.189	17.5510	18.563	22.6739	27.517

Table 5.4 Comparison of $\lambda_1(a)$ for $Kn = 0.00$ with previously known values

$\lambda_1(a)$	$\lambda_1(1)$	$\lambda_1(2/3)$	$\lambda_1(1/2)$	$\lambda_1(1/4)$	$\lambda_1(1/8)$
This work	12.0305	12.6418	13.7316	17.9174	22.487
Dennis et al.	11.91	12.49	13.57	17.76	22.38
difference%	1.01	1.21	1.19	0.89	0.48

and it shows that all of the differences are less than 1.3 percent. From this comparison, we know that the first eigenvalues calculated by the first term are sufficiently accurate for all different aspect ratios.

Table 5.5 shows the computed results of $Nu_\infty(a)$ for different aspect ratios by Eq.(5.9), and Figure 5.2 shows $Nu_\infty(a)$ as functions of *Kn*. It shows that Nusselt number Nu_∞ increase as the Knudsen number *Kn* increases and that the values of Nu_∞ increase as the aspect ratio, *a*, decreases for a fixed *Kn*.

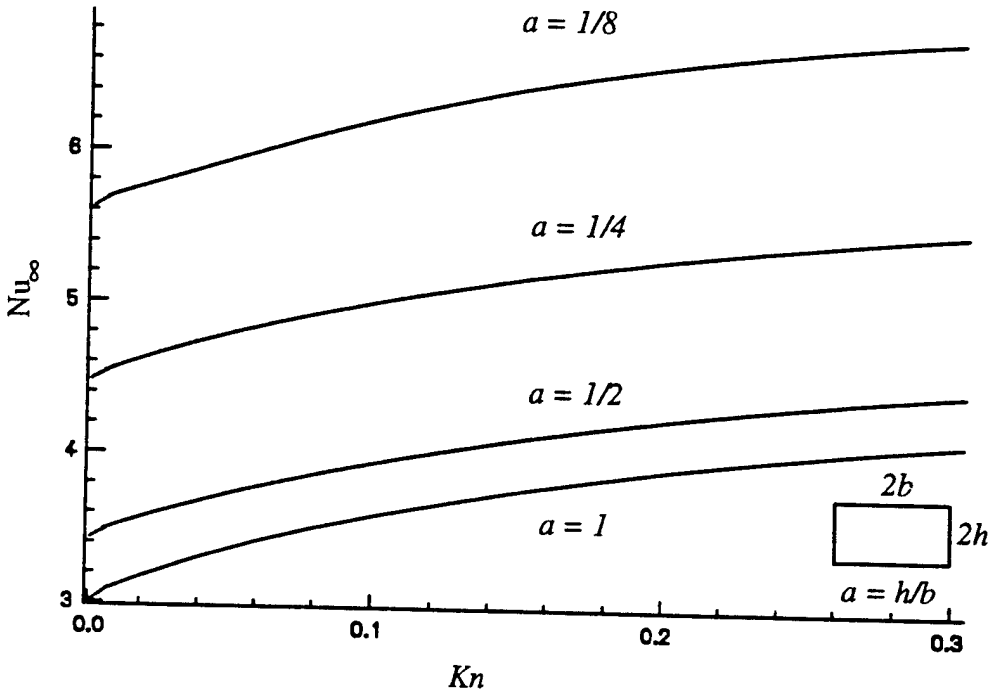

Fig. 5.2 Fully developed *Nu* as a function of *Kn* for different aspect ratio

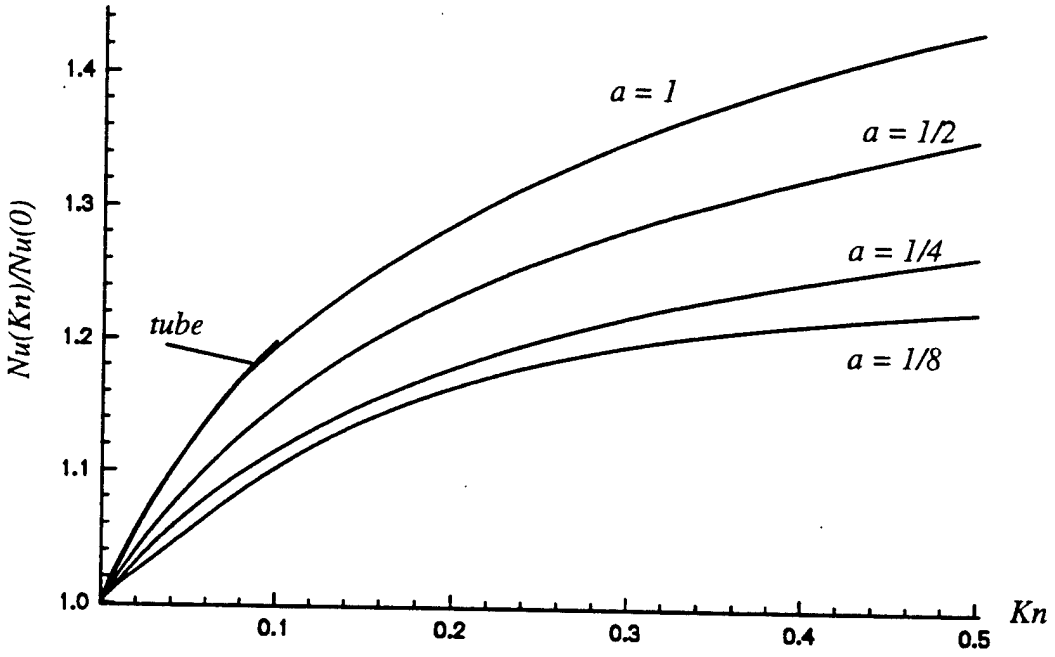

Fig. 5.3 Ratio k as a function of Kn for different aspect ratio

[$k = Nu(Kn)/Nu(0)$]

Table 5.5 $Nu_\infty(a)$ for different aspect ratios

Kn	$Nu_\infty(1)$	$Nu_\infty(2/3)$	$Nu_\infty(1/2)$	$Nu_\infty(1/4)$	$Nu_\infty(1/8)$
0	3.0076	3.1605	3.429	4.4794	5.6217
0.005	3.0548	3.1974	3.468	4.5164	5.6632
0.01	3.0950	3.2482	3.518	4.5670	5.7098
0.02	3.1700	3.2990	3.566	4.6177	5.7563
0.04	3.3010	3.3949	3.660	4.7122	5.8662
0.06	3.4115	3.4908	3.753	4.8038	5.9761
0.08	3.5068	3.5867	3.846	4.8969	6.0861
0.10	3.5898	3.6826	3.939	4.9957	6.1961
0.20	3.8873	3.9688	4.320	5.2209	6.3668
0.30	4.0736	4.1590	4.405	5.4462	6.5376
0.50	4.2970	4.3878	4.6408	5.6685	6.8792

Table 5.6 $k(a)$ for different aspect ratios

Kn	k_{tube}	$k(1)$	$k(2/3)$	$k(1/2)$	$k(1/4)$	$k(1/8)$
0	1	1	1	1	1	1
0.005	1.015	1.016	1.012	1.011	1.008	1.007
0.01	1.028	1.029	1.028	1.026	1.020	1.016
0.02	1.054	1.054	1.044	1.040	1.031	1.024
0.04	1.099	1.100	1.074	1.067	1.052	1.043
0.06	1.138	1.137	1.105	1.094	1.072	1.063
0.08	1.170	1.169	1.135	1.122	1.093	1.083
0.10	1.198	1.194	1.165	1.149	1.115	1.102
0.20	–	1.292	1.256	1.260	1.166	1.133
0.30	–	1.354	1.316	1.285	1.216	1.163
0.50	–	1.459	1.388	1.353	1.266	1.224

Note: $k = Nu_\infty(Kn)/Nu_\infty(0)$, k_c – for channel and k_{tube} – for round tube

To see the effect of the Knudsen number Kn on the Nusselt number Nu_∞ for a certain aspect ratio with respect to the case of non–slip–flow, a ratio $k = Nu_\infty(Kn)/Nu_\infty(0)$ was

introduced. Table 5.6 gives the computed results of $k(a)$ for different aspect ratios.

Figure 5.3 shows that the ratio k as a function of the Nusselt number Kn for different aspect ratios. It shows that the ratio k increases as Kn increases for all aspect ratios and that the ratio k decreases as the aspect ratio decreases for $0< Kn <0.30$. The maximum increase of k (or the Nusselt number Nu_∞) is as follows: 35.4 percent ($Kn = 0.30$) for $a = 1$; 31.6 percent for $a = 2/3$; 28.5 percent for $a = 1/2$; 21.6 percent for $a = 1/4$; and 16.3 percent for $a = 1/8$. Figure 5.4 shows the comparison of Nusselt number values with that of a round tube. The result of an aspect ratio $a = 1$ agrees with that of the round tube (the maximum difference is 0.33 percent), because the "aspect ratio" of the round tube can be regarded as around 1 while the ratio k becomes smaller with a decreasing aspect ratio.

The aspect ratio a also affects the Nusselt number Nu_∞. Fig. 5.5 shows the ratio of the Nusselt number with the aspect ratio ($a < 1$) to Nusselt number with $a = 1$, or $Nu(a)/Nu(1)$, as a function of aspect ratio a. As shown in Fig. 5.5, these ratios increase greatly as the aspect ratio a moves toward 0; however, the effects are weaked slightly with the increase of the Knudsen number Kn.

5.7 Local Heat Transfer Coefficient for the Case of a Microtube

The local heat transfer coefficient Nu_x plays an important role in determining the thermal effect of Kn in the entrance length. To depict how the local heat transfer coefficient Nu_x behaves with length, at least two eigenvalues are needed. Unfortunately, it is extremly difficult at present to obtain the second eigenvalue in the case of a microchannel. However, based on the similarity of the circular microtube and the square microchannel, the situation in the Graetz problem with slip–flow condition can be revealed by considering the microtube solution.

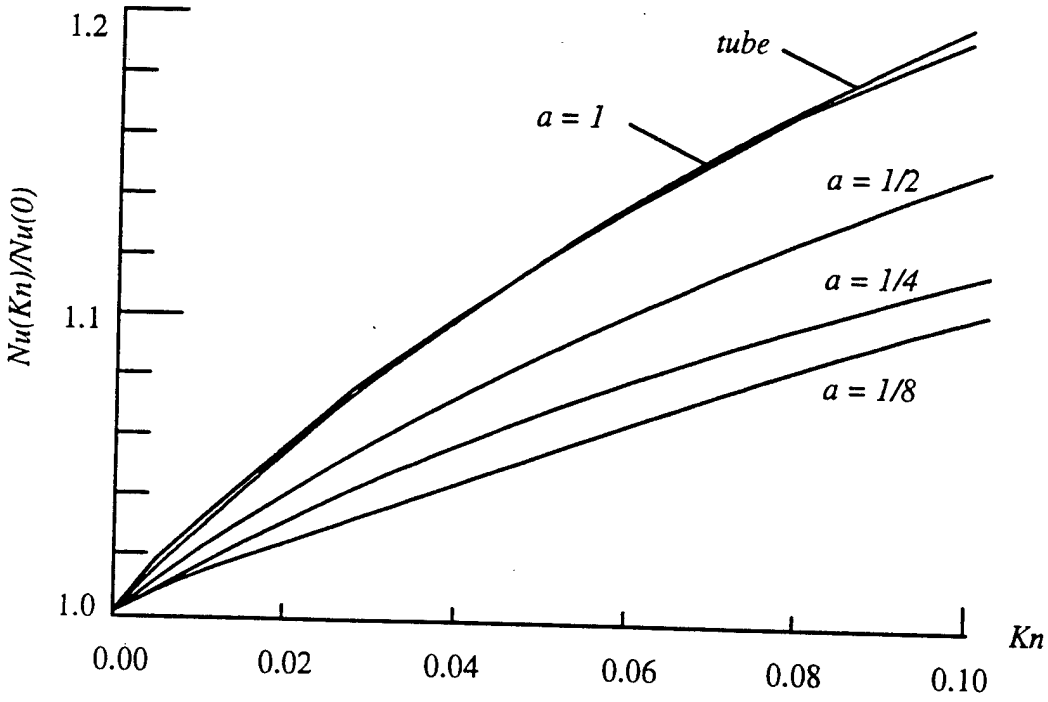

Fig. 5.4 Comparison of ratio *k* between microchannel and microtube
[*k = Nu(Kn)/Nu(0)*]

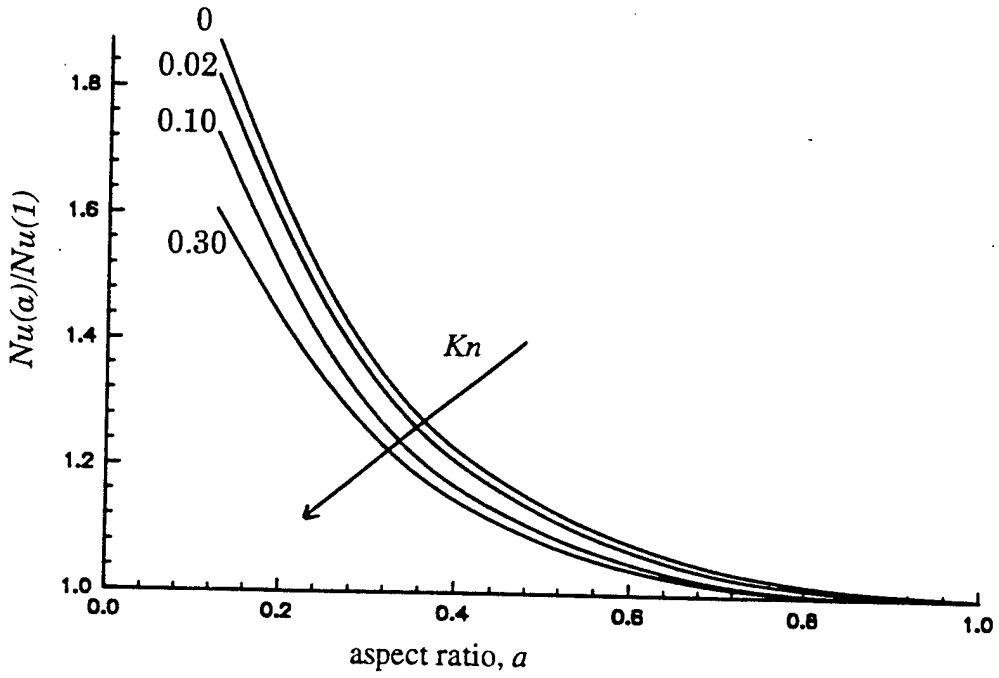

Fig. 5.5 Ratio of Nu(a)/Nu(1) as a function of aspect ratio

Figure 5.6 shows the local Nu_x value in the case of a microtube as a function of x*/Gz for $Kn = 0.02$ and with the number of eigenvalues as a parameter. The value of the local Nusselt number converges dramatically with the increase in the number of eigenvalues in the computation. When x*/Gz is 0.02, the error in Nu_x is 0.7 percent when two eigenvalues are used and, comparing to the straight line (using one eigenvalue), the error is 14 percent. It can be concluded that the results using four eigenvalues are sufficiently accurate for x*/Gz > 0.02. When x*/Gz is greater than 0.05, the error is at most 1.3 percent – that is, all three plots become nearly flat, indicating a thermally fully–developed condition.

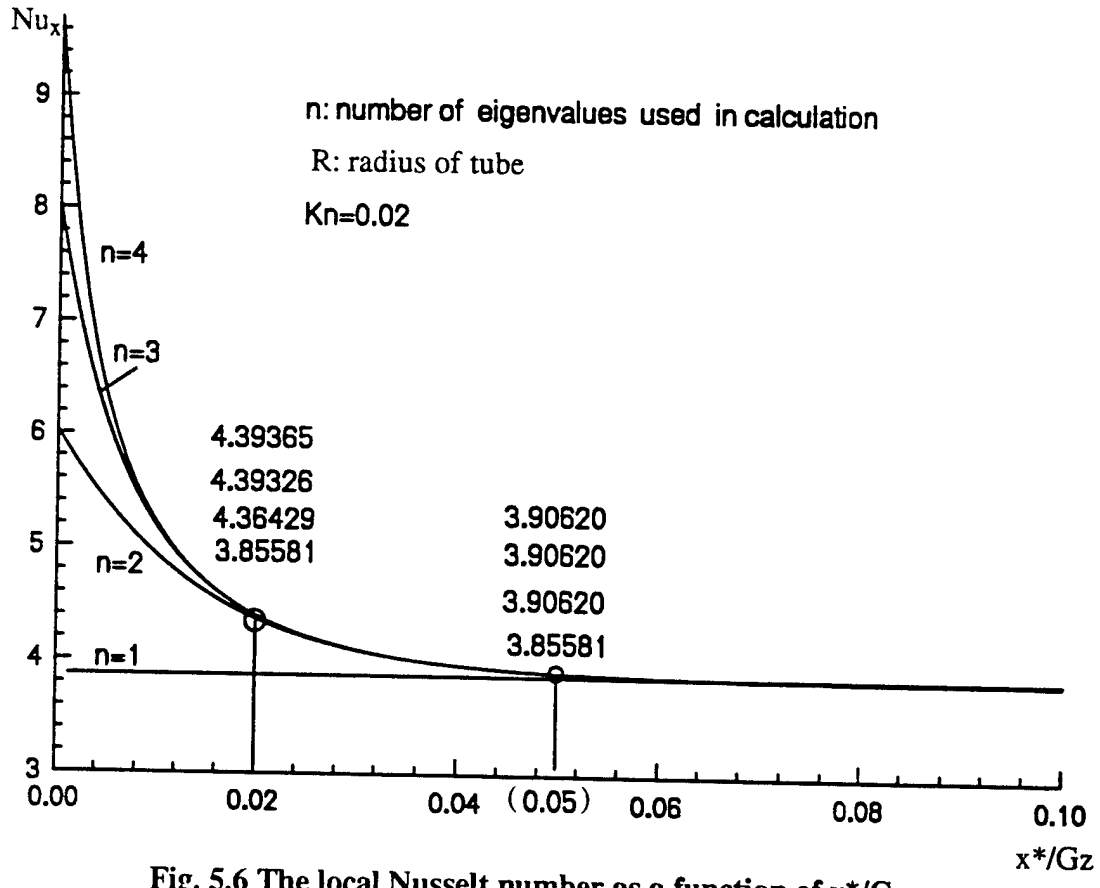

Fig. 5.6 The local Nusselt number as a function of x*/Gz

Figure 5.7 shows the local Nusselt number as a function of *Kn*. It is obvious that *Kn* has an influence on the Nusselt number. All the plots in Fig. 5.7 show that the Nusselt number increases as *Kn* increases and that this effect is magnified near the entrance. When x*/Gz is greater than 0.05, all the plots become nearly flat, indicating a thermally fully–developed condition.

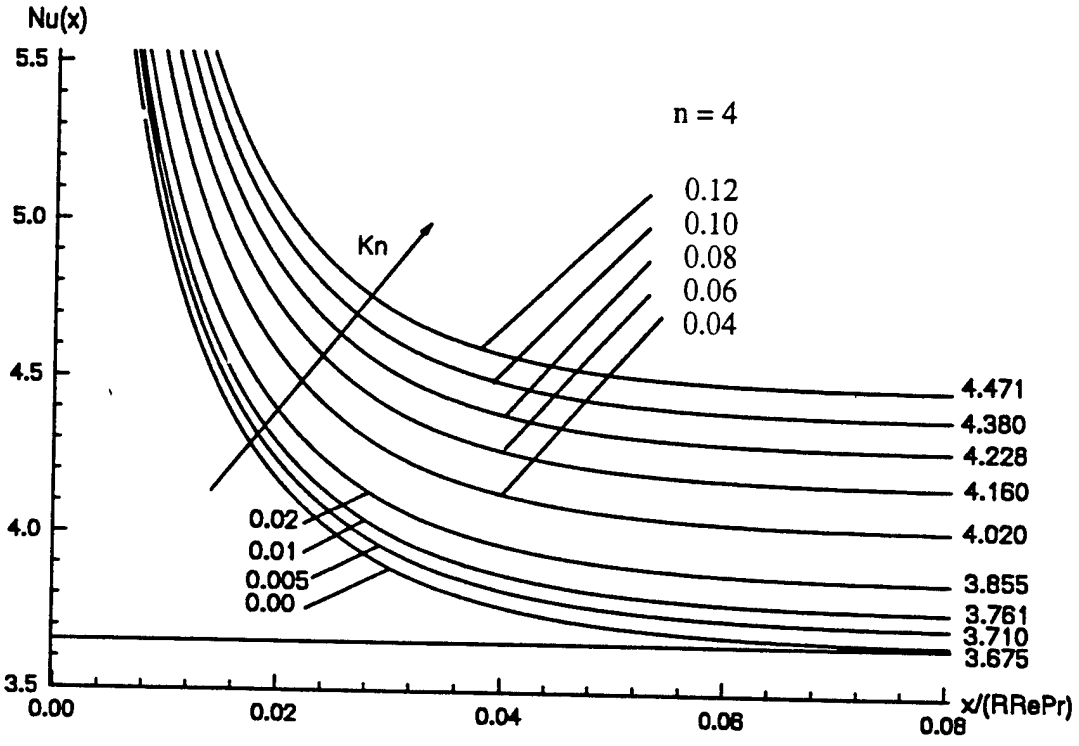

Fig. 5.7 The local Nusselt numbers as functions of x*/Gz and *Kn*

From the above discussion, we can see that:

(1) slip–flow has a positive influence on the heat transfer coefficient and can enhance the heat transfer efficiency;

(2) the influence depends on the Knudsen number and increases as *Kn* increases;

(3) when *Kn* is equal or greater than 0.02, the increase in the fully–developed Nu is greater than 5 percent so that the effect of slip–flow should be taken into

consideration in the computations of the heat transfer coefficient; and

(4) that the influence of *Kn* on Nu_∞ will decrease as *Kn* increases.

5.8 Discussion on Other Eigenvalues

In the expressions of $\Delta_p(\lambda)$, if we take X_m to be an ixi matrix, then there should exist ip eigenvalues. For example, for p = 1 and i = 1, there exists only one eigenvalue; for p = 1 and i = 3, that is $\Delta_1(\lambda)$ in the calculations, there exists three eigenvalues; and for p = 3 and i = 3, that is $\Delta_3(\lambda)$ in the calculations, there should exist nine eigenvalues rather than the five shown in Table 5.7 (four eigenvalues are missing). The calculated results are shown in Table 5.7 (see Appendix A in details). From the results in Table 5.7, it is obvious that the first eigenvalue is reliable, while the others are not reliable due to truncation error. Therefore, in this research, only first eigenvalues were evaluated.

Table 5.7 Comparison of $\lambda_n(a = 1, \mathrm{Kn} = 0.00)$ calculated by different approximation

	Dennis et al.	$\Delta_1(\lambda)$ or X_1	X_2	X_3	$\Delta_3(\lambda)$
λ_1	11.91	11.962893	–	–	11.962888
λ_2	–	35.62984	34.96576	–	35.62984
λ_3	71.07	77.06352	67.20875	71.40406	71.40407
λ_4	–	–	121.27253	113.90901	113.90902
λ_5	157.9	–	–	180.87005	121.27253

5.9 Summary

In this chapter, the procedures for the evaluation of eigenvalues for the heat transfer problem through microchannels in slip–flow were developed. The first eigenvalues and the fully–developed Nusselt number Nu_∞ were found for different aspect ratios. From the comparison and discussion, it is evident that the new technique for evaluation of the first eigenvalues and the fully–developed Nusselt numbers of the Graetz Problem through

rectangular microchannels in slip–flow is computionally effective, and the calculated Nusselt numbers are valuable to predict the heat transfer coefficients for the dimensionless length x*/Gz greater than 0.05.

CHAPTER 6

EXPERIMENTAL APPARATUS AND PROCEDURE

The purpose of this work was to determine the heat transfer coefficient and Nusselt number in the rectangular microchannel and microtube in a laminar flow region and compare the analytical results with experimental measurements. Section 6.1 details the test section with the microchannel and microtube. The flow loop and the data acquisition system are described. Section 6.2 discusses the design background for the apparatus. Section 6.3 describes the procedure used to obtain the data in the experiment. It should be noted that while an attempt was made to verify the analytical results experimentally, the data obtained from the experiments was inconclusive. It is hoped that the details of the experiments contained in the next two chapters may aid others what attempt similar experiments in slip–flow.

6.1. Experimental Apparatus

6.1.1 Test Section

The test section is the part of the experimental apparatus where the microchannel and microtube are tested. The microchannel/microtube were fabricated from 3.2 mm (0.125 in) thick 6061–T6 aluminum bar. Aluminum was chosen for its high thermal conductivity. Conventional cutting and milling processes were used to machine the aluminum pieces and channel blanks, to the final 25.4 mm x 101.6 mm (1 in x 4 in) shape. The fabrication technique was discussed in detail by Bailey (1996).

The microchannel blank configuration is shown in Figure 6.1. The macrochannel with dimensions of 117 μm x 24 μm x 63.5 mm was milled by Dr. Craig Friedrich of the Institute for Micromanufacturing. The milling machine, referred to as the Ultra Precision Milling Center, is a one–of–a–kind machine that was specially built by Dover Instrument Corporation for the Institute for Micromanufacturing at Louisiana Tech University.

The roughness of the channel was obtained by using a WYKO Roughness/Step Tester (RST) along the channel at 30 locations. The raw data are shown in Appendix D. The average roughness was shown to be 2.28 μm.

The WYKO RST was also used to determine the channel width and depth. The average top width is 120.43 μm, and the average bottom width is 112.76 μm; the average depth is 24.04 μm.

An aluminum cover was glued onto the surface of the blank with epoxy. A 70 mm long microtube (shown in Fig. 6.2) was glued into the channel having dimensions of 350 μm x 350 μm x 63.5 mm. Two pieces of lexan also were glued onto the glued aluminum parts to form the whole test section with a water jacket. Lexan was chosen based on its combination of the properties of insulation, strength, and machinability. Care was exercised to prevent the glue from entering the microchannel section.

6.1.2 Flow Loop

Figure 6.3. shows the flow loop used to conduct heat transfer experiments. It consisted of (a) a helium gas cylinder (full pressure of 2200 psi), (b) three flowmeters, (c) two metering valves, (d) a heater, (e) a test section, (f) two vacuum gages, (g) a vacuum pump, and (h) a constant temperature water bath. The test section, as shown in Fig. 6.3, consisted of a microchannel and a water jacket with two thermocouples. As shown in Fig. 6.4, two other thermocouples located at the ends of the microchannel fixed in the test fixture (Bailey, 1996) were used to measure the inlet and outlet conditions of the

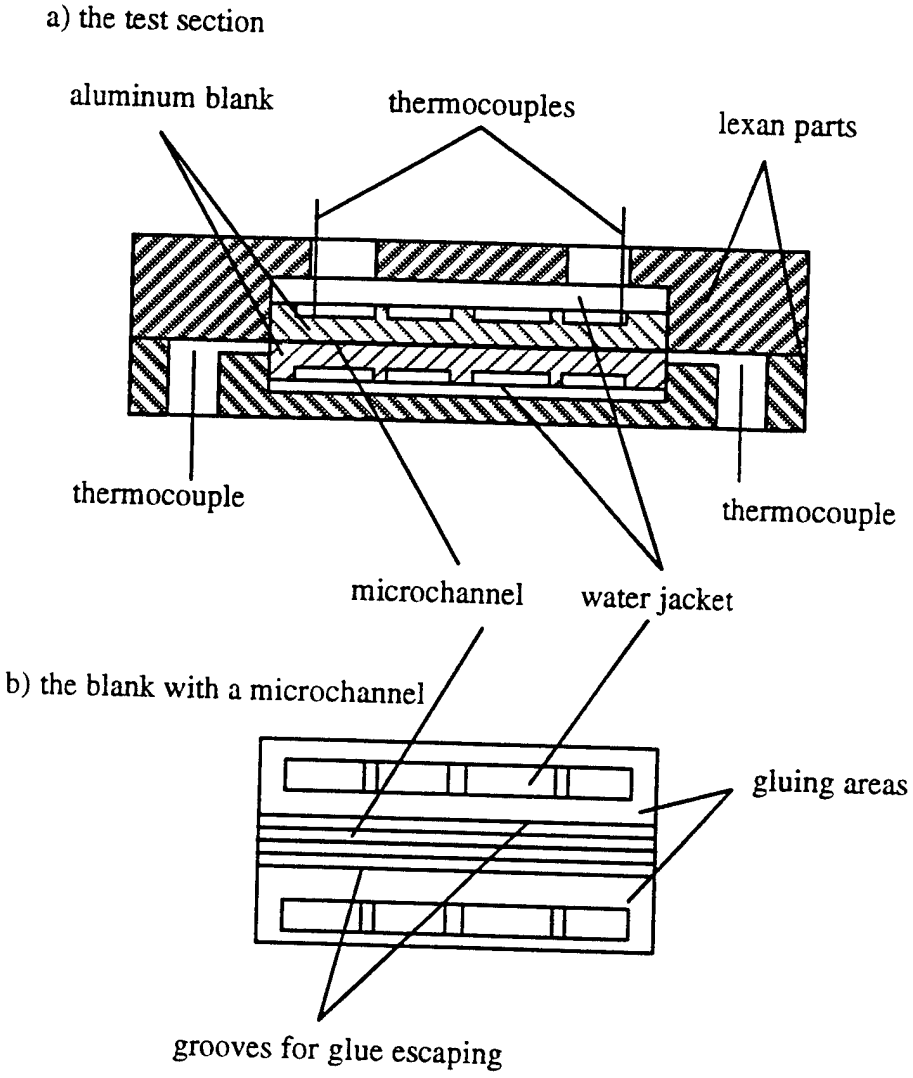

Fig. 6.1 Side cut–away view of the test section and the blank with microchannel

(117 μm x 24 μm x 63.5 mm)

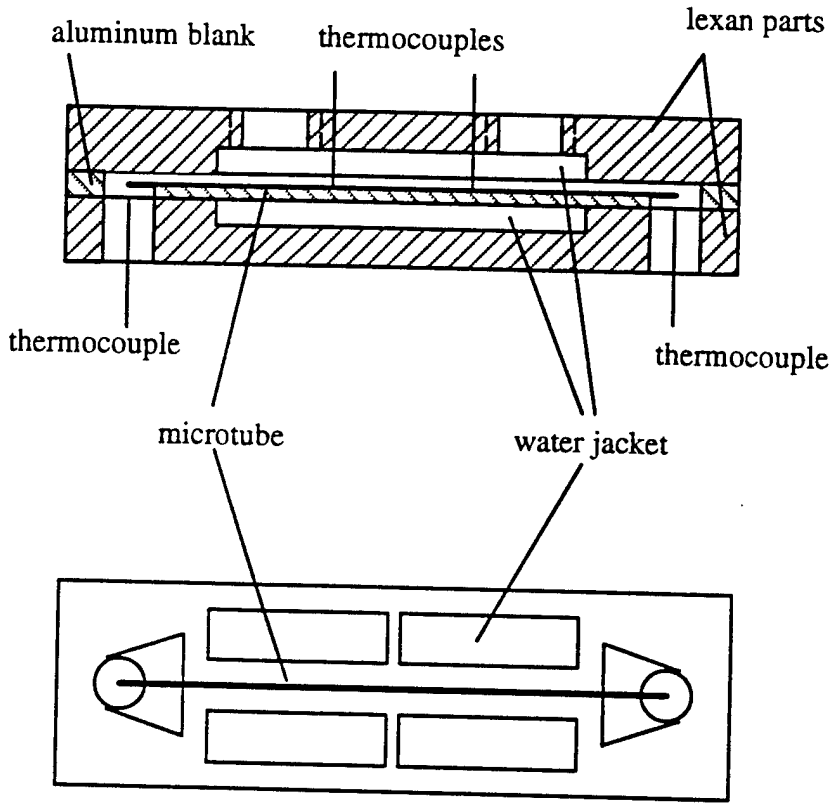

Fig. 6.2 Side cut–away view of the test section and the blank with microtube
(D_i = 52.1 μm, D_o = 350 μm, L = 70 mm)

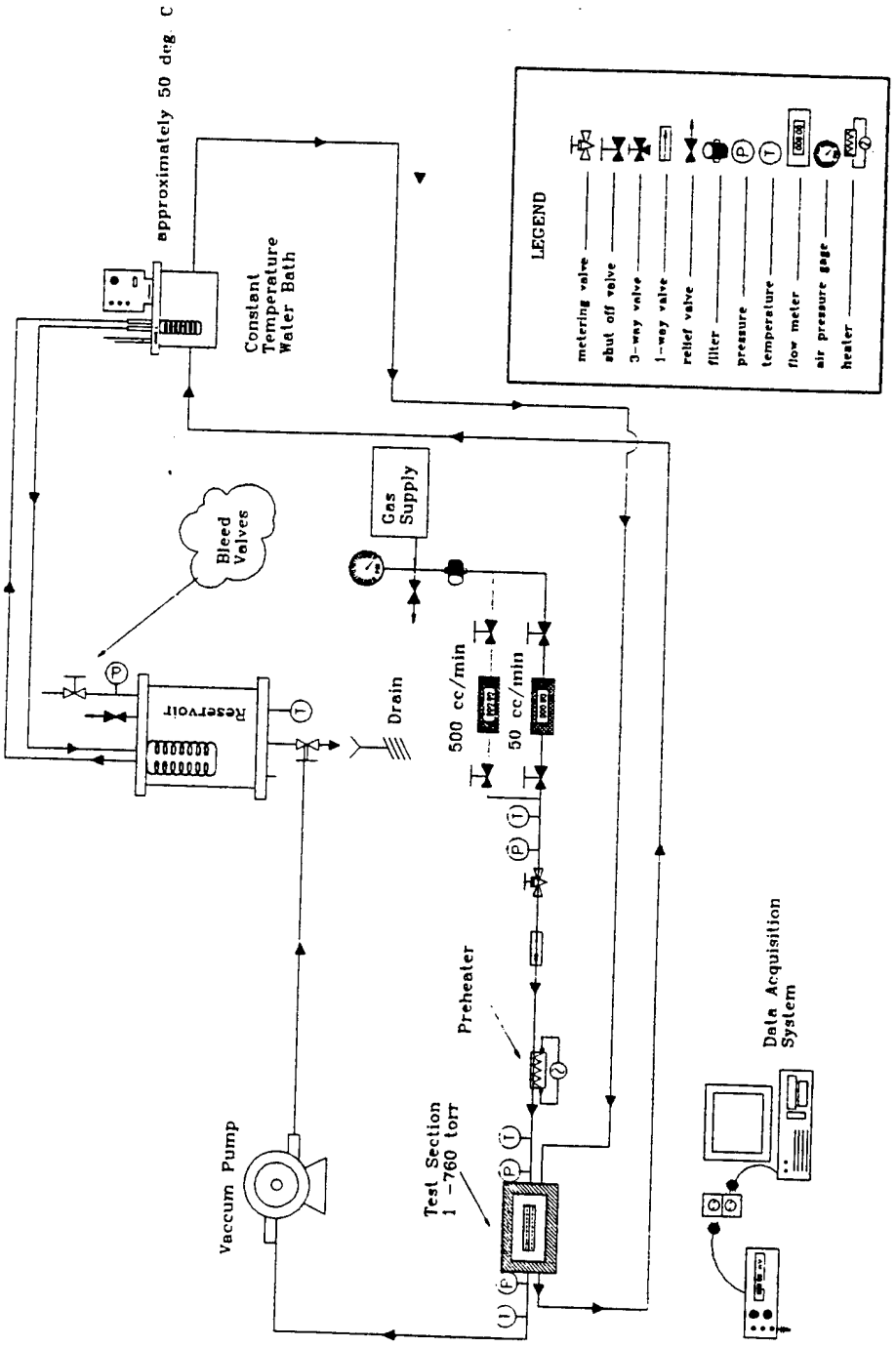

Fig. 6.3 Flow loop for micro heat transfer experiments

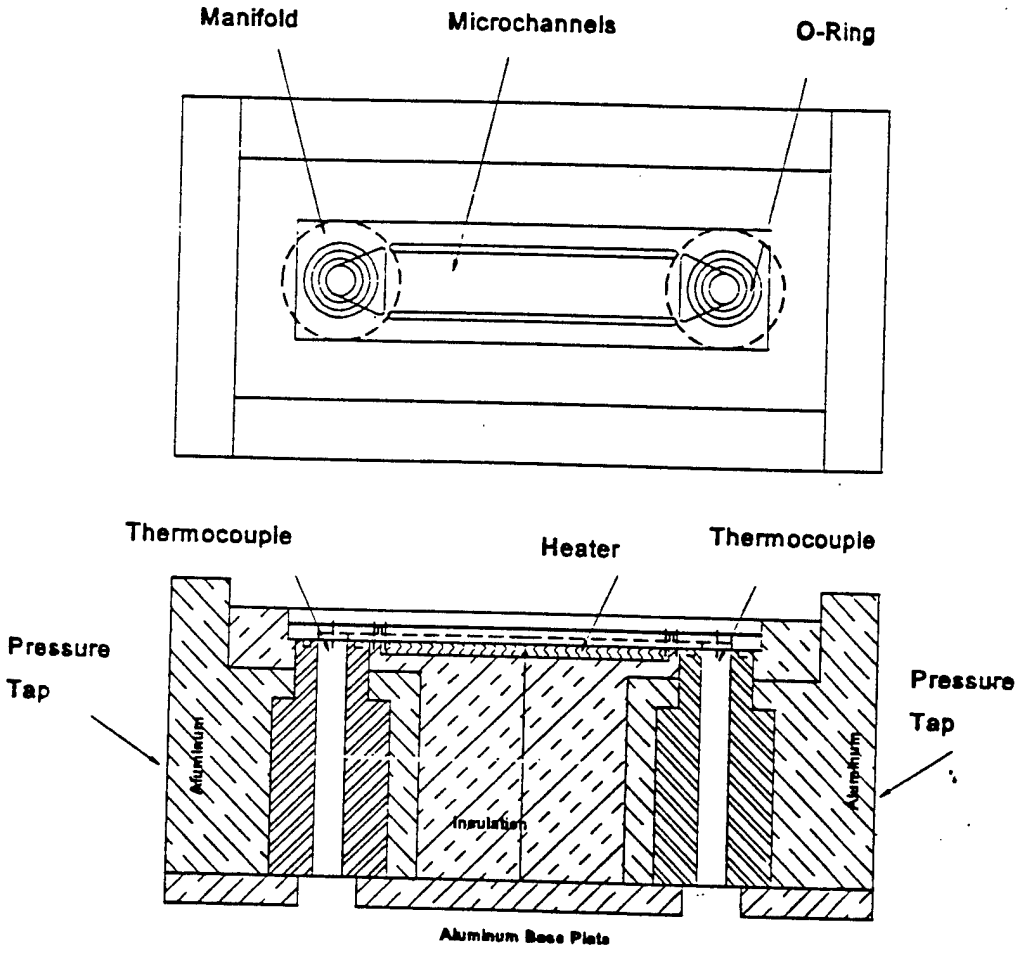

Fig. 6.4 Top view and side cut–away view of test fixture

microchannel or microtube. The reading from the thermocouple in the water jacket was used to determine the overall heat transfer coefficient.

6.1.3 Data Acquisition

The data acquisition system consisted of a Gateway 2000 personal computer equipped with a LabVIEW for Windows data acquisition system. The raw data consisted of temperature readings (°C) from the thermocouples, voltage output from the pressure transducers, and frequency from the flowmeters. Converted data are displayed on the monitor to allow the user to determine when a steady state has been reached. The raw data can be sent to an Excel spreadsheet when desired. Once in the spreadsheet, the voltage output can be converted into pressure, and the frequency output can be converted into volumetric flow rate by using the calibration curve supplied with the meters. In addition, the pressure and temperature readings at the exit of the flowmeter can be used to convert the volumetric flow rate into a mass flow rate.

6.2 Design Background

There are two restrictions that must be achieved in the experimental apparatus:

1) The flow must be in the slip–flow regime, so

$0.01 < Kn < 0.30$

2) The flow must be laminar, so

$Re < 2300$

6.2.1 Working Fluid, Sizing and Pressure

For a gas, the Knudsen number is found from:

$$Kn = \frac{\mu}{pD_H}\sqrt{\frac{\pi R_u T}{2g_c M}} \qquad (6.1)$$

Therefore, there are three factors which may be chosen to achieve slip flow:

1) Small geometry (small hydraulic diameter),

2) Low pressure, and

3) Large value of gas viscosity.

Table 6.1 shows the corresponding pressure ranges for different D_H for nitrogen and helium from Eq. (6.1). Knowing that a microchannel of 10 μm on aluminum could not be milled on the Ultra Precision Milling Center, D_H = 50 μm is chosen. Thus, for the case of the microtube, the diameter D = 50 μm, and for the case of microchannel, the dimension is 100 μm wide x 25 μm deep, D_H = 40 μm. Helium gas was chosen as the working fluid because its required pressure for a given Knudsen number is three times higher than that of nitrogen. Note that the atmospheric pressure is p_{atm} = 14.7 psia (101.3 kPa). Thus, we conclude that a vacuum must be used to achieve slip flow. Table 6.2 lists the fluid properties for two gases.

Table 6.1 Corresponding pressure for different D_H for nitrogen and helium

D_H: μm		10		50		100	
Kn		0.01	0.3	0.01	0.30	0.01	0.30
p (psia)	N_2	9.7	0.32	1.94	0.064	0.97	0.032
	He	29.1	0.96	5.82	0.190	2.91	0.096

Table 6.2 Properties of nitrogen and helium gases

	g_c kg–m/N–s^2	μ kg/m s	M g/mol	R_u J/mol–K	T K
N_2	1	1.784×10^{-5}	28.95	8.3144	300
He	1	1.987×10^{-5}	4.003	8.3144	300

6.2.2 Flow Rate

To assure the gas flow in the slip flow condition, we let $p_1 = 5.82$ psia (300 torr) and $p_2 = 0.19$ psia (9.79 torr) or less. Thus, we assume that flow in such a condition (rarefied gas) should be treated as a compressible flow. Consequently, the estimation of pressure drop, Reynolds number, and flow rate become complicated problems.

The exit pressure and inlet pressure are related by (Shapiro,1953):

$$\frac{p_2}{p_1} = \frac{(p/p^*)_2}{(p/p^*)_1} \tag{6.2}$$

where

$$\frac{p}{p^*} = \frac{1}{M}\sqrt{\frac{\gamma + 1}{2[1 + (\gamma-1)M^2/2]}} \tag{6.3}$$

for helium gas $\gamma = 1.667$. Although the flow can be treated as choked flow, that is, $M_2 = 1$, M_1 must be known for the estimation of inlet pressure, while the determination of M_1 (or the velocity of the fluid at the inlet) depends on the inlet pressure and outlet pressure. Also, the Reynolds number is a function of pressure and may increase at most ten times of that at STP (standard temperature and pressure, 300 °K and 101.325 kPa or 1 atm) (White,1991).

The rough estimation of the Reynolds number is carried by using the formulas for incompressible flow. The maximum mass flow rate to achieve laminar flow may be found as follows:

$$\mathrm{Re} = \frac{D\,G}{\mu} = 2300$$

$$G = \frac{m}{A_c} = \frac{(2300)(0.01987)(10^{-3})}{(50)(10^{-6})} = 914.0 \text{ kg/s-m}^2$$

$$m = (914.0)(\pi/4)(50 \times 10^{-6})^2 = 1.795 \times 10^{-6} \text{ kg/s}$$

The corresponding volumetric flow rate at STP is:

$$\dot{v} = \frac{m}{\varrho_o} = \frac{(1.795)(10^{-6})}{(0.1625)} = 11.04 \times 10^{-6} \text{ m}^3/\text{s}$$

$$\dot{v} = 11.04 \text{ cm}^3/\text{s} = 662.6 \text{ cm}^3/\text{min. at STP}$$

This is the maximum flow rate for the slip flow condition, corresponding to a Reynolds number of 2300. If the flow rate is reduced to 10 cm^3/min. at STP, which is the minimum flow rate for the flowmeter in the lab in the Institute for Micromanufacturing, the corresponding Reynolds number is:

$$Re = (2300)(10/662.4) = 34.7$$

Even ten times this value (347) is much less than 2300, the value of Reynolds number for laminar flow. Thus, laminar flow should be assured with the design parameters. Taking the experiment conducted by Yu (1994) as a reference ($D_i = 52.1$ μm, nitrogen, $p_1 = 42.64$ psia, flow rate = 9.81 ml/min, Re = 255.91), the flow rate maybe higher than 10 ml/min. Therefore, the experiments should be carried out without technical problems.

6.3 Experimental Procedure

The test gas was supplied from an industrial helium gas cylinder and the pressure of the test gas was reduced down to the proper pressure (about 100 psia) by the coarse valve. The pressure and the flow rate were controlled precisely by the fine metering valve.

Before entering the test component, the gas was heated to the desired temperature range by a heater strip with a length of 400 mm wrapped around the stainless steel tube. The input power was controlled by a temperature controller. In the test section, water was circulated on the outside of the microchannel by a recirculating pump in the constant

temperature water bath.

The experimental procedures in the experiments were as follows:

1) Pump the test section including the steel pipes connected to the flow meter over 40 hours to check gas leakage and water leakage.

2) Run the acquisition system half an hour.

3) Control the metering valve to desired flow rate.

4) Take the data when the flow reaches steady–state. It took about 20 minutes for stabilization.

6.4 Data Reduction

6.4.1 Data Reduction of the Microchannel

For the heat transfer test, the heat transfer coefficient of the inside channel is derived by the following procedures. From the energy balance of the control volume as shown in Figure 6.5, we have

$$-h\frac{A_w}{L}\,dx\,(T-T_w) = \dot{m}\,C_p\,dT \qquad (6.4)$$

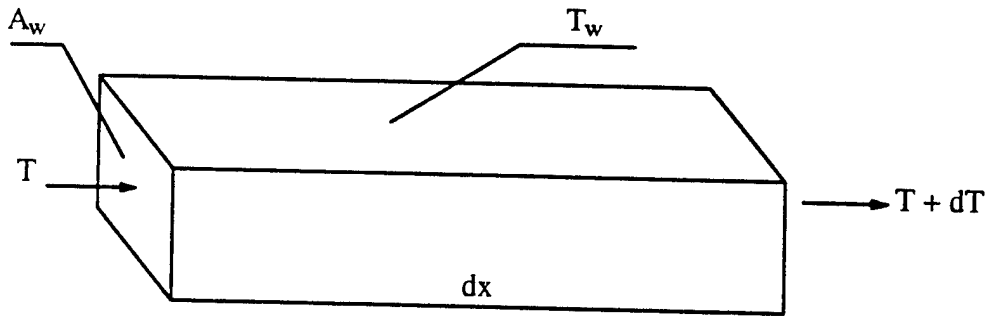

Fig.6.5 Control volume of heat transfer in microchannel

Integrating Eq. (6.4) over the entire length of the channel yields

$$-\frac{hA_w}{\dot{m}\,C_p}\int_0^L \frac{dx}{L} = \int_{T_1-T_{w2}}^{T_2-T_{w2}} \frac{dT}{T-T_{w2}} \tag{6.5}$$

resulting in

$$\frac{T_2-T_{w2}}{T_1-T_{w2}} = \exp\left(-\frac{hA_w}{\dot{m}\,C_p}\right) \tag{6.6}$$

The wall temperature was considered constant along the microchannel so that the heat transfer coefficient h was estimated by Eq. (6.6) and the Nusselt number by Eq. (6.7)

$$Nu = \frac{DG_v\varrho C_p}{A_w k}\ln\left(\frac{T_2-T_{w2}}{T_1-T_{w2}}\right) \tag{6.7}$$

Fluid properties were evaluated at the mean bulk temperature of the fluid. The Reynolds number is evaluated as follows:

$$Re = G_v\frac{4}{\pi D\nu} \tag{6.8}$$

6.4.2 Data Reduction of the Microtube

In the case of the microtube, because the tube is made of polymide (low thermal conductivity), the wall temperature will change along the microtube, decreasing from T_{w1} to T_{w2} so that the average temperature difference is over–estimated by Eq. (6.6). Traditionally, a correction factor is used to correct the error, where F is a function of parameters $F(T_1, T_2, T_{w1}, T_{w2})$ and the function is readily available from Holman (1986).

The heat transfer process in the tube involves a combination of convection and conduction. The overall heat transfer is expressed in terms of an overall heat transfer coefficient U as:

$$Q = U A_w \Delta T$$

where U is dependent on the definition of ΔT. If $\Delta T = T_{fluid} - T_w$, the h is given by

$$\frac{1}{U\pi D_i} = \frac{1}{h_i \pi D_i} + \frac{\ln(\frac{D_o}{D_i})}{2\pi k_t} + \frac{\ln(\frac{D_c}{D_o})}{2\pi k_c} \qquad (6.9)$$

Once U (= h) is evaluated from Eq. (6.6), h_i can be calculated from the above equation. Fluid properties were evaluated at the mean bulk temperature of the fluid.

CHAPTER 7

EXPERIMENTAL RESULTS

In this chapter, the experimental results involving the microchannel and the microtube are discussed. It was noted that there was a significant discrepancy between the Nusselt number measured experimentally and the Nusselt number calculated from the analytical model involving slip–flow. The fact that the gas temperature did not increase from inlet to outlet as heat was added to the flow passage indicated that there was some problem in measurement of the gas temperature at the exit. Upon examination of the thermocouple location at the flow passage exit, it was noted that the thermocouple position was not at the centerline of the flow channel; therefore, the indicated temperature was not the gas exit temperature, in all likelihood. It is possible (but not probable) that micro–specific mechanisms caused the results of the experimental study to deviate significantly from the analytical model.

7.1. Heat Transfer with Microchannel

In this experiment, inlet and outlet pressures, flow rate, and inlet and outlet fluid temperatures were measured. These readings were used to determine the heat transfer coefficient of the microchannel with a certain Knudsen number. It was found that the temperature drop of the flow media depended on the flow rate, as shown in Table 7.1.

In Figure 7.1, Nusselt number was plotted as a function of Reynolds number, Re.

From this experiment, one can observe:

1) Constant wall temperature. As shown in Table 7.1, the temperature differences of wall are less than 0.2°C; it is reasonable to regard the condition as an isothermal wall.

Table 7.1 Experiment with microchannel

G_v ml/min	T_{inlet} °C	T_{outlet} °C	T_{w1} °C	T_{w2} °C	Nu	Re
343.3	29.90	37.47	78.41	78.56	80.96	720
300.9	29.62	33.56	74.89	74.96	43.18	618
246.7	29.84	32.15	69.83	69.88	20.43	507
198.6	29.77	31.69	74.81	74.89	11.78	408
173.3	29.42	30.54	70.65	70.69	6.59	356
149.2	29.31	30.12	72.13	72.22	3.59	307
125.9	29.21	29.67	71.07	71.12	1.76	259
101.8	29.11	29.18	68.69	68.74	0.11	208
*47.3	29.33	28.79	70.65	70.71	0.52	97

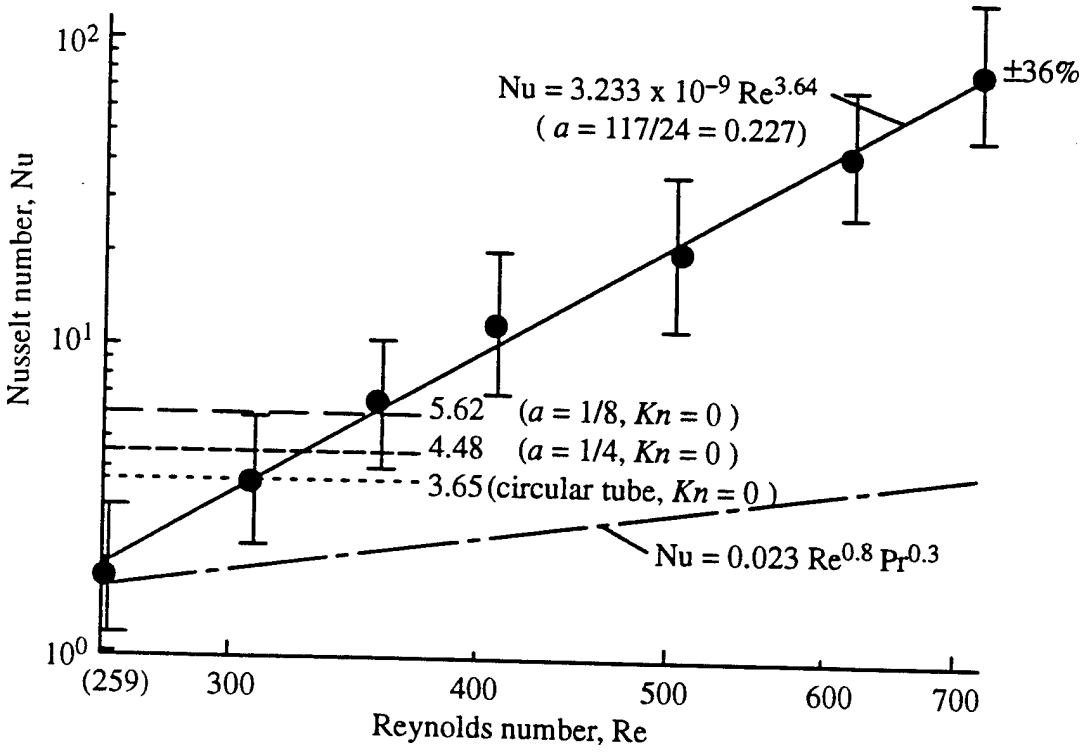

Fig. 7.1 Nusselt number as a function of Reynolds number
(microchannel of 117 μm x 24 μm x 63.5 mm)

In Figure 7.1, Nusselt number was plotted as a function of Reynolds number, Re. From this experiment, one can observe:

1) Constant wall temperature. As shown in Table 7.1, the temperature differences of the wall are less than 0.2°C; it is reasonable to regard the condition as an isothermal wall.

2) Microchannel flow. Fig. 7.1 shows that Nusselt numbers were much larger than those of the empirical formula (Dittus et al. 1930) for laminar flow if the flow rate is greater than 200 ml/min (Re > 400). It is obvious that the flow condition cannot be explained simply by slip–flow or even turbulent flow. For the case of laminar with Kn = 0.00 and a = 1/4, Nu = 4.48; when a = 1/8, Nu = 5.62 ; and, even in slip–flow with Kn = 0.30 and a = 1/8, Nu = 6.54. Therefore, there is likely a different mechanism in a flow through a microchannel/microtube to explain such a large discrepancy. It will be discussed in detail later in the next section of this chapter.

3) Non–heating–up–phenomenon. The experimentally measured gas temperature at the outlet was higher than the inlet gas temperature when the flow rate was relatively large (343.3 ml/min., for example). As the gas flow rate was decreased to a value less than 125 ml/min., the gas temperature difference became quite small. In fact, a negative temperature increase (i.e., a temperature decrease) was indicated when the flow rate was less than 47.3 ml/min. This phenomenon was not anticipated.

Upon examination of the test apparatus, it was noted that the thermocouple at the flow channel exit was not positioned exactly along the centerline of the flow channel. As the gas exited the test flow channel, instead of impinging directly on the thermocouple, the gas mixed with the gas already within the plenum chamber at the flow passage exit. The thermocouple indicated the gas temperature in the exit plenum instead of indicating the exit gas temperature.

This thermocouple measurement error is the most probable source of the so–called "non–heating–up" phenomenon observed in the experiments. For high flow rates, the gas in the plenum chamber was rapidly replaced by gas exiting the flow passage; therefore, the thermocouple indication was more nearly that of the exit gas temperature. On the other hand, at low flow rates, the warm gas exiting from the flow passage mixed with the much larger volume of colder gas already in the plenum chamber. As a result, the gas mixture temperature (measured by the thermocouple) was significantly lower than the gas exit temperature.

It is also possible that there was some leakage along the length of the microchannel, although gas leakage would not result in a decrease of the gas temperature while the gas was being heated.

7.2. Heat Transfer with Microtube

In this experiment, the flow rate was carefully controlled to 0.1 ml/min in an attempt to keep the inlet pressure in the vacuum regime. After twenty minutes, the data were measured with the inlet pressure 737 torr (14.3 psia) and outlet pressure 5 torr (0.097 psia); the gas temperature in the pipe far away from the test section was 25°C. The results are shown in Table 7.2.

Table 7.2 Experiment with microtube

Run no.	G_v ml/min	T_{inlet} °C	T_{outlet} °C	T_{w1} °C	T_{w2} °C	Nu	Re
1	0.11	29.50	25.11	88.41	82.56		0.27
2	0.11	30.05	25.58	91.35	85.43		0.27
3	0.11	30.28	25.87	89.50	84.12		0.27
4	0.11	30.29	25.92	87.73	82.93	0.015	0.27

From Table 7.2, one can observe that:

1) Non–constant wall temperature. It is obvious that constant wall temperature condition cannot be achieved by the current designed apparatus. The temperature difference between the inlet wall temperature T_{w1} and the outlet wall temperature T_{w2} (approximately) is about 6 °C. It is due to that the microtube wall being made of polymite (k = 0.155 W/m–K) rather than aluminum (k = 204 W/m–K). Therefore, it cannot be regarded as an isothermal wall.

2) Non–heating–up–phenomenon. The experimental results shows that the inlet gas temperature T_{inlet} is higher than the outlet gas temperature T_{outlet} by about 4.5°C, which was not the anticipated situation. This phenomenon happened also in the experiment with the microchannel when the flow rate was 47.3 ml/min.

One explanation is that the Joule–Thomson effect caused by the expansion of the gas at the outlet may result in a cooling effect to such an extent that the outlet gas temperature T_{outlet} is of a smaller value. The expansion of a real gas from a high to a lower pressure in an isenthalpic (constant–enthalpy) process will result in a temperature change, which may be either positive or negative, depending on the pressure and temperature and type of gas. For helium gas expanding from T_1 = 300 K = 26.8°C to an exit pressure of 1 atm, we find the following values (Table 7.3) for the exit temperature, using $h_1 = h_2$ (Mann, 1962). Note that the temperature increases during the Joule–Thomson expansion for helium gas. We may conclude that any decrease in temperature of the helium gas could not be caused by the Joule–Thomson expansion effect. Any Joule–Thomson effect for helium gas around the ambient temperature would result in a warming effect or an increase in temperature. Unless the inlet pressure is greater than about 30 atm (440 psia), the temperature change is small (less than 2°C or 4°F).

Table 7.3 Temperature change vs. pressure for helium gas

PRESSURE, p_1			EXIT TEMPERATURE, T_2			$(T_2 - T_1)$	
atm	psia	kPa	K	°F	°C	°C	°F
4	58.8	405	300.2	80.6	27.0	0.2	0.4
6	88.2	608	300.3	80.8	27.1	0.3	0.5
8	117.6	811	300.4	81.0	27.2	0.4	0.7
10	147.0	1013	300.6	81.3	27.4	0.6	1.1
20	294.0	2027	301.2	82.4	28.0	1.2	2.2
50	735.0	5066	303.2	86.0	30.0	3.2	5.8

Other explanations are as follows:

Wang et al. (1994) pointed out, based on their experiments:

> Microscale heat transfer and transport phenomena are expected to be quite different from those in customary situation. . . .
>
> (1) For single–phase liquid forced convection through microchannel, a fully developed heat transfer regime is initiated at about Re = 1000–1500. The transition to turbulent mode is influenced by liquid temperature, velocity and micro size. . . .
>
> (2) T*ransition and laminar heat transfer in microchannels are highly strange and complicated* [italics added], compared with the conventionally sized situation. The range of transition zone, and heat transfer characteristics of both transition and laminar flow are highly affected by liquid temperature, velocity and micro size.

Yu (1994) pointed out in his dissertation:

> One may ask the reason and significance of the shifting. It is well known now that the process of convective heat transfer depends on flow field. The relative rates of diffusion of heat and momentum are related by the Prandtl number. In the micro tube experiments, it has been shown that flow resistance was reduced both in laminar and turbulent flow. As it is well known, if the velocity profile follows a parabolic curve, then the friction factor f times the Reynolds number should be 64. But in various micro tube experiments, the number is around 50. As discussed before in Section 1, *it cannot be caused by a slip boundary condition. This*

> *manifests that there are some alterations in velocity profile, and this in turn will affect convective heat transfer* [italics added]. Similarly, flow resistance reduction is also found in turbulent flow. **All of these will lead one to expect that heat transfer in micro tubes will behave differently both in laminar and turbulent flow [bolds added].**

Also Bailey et al. (1995) pointed out:

> Several effects and conditions can exist in micro–scale convection that are normally neglected when considering macro–scale flow. . . . Another observed micro–scale effect is that of *large temperature variations of the transport fluid* [italics added] (Wang and Peng, 1994). This can cause a significant variation in fluid properties throughout a micro–system, invalidating the often used assumption of constant properties. . . . As of yet, it is not completely clear when these factors come into play as fluid convection systems are reduced in size. At present, there are not enough experimental data to make this determination. Additionally, **there are likely more micro–specific effects and conditions that have yet to be observed [bolds added].**

The experimental results for the heat transfer in the microtube and the microchannel were different in this study. In both the microchannel and the microtube, the Reynolds number was significantly less than 2000; therefore, the flow pattern was completely within the laminar flow regime. Although it is possible that unrecognized micro–specific phenomena could be responsible for the unusual experimental results, it is more probable that the placement error of the thermocouple at the flow channel exit caused the unanticipated experimental results at the very low flow rates.

The fact that the dimension of the flow passages and the thermocouple bead were the same order of magnitude could also contribute to the thermocouple measurement error. Because of these uncertainties, the experimental data obtained in this research are likely to be of little value in assessing the validity of the analytical solutions.

7.3 Uncertainty Analysis for the Experimental Data

Along with statistical analysis, uncertainly analysis mainly concerns uncertainty in the final results because of uncertainties in the primary measurements. The method presented by Kline and McClintock (1953) was used in this research. If the final result R is a function of several independent variables, $x_1, x_2, \ldots, x_n$,

$$R = R(x_1, x_2, \ldots, x_n),$$

then the uncertainty of R associated with the uncertainties in measuring the primary variables is:

$$U_R = [(\frac{\partial R}{\partial x_1}U_1)^2 + (\frac{\partial R}{\partial x_2}U_2)^2 + \ldots + (\frac{\partial R}{\partial x_n}U_n)^2]^{1/2}$$

or

$$\frac{U_R}{R} = [(\frac{U_1}{x_1})^2 + (\frac{U_2}{x_2})^2 + \ldots + (\frac{U_n}{x_n})^2]^{1/2}$$

From the manufacturers' data, the measuring uncertainties for each independent variable are:

$U_D/D = 0.0025$, $U_L/L = 0.001$, $U_{Gv}/G_v = 0.0128$

$U_P/P = 0.0025$, $U_T = 0.4$ °C, $U_c/c_P = U_\varrho/\varrho = U_\nu/\nu = U_k/k = 0.005$

(1) uncertainty in the Reynolds number

$$\frac{U_{Re}}{Re} = [(\frac{U_{Gv}}{G_v})^2 + (\frac{U_D}{D})^2 + (\frac{U_\nu}{\nu})^2]^{1/2}$$

and $U_{Re}/Re = 1.4\%$.

(2) uncertainty in dimensionless temperature

$$\frac{U_\theta}{\theta} = \sqrt{2}\ \left(\frac{U_T}{\Delta T}\right)\ [1 + (\frac{1}{\theta})^2]^{1/2}$$

$U_\theta/\theta = 1.45\%$ for the case of microtube; $U_\theta/\theta = 2.13\%$ for the case of a microchannel with $G_v = 343.3$ ml/min and $U_\theta/\theta = 1.92\%$ with $G_v = 149.2$ ml/min

(2) uncertainty in the Nusselt number

$$\frac{U_{Nu}}{Nu} = [(\frac{U_{Gv}}{G_v})^2 + (\frac{U_D}{D})^2 + (\frac{U_k}{k})^2 + (\frac{U_c}{c_p})^2 + (\frac{U_\varrho}{\varrho})^2 + (\frac{U_\theta}{\theta \ln \theta})^2]^{1/2}$$

$U_{Nu}/Nu = 18.3\%$ for the case of a microtube; $U_{Nu}/Nu = 36.0\%$ for the case of a microchannel with $G_v = 343.3$ ml/min and $U_{Nu}/Nu = 14.9\%$ with $G_v = 149.2$ ml/min.

CHAPTER 8

CONCLUSIONS AND RECOMMENDATIONS

8.1 Conclusions

In the previous chapters, the mathematical models of velocity distribution and temperature distribution were established, and the expression for the series solution shows the importance of the eigenvalues. Since those eigenvalues were extremely difficult to evaluate directly from the original expansion, a concise matrix was derived based on the properties of the elements in the original matrix. A truncated eigenfunction was obtained which can be used to evaluate the eigenvalues. The procedures were developed and some results were obtained. Also, the heat transfer experiments were conducted with a single microchannel and with a microtube. From the discussions of analytical and experimental results, the following conclusions can be drawn:

1) The technique for evaluation of the eigenvalues of the heat transfer problem in slip–flow is computationally effective in the evaluation of the first eigenvalues;

2) The Nusselt number increases as *Kn* increases, or the heat transfer is enhanced under slip–flow conditions for a given aspect ratio;

3) When *Kn* is equal to or greater than 0.02, the increase in Nu_∞ is greater than 5 percent so that the effect of slip flow conditions should be taken into consideration in the computations of the heat transfer coefficient;

4) The experiments were of no value in assessing the validity of the analytical solutions in this research.

8.2 Recommendations for Future Study

Considering the results such as the non–heating–up–phenomenon occurring in the heat transfer experiment with a microchannel/microtube may be caused totally by measurement errors due to the small flow rate and the fact that both the dimensions of the microtube to be measured and that of the t–c bead are of the same dimension level, it is suggested that further experiments which may result in acceptable data be conducted. The suggested changes to the experiment include the following:

1) A microchannel machined in the aluminum should be used to reach an approximate isothermal wall condition. The wall made of a material with high heat conductivity can easily maintain a small temperature difference between the inlet and the outlet, better approximating the isothermal boundary condition.

2) A much shorter microchannel or several parallel microchannels should be employed to increase the flow rate for a reasonable pressure drop.

3) A hot gas that is cooled by a surrounding cold water jacked should be used rather than the reverse situation. A high temperature is desired at the inlet in order to produce a relatively large *Kn*.

For the analytical solution, the evaluation of the eigenvalues is very important for the solution of the heat transfer problem through microchannels in slip–flow. Although the technique is effective for the first values, it is extremely time–consuming and the computational error is a problem for other eignevalues. It is suggested that new codes be developed on a supercomputer to solve the extremely large matrices to obtain more eigenvalues more effectively so that the thermal entrance effect in the rectangular microchannels can be established.

APPENDIX A

CALCULATION OF EIGENVALUE λ FOR Kn = 0.00

WITH ASPECT RATIO $a = 1$

Calculation of Eigenvalue λ for Kn = 0.00 with Aspect Ratio *a* = 1 10/27/95

l1 = β = (1+a)/2 and l2 = β' = (1+1/a)/2

$l1 := 1 \quad l2 := 1 \quad a := 1$

$i := 0,1..10 \quad j := 0,1..10$

$$R0 := -\frac{8}{\pi^4}\cdot\sum_{k=1}^{3}\frac{1}{(2\cdot k-1)^4}\cdot\left[1-\frac{2}{(2\cdot k-1)\cdot\pi}\cdot\tanh\left[\frac{(2\cdot k-1)\cdot\pi}{2}\right]\right]$$

$$R(x,y) := -\frac{4}{\pi^3}\cdot\sum_{k=1}^{8}\frac{1}{(2\cdot k-1)^3}\cdot\sin\left[(2\cdot k-1)\cdot\pi\cdot\frac{y}{a}\right]\cdot\left[1-\frac{\cosh\left[\frac{(2\cdot k-1)\cdot\pi\cdot(x-0.5)}{a}\right]}{\cosh\left[\frac{(2\cdot k-1)\cdot\pi}{2}\right]}\right]$$

Calculating time is about 30 minutes for i = j = 10

$$d_{i,j} := \int_0^{l1}\int_0^{l2}\frac{R(x,y)}{R0}\cdot\cos\left(i\cdot\pi\cdot\frac{x}{l1}\right)\cdot\cos\left(j\cdot\pi\cdot\frac{y}{l2}\right)dy\,dx$$

uncompiled

$$d = \begin{bmatrix}
1.00147 & 0 & -0.27819 & 0 & -0.08309 & 0 & -0.03854 & 0 & -0.02209 & 0 & -0.01431 \\
0 & 0 & 0 & 0 & 0 & 0 & 0 & 0 & 0 & 0 & 0 \\
-0.27809 & 0 & 0.08285 & 0 & 0.02237 & 0 & 0.00979 & 0 & 0.00542 & 0 & 0.00343 \\
0 & 0 & 0 & 0 & 0 & 0 & 0 & 0 & 0 & 0 & 0 \\
-0.08299 & 0 & 0.02237 & 0 & 0.00725 & 0 & 0.00338 & 0 & 0.00192 & 0 & 0.00122 \\
0 & 0 & 0 & 0 & 0 & 0 & 0 & 0 & 0 & 0 & 0 \\
-0.03844 & 0 & 0.00979 & 0 & 0.00338 & 0 & 0.00167 & 0 & 9.73085\cdot10^{-4} & 0 & 6.30798\cdot10^{-4} \\
0 & 0 & 0 & 0 & 0 & 0 & 0 & 0 & 0 & 0 & 0 \\
-0.02198 & 0 & 0.00542 & 0 & 0.00191 & 0 & 9.72637\cdot10^{-4} & 0 & 5.81959\cdot10^{-4} & 0 & 3.83988\cdot10^{-4} \\
0 & 0 & 0 & 0 & 0 & 0 & 0 & 0 & 0 & 0 & 0 \\
-0.01418 & 0 & 0.00343 & 0 & 0.00122 & 0 & 6.29649\cdot10^{-4} & 0 & 3.93537\cdot10^{-4} & 0 & 2.62711\cdot10^{-4}
\end{bmatrix}$$

$m = 0 \quad n = 0$

$p = 0,1..5 \quad q = 0,1..5 \quad b_{6,0} = 0 \quad b_{7,0} = 0 \quad b_{8,0} = 0$

$$b_{p,q} = \frac{1}{4}\cdot\left(d_{|m-p|,|n-q|} - d_{|m-p|,n-q} + d_{m-p,n-q} - d_{m-p,|n-q|}\right)$$

$$b = \begin{bmatrix} 0 & 0 & 0 & 0 & 0 & 0 \\ 0 & 0 & 0 & 0 & 0 & 0 \\ 0 & 0 & 0 & 0 & 0 & 0 \\ 0 & 0 & 0 & 0 & 0 & 0 \\ 0 & 0 & 0 & 0 & 0 & 0 \\ 0 & 0 & 0 & 0 & 0 & 0 \\ 0 & 0 & 0 & 0 & 0 & 0 \\ 0 & 0 & 0 & 0 & 0 & 0 \\ 0 & 0 & 0 & 0 & 0 & 0 \end{bmatrix} \qquad b00 = \begin{bmatrix} 0 & 0 & 0 & 0 & 0 & 0 \\ 0 & 0 & 0 & 0 & 0 & 0 \\ 0 & 0 & 0 & 0 & 0 & 0 \\ 0 & 0 & 0 & 0 & 0 & 0 \\ 0 & 0 & 0 & 0 & 0 & 0 \\ 0 & 0 & 0 & 0 & 0 & 0 \\ 0 & 0 & 0 & 0 & 0 & 0 \\ 0 & 0 & 0 & 0 & 0 & 0 \\ 0 & 0 & 0 & 0 & 0 & 0 \end{bmatrix}$$

$m = 1 \quad n = 1$

$p = 0,1..5 \quad q = 0,1..5$

$$b_{p,q} = \frac{1}{4}\cdot\left(d_{|m-p|,|n-q|} - d_{|m-p|,n-q} + d_{m-p,n-q} - d_{m-p,|n-q|}\right)$$

$$b = \begin{bmatrix} 0 & 0 & 0 & 0 & 0 & 0 \\ 0 & 0.41015 & 0 & -0.063895 & 0 & -0.0142825 \\ 0 & 0 & 0 & 0 & 0 & 0 \\ 0 & -0.063895 & 0 & 0.01134 & 0 & 0.0021775 \\ 0 & 0 & 0 & 0 & 0 & 0 \\ 0 & -0.0142825 & 0 & 0.0021775 & 0 & 5.4\cdot 10^{-4} \\ 0 & 0 & 0 & 0 & 0 & 0 \\ 0 & 0 & 0 & 0 & 0 & 0 \\ 0 & 0 & 0 & 0 & 0 & 0 \end{bmatrix} \qquad b11 = \begin{bmatrix} 0 & 0 & 0 & 0 & 0 & 0 \\ 0 & 0.41015 & 0 & -0.063895 & 0 & -0.0142825 \\ 0 & 0 & 0 & 0 & 0 & 0 \\ 0 & -0.063895 & 0 & 0.01134 & 0 & 0.0021775 \\ 0 & 0 & 0 & 0 & 0 & 0 \\ 0 & -0.0142825 & 0 & 0.0021775 & 0 & 5.4\cdot 10^{-4} \\ 0 & 0 & 0 & 0 & 0 & 0 \\ 0 & 0 & 0 & 0 & 0 & 0 \\ 0 & 0 & 0 & 0 & 0 & 0 \end{bmatrix}$$

$$b12 = \begin{bmatrix} 0 & 0 & 0 & 0 & 0 & 0 \\ 0 & 0 & 0.346255 & 0 & -0.0781775 & 0 \\ 0 & 0 & 0 & 0 & 0 & 0 \\ 0 & 0 & -0.052555 & 0 & 0.0135175 & 0 \\ 0 & 0 & 0 & 0 & 0 & 0 \\ 0 & 0 & -0.012105 & 0 & 0.0027175 & 0 \\ 0 & 0 & 0 & 0 & 0 & 0 \\ 0 & 0 & 0 & 0 & 0 & 0 \\ 0 & 0 & 0 & 0 & 0 & 0 \end{bmatrix}$$

$$b13 = \begin{bmatrix} 0 & 0 & 0 & 0 & 0 & 0 \\ 0 & -0.063895 & 0 & 0.3319725 & 0 & -0.0833825 \\ 0 & 0 & 0 & 0 & 0 & 0 \\ 0 & 0.01134 & 0 & -0.0503775 & 0 & 0.014245 \\ 0 & 0 & 0 & 0 & 0 & 0 \\ 0 & 0.0021775 & 0 & -0.011565 & 0 & 0.0029083 \\ 0 & 0 & 0 & 0 & 0 & 0 \\ 0 & 0 & 0 & 0 & 0 & 0 \\ 0 & 0 & 0 & 0 & 0 & 0 \end{bmatrix}$$

$$b14 = \begin{bmatrix} 0 & 0 & 0 & 0 & 0 & 0 \\ 0 & 0 & -0.0781775 & 0 & 0.3267675 & 0 \\ 0 & 0 & 0 & 0 & 0 & 0 \\ 0 & 0 & 0.0135175 & 0 & -0.04965 & 0 \\ 0 & 0 & 0 & 0 & 0 & 0 \\ 0 & 0 & 0.0027175 & 0 & -0.0113742 & 0 \\ 0 & 0 & 0 & 0 & 0 & 0 \\ 0 & 0 & 0 & 0 & 0 & 0 \\ 0 & 0 & 0 & 0 & 0 & 0 \end{bmatrix}$$

$$b15 = \begin{bmatrix} 0 & 0 & 0 & 0 & 0 & 0 \\ 0 & -0.0142825 & 0 & -0.0833825 & 0 & 0.324325 \\ 0 & 0 & 0 & 0 & 0 & 0 \\ 0 & 0.0021775 & 0 & 0.014245 & 0 & -0.0493275 \\ 0 & 0 & 0 & 0 & 0 & 0 \\ 0 & 5.4\cdot10^{-4} & 0 & 0.0029083 & 0 & -0.0112848 \\ 0 & 0 & 0 & 0 & 0 & 0 \\ 0 & 0 & 0 & 0 & 0 & 0 \\ 0 & 0 & 0 & 0 & 0 & 0 \end{bmatrix}$$

$$b21 = \begin{bmatrix} 0 & 0 & 0 & 0 & 0 & 0 \\ 0 & 0 & 0 & 0 & 0 & 0 \\ 0 & 0.346255 & 0 & -0.052555 & 0 & -0.012105 \\ 0 & 0 & 0 & 0 & 0 & 0 \\ 0 & -0.0781775 & 0 & 0.0135175 & 0 & 0.0027175 \\ 0 & 0 & 0 & 0 & 0 & 0 \\ 0 & 0 & 0 & 0 & 0 & 0 \\ 0 & 0 & 0 & 0 & 0 & 0 \\ 0 & 0 & 0 & 0 & 0 & 0 \end{bmatrix}$$

$$b22 = \begin{bmatrix} 0 & 0 & 0 & 0 & 0 & 0 \\ 0 & 0 & 0 & 0 & 0 & 0 \\ 0 & 0 & 0.2937 & 0 & -0.06466 & 0 \\ 0 & 0 & 0 & 0 & 0 & 0 \\ 0 & 0 & -0.06466 & 0 & 0.016235 & 0 \\ 0 & 0 & 0 & 0 & 0 & 0 \\ 0 & 0 & 0 & 0 & 0 & 0 \\ 0 & 0 & 0 & 0 & 0 & 0 \\ 0 & 0 & 0 & 0 & 0 & 0 \end{bmatrix}$$

$$b23 = \begin{bmatrix} 0 & 0 & 0 & 0 & 0 & 0 \\ 0 & 0 & 0 & 0 & 0 & 0 \\ 0 & -0.053331 & 0 & 0.319167 & 0 & -0.0698377 \\ 0 & 0 & 0 & 0 & 0 & 0 \\ 0 & 0.0123898 & 0 & -0.0629381 & 0 & 0.0156838 \\ 0 & 0 & 0 & 0 & 0 & 0 \\ 0 & 0 & 0 & 0 & 0 & 0 \\ 0 & 0 & 0 & 0 & 0 & 0 \\ 0 & 0 & 0 & 0 & 0 & 0 \end{bmatrix}$$

$$b24 = \begin{bmatrix} 0 & 0 & 0 & 0 & 0 & 0 \\ 0 & 0 & 0 & 0 & 0 & 0 \\ 0 & 0 & -0.06466 & 0 & 0.2771175 & 0 \\ 0 & 0 & 0 & 0 & 0 & 0 \\ 0 & 0 & 0.016235 & 0 & -0.0610242 & 0 \\ 0 & 0 & 0 & 0 & 0 & 0 \\ 0 & 0 & 0 & 0 & 0 & 0 \\ 0 & 0 & 0 & 0 & 0 & 0 \\ 0 & 0 & 0 & 0 & 0 & 0 \end{bmatrix}$$

$$b25 = \begin{bmatrix} 0 & 0 & 0 & 0 & 0 & 0 \\ 0 & 0 & 0 & 0 & 0 & 0 \\ 0 & -0.012105 & 0 & -0.0691375 & 0 & 0.2749975 \\ 0 & 0 & 0 & 0 & 0 & 0 \\ 0 & 0.0027175 & 0 & 0.0171533 & 0 & -0.0606123 \\ 0 & 0 & 0 & 0 & 0 & 0 \\ 0 & 0 & 0 & 0 & 0 & 0 \\ 0 & 0 & 0 & 0 & 0 & 0 \\ 0 & 0 & 0 & 0 & 0 & 0 \end{bmatrix}$$

$$b31 = \begin{bmatrix} 0 & 0 & 0 & 0 & 0 & 0 \\ 0 & -0.063895 & 0 & 0.01134 & 0 & 0.0021775 \\ 0 & 0 & 0 & 0 & 0 & 0 \\ 0 & 0.3319725 & 0 & -0.0503775 & 0 & -0.011565 \\ 0 & 0 & 0 & 0 & 0 & 0 \\ 0 & -0.083385 & 0 & 0.0142425 & 0 & 0.0029107 \\ 0 & 0 & 0 & 0 & 0 & 0 \\ 0 & 0 & 0 & 0 & 0 & 0 \\ 0 & 0 & 0 & 0 & 0 & 0 \end{bmatrix}$$

$$b32 = \begin{bmatrix} 0 & 0 & 0 & 0 & 0 & 0 \\ 0 & 0 & -0.052555 & 0 & 0.0135175 & 0 \\ 0 & 0 & 0 & 0 & 0 & 0 \\ 0 & 0 & 0.281595 & 0 & -0.0619425 & 0 \\ 0 & 0 & 0 & 0 & 0 & 0 \\ 0 & 0 & -0.0691425 & 0 & 0.0171532 & 0 \\ 0 & 0 & 0 & 0 & 0 & 0 \\ 0 & 0 & 0 & 0 & 0 & 0 \\ 0 & 0 & 0 & 0 & 0 & 0 \end{bmatrix}$$

$$b33 = \begin{bmatrix} 0 & 0 & 0 & 0 & 0 & 0 \\ 0 & 0.0104014 & 0 & -0.051343 & 0 & 0.0130546 \\ 0 & 0 & 0 & 0 & 0 & 0 \\ 0 & -0.0513426 & 0 & 0.3075718 & 0 & -0.0672085 \\ 0 & 0 & 0 & 0 & 0 & 0 \\ 0 & 0.0130546 & 0 & -0.0672105 & 0 & 0.0165824 \\ 0 & 0 & 0 & 0 & 0 & 0 \\ 0 & 0 & 0 & 0 & 0 & 0 \\ 0 & 0 & 0 & 0 & 0 & 0 \end{bmatrix}$$

$$b34 = \begin{bmatrix} 0 & 0 & 0 & 0 & 0 & 0 \\ 0 & 0.01134 & 0 & -0.0503775 & 0 & 0.014245 \\ 0 & 0 & 0 & 0 & 0 & 0 \\ 0 & -0.0503775 & 0 & 0.27003 & 0 & -0.0662292 \\ 0 & 0 & 0 & 0 & 0 & 0 \\ 0 & 0.0142425 & 0 & -0.0662318 & 0 & 0.018148 \\ 0 & 0 & 0 & 0 & 0 & 0 \\ 0 & 0 & 0 & 0 & 0 & 0 \\ 0 & 0 & 0 & 0 & 0 & 0 \end{bmatrix}$$

$$b35 = \begin{bmatrix} 0 & 0 & 0 & 0 & 0 & 0 \\ 0 & 0.0021775 & 0 & 0.014245 & 0 & -0.0493275 \\ 0 & 0 & 0 & 0 & 0 & 0 \\ 0 & -0.011565 & 0 & -0.0662292 & 0 & 0.2637127 \\ 0 & 0 & 0 & 0 & 0 & 0 \\ 0 & 0.0029107 & 0 & 0.018148 & 0 & -0.064789 \\ 0 & 0 & 0 & 0 & 0 & 0 \\ 0 & 0 & 0 & 0 & 0 & 0 \\ 0 & 0 & 0 & 0 & 0 & 0 \end{bmatrix}$$

Comparison of different approximation used in evaluation of eigenvalue

$\lambda := 11, 11.1 .. 80$

$X1(\lambda) := (4.9348 - \lambda \cdot 0.41015) \cdot (12.33701 - \lambda \cdot .346255) \cdot (24.67401 - \lambda \cdot .331973) \cdot (1) -$

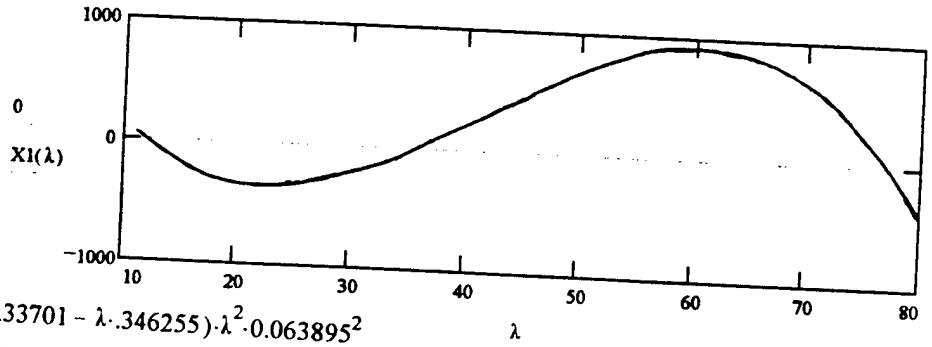

$- (12.33701 - \lambda \cdot .346255) \cdot \lambda^2 \cdot 0.063895^2$

$\lambda := 10$

$\text{root}(X1(\lambda), \lambda) = 11.96289$ $\qquad \frac{4.9348}{0.41015} = 12.0317$

$\lambda := 40$

$\text{root}(X1(\lambda), \lambda) = 35.62984$ $\qquad \frac{12.33701}{0.346255} = 35.62984$

$\lambda := 70$

$\text{root}(X1(\lambda), \lambda) = 77.06352$ $\qquad \frac{19.73921}{0.2937} = 67.20875$

$\lambda := 30, 30.1 .. 130$

$X2(\lambda) := (19.73921 - \lambda \cdot 0.2937) \cdot (12.33701 - \lambda \cdot 0.346255) \cdot (32.07621 - \lambda \cdot 0.281595) -$

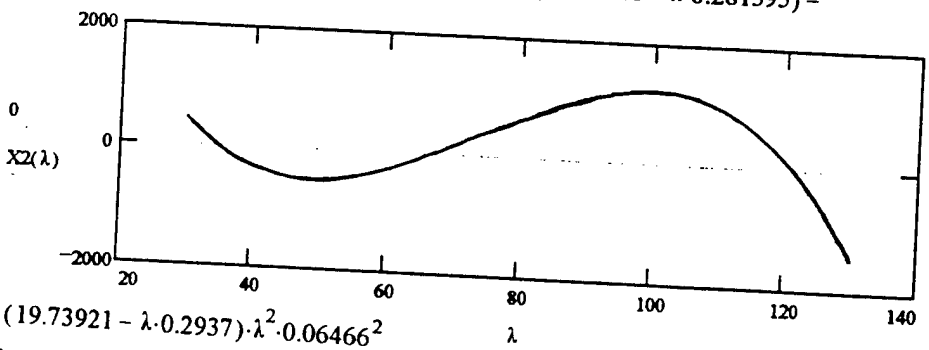

$- (19.73921 - \lambda \cdot 0.2937) \cdot \lambda^2 \cdot 0.06466^2$

$\lambda := 10$

$\text{root}(X2(\lambda), \lambda) = 34.96576$ $\qquad \frac{12.33701}{0.346255} = 35.62984$

$\lambda := 70$

$\text{root}(X2(\lambda), \lambda) = 67.20875$ $\qquad \frac{19.73921}{0.2937} = 67.20875$

$\lambda := 120$

$\text{root}(X2(\lambda), \lambda) = 121.27253$ $\qquad \frac{32.07621}{0.281595} = 113.90902$

$\lambda := 70, 70.05 .. 190$

$X3(\lambda) := (24.674 - \lambda \cdot 0.331973) \cdot (32.07621 - \lambda \cdot 0.281595) \cdot (44.41322 - \lambda \cdot 0.270)$

$- (32.07621 - \lambda \cdot 0.281595) \cdot \lambda^2 \cdot 0.0691425^2$

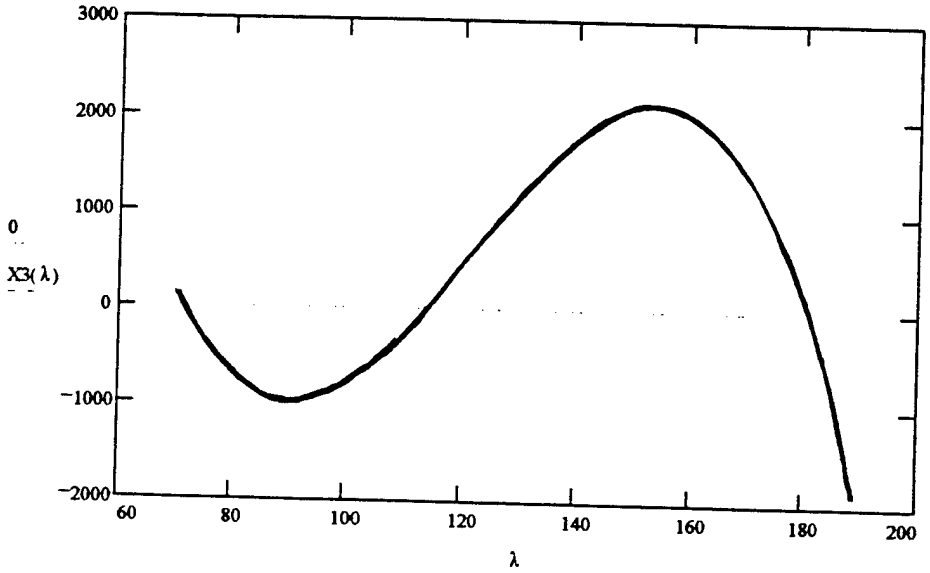

$\lambda := 70$

$root(X3(\lambda), \lambda) = 71.40406$ $\qquad \frac{24.67401}{0.331973} = 74.32535$

$\lambda := 110$

$root(X3(\lambda), \lambda) = 113.90901$ $\qquad \frac{32.07621}{0.281595} = 113.90902$

$\lambda := 180$

$root(X3(\lambda), \lambda) = 180.87005$ $\qquad \frac{44.41322}{0.27003} = 164.47513$

$\lambda := 11, 11.05 .. 125$

$$x(\lambda) := \lambda^3 \cdot 0.063895 \cdot 0.0503775 \cdot 0.00291065925 - \lambda^3 \cdot 0.083385 \cdot 0.0503775 \cdot 0.0021775$$

$$X123(\lambda) := X1(\lambda) \cdot X2(\lambda) \cdot X3(\lambda) - X2(\lambda) \cdot x(\lambda)^2$$

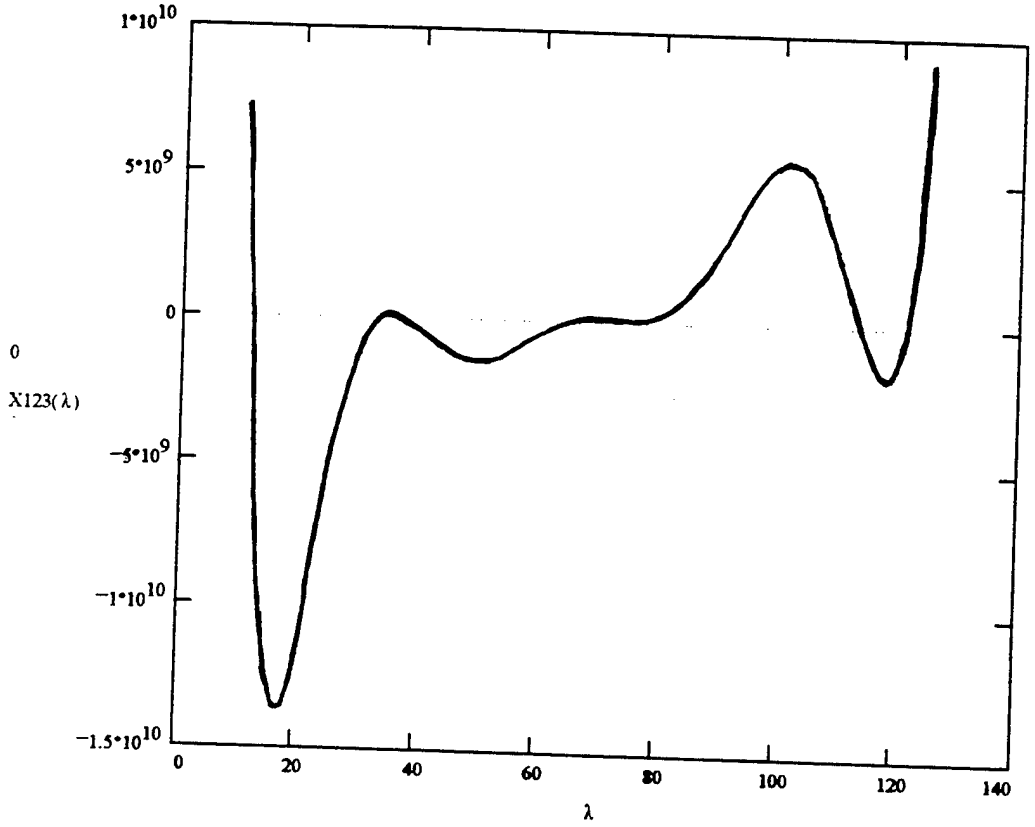

$\lambda := 10$

root(X123(λ), λ) = 11.96288801491174

$\lambda := 40$

root(X123(λ), λ) = 35.62984

$\lambda := 70$

root(X123(λ), λ) = 71.40407

$\lambda := 110$

root(X123(λ), λ) = 113.90902

$\lambda := 165$

root(X123(λ), λ) = 121.27253

a = h/b aspect ratio

$a := 1 \quad \lambda := 1$

$n := 0, 1 .. 5$

$m := 0, 1 .. 5$

$$\delta_{m,n} := \frac{\pi^2}{4 \cdot a} \cdot (m^2 + a^2 \cdot n^2)$$

$$\delta = \begin{bmatrix} 0 & 2.4674011 & 9.8696044 & 22.2066099 & 39.4784176 & 61.6850275 \\ 2.4674011 & 4.9348022 & 12.3370055 & 24.674011 & 41.9458187 & 64.1524286 \\ 9.8696044 & 12.3370055 & 19.7392088 & 32.0762143 & 49.348022 & 71.5546319 \\ 22.2066099 & 24.674011 & 32.0762143 & 44.4132198 & 61.6850275 & 83.8916374 \\ 39.4784176 & 41.9458187 & 49.348022 & 61.6850275 & 78.9568352 & 101.1634451 \\ 61.6850275 & 64.1524286 & 71.5546319 & 83.8916374 & 101.1634451 & 123.370055 \end{bmatrix}$$

APPENDIX B

CALCULATION OF $d_{i,j}$ AND $bmn_{p,q}$ FOR Kn = 0.02

WITH ASPECT RATIO $a = 1$

Calculation of $d_{i,j}$ and $bmn_{p,q}$ for Kn = 0.02 with Aspect Ratio a = 1

$Kn = 0.02 \quad \alpha = .01, .02 .. 22$

$f(\alpha) = 2 \cdot Kn \cdot \alpha \cdot \tan(\alpha) - 1. \qquad tg(\alpha) = \tan(\alpha) \cdot \alpha \qquad u(\alpha) = \frac{1}{(2 \cdot Kn)}$

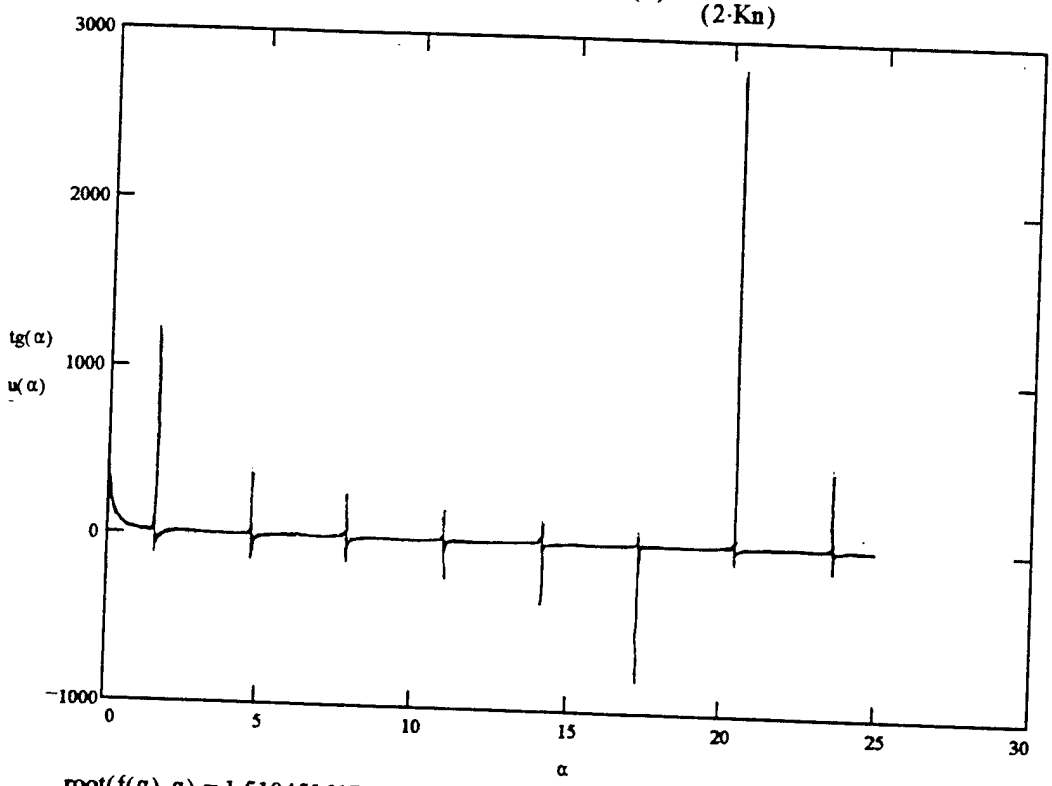

root(f(α), α) = 1.510451617057772 b_1 = 1.510451617057772

α = 4.533017031227471

root(f(α), α) = 4.533017098853988 b_2 = 4.533017098853988

α = 7.560312429685289

root(f(α), α) = 7.560312976908389 b_3 = 7.560312976908389

α = 10.59472926320076

root(f(α), α) = 10.59472964716824 b_4 = 10.59472964716824

α = 13.63777351248604

root(f(α), α) = 13.63777658025087 b_5 = 13.63777658025087

α = 16.69010436230128

root(f(α), α) = 16.69010802858231 b_6 = 16.69010802858231

α = 19.75169253134426

root(f(α), α) = 19.75169677799757 b_7 = 19.75169677799757

α = 22.82205687896281

root(f(α), α) = 22.82205788967408 b_8 = 22.82205788967408

w/w0 (w) for 8 α's for ratio a =1 (here $\alpha = b$) in Eq.(19) [Eqs. (12) and (13)]

$$w0 = -2\cdot \sum_{i=1}^{3} \frac{a}{(b_i)^5}\cdot\frac{\sin(b_i)^2}{1+2\cdot Kn\cdot\sin(b_i)^2}\cdot\left[\frac{b_i}{a}-\frac{\sinh\left(\frac{b_i}{a}\right)}{\cosh\left(\frac{b_i}{a}\right)+2\cdot Kn\cdot b_i\cdot\sinh\left(\frac{b_i}{a}\right.}\right.$$

$w0 = -0.16265$

$$w0 = -2\cdot \sum_{i=1}^{8} \frac{a}{(b_i)^5}\cdot\frac{\sin(b_i)^2}{1+2\cdot Kn\cdot\sin(b_i)^2}\cdot\left[\frac{b_i}{a}-\frac{\sinh\left(\frac{b_i}{a}\right)}{\cosh\left(\frac{b_i}{a}\right)+2\cdot Kn\cdot b_i\cdot\sinh\left(\frac{b_i}{a}\right.}\right.$$

$i = 1,2..8$

$w0 = -0.16284$

$$c_i = \frac{\sin(b_i)}{1+2\cdot Kn\cdot\sin(b_i)^2}\cdot\frac{1}{(b_i)^3} \qquad g_i = \frac{1}{\cosh\left(\frac{b_i}{a}\right)+2\cdot Kn\cdot b_i\cdot\sinh\left(\frac{b_i}{a}\right.}$$

$$w(x,y) = -2\cdot \sum_{i=1}^{3} \cos\left[\left[b_i\cdot\left(2\cdot\frac{y}{11}-1\right)\right]\right]\cdot c_i\cdot\left[1-\cosh\left[\frac{b_i}{a}\cdot\left(2\cdot\frac{x}{12}-1\right)\right]\cdot g_i\right]$$

$w(0,0.5) = -0.02681$
$w(1,1) = -0.00259$
$w(0.5,0) = -0.02498$

$$w(x,y) = -2\cdot \sum_{i=1}^{8} \cos\left[\left[b_i\cdot\left(2\cdot\frac{y}{11}-1\right)\right]\right]\cdot c_i\cdot\left[1-\cosh\left[\frac{b_i}{a}\cdot\left(2\cdot\frac{x}{12}-1\right)\right]\cdot g_i\right]$$

$w(0,0.5) = -0.0265$
$w(1,1) = -0.00305$
$w(0.5,0) = -0.02629$

Therefore, using 8 α's is accurate enough

$m := 1 \quad n := 1$

$p := 0,1..5 \quad q := 0,1..5$

$$b_{p,q} := \frac{1}{4}\cdot\left(d_{|m-p|,|n-q|} - d_{|m-p|,n+q} - d_{m-p,n-q} - d_{m+p,|n-q|}\right)$$

$$b = \begin{bmatrix} 0 & 0 & 0 & 0 & 0 & 0 \\ 0 & 0.38917 & 0 & -0.05173 & 0 & -0.01325 \\ 0 & 0 & 0 & 0 & 0 & 0 \\ 0 & -0.05191 & 0 & 0.0079 & 0 & 0.00198 \\ 0 & 0 & 0 & 0 & 0 & 0 \\ 0 & -0.01406 & 0 & 0.00199 & 0 & 4.625\cdot10^{-4} \\ 0 & 0 & 0 & 0 & 0 & 0 \\ 0 & 0 & 0 & 0 & 0 & 0 \\ 0 & 0 & 0 & 0 & 0 & 0 \end{bmatrix} \qquad b11 = \begin{bmatrix} 0 & 0 & 0 & 0 & 0 & 0 \\ 0 & 0.38917 & 0 & -0.05173 & 0 & -0.01325 \\ 0 & 0 & 0 & 0 & 0 & 0 \\ 0 & -0.05191 & 0 & 0.0079 & 0 & 0.00198 \\ 0 & 0 & 0 & 0 & 0 & 0 \\ 0 & -0.01406 & 0 & 0.00199 & 0 & 4.625\cdot10^{-4} \\ 0 & 0 & 0 & 0 & 0 & 0 \\ 0 & 0 & 0 & 0 & 0 & 0 \\ 0 & 0 & 0 & 0 & 0 & 0 \end{bmatrix}$$

$b_{1,1} = 0.38917$

similarly,

$$b12 = \begin{bmatrix} 0 & 0 & 0 & 0 & 0 & 0 \\ 0 & 0 & 0.33744 & 0 & -0.06498 & 0 \\ 0 & 0 & 0 & 0 & 0 & 0 \\ 0 & 0 & -0.04401 & 0 & 0.00988 & 0 \\ 0 & 0 & 0 & 0 & 0 & 0 \\ 0 & 0 & -0.01207 & 0 & 0.00245 & 0 \\ 0 & 0 & 0 & 0 & 0 & 0 \\ 0 & 0 & 0 & 0 & 0 & 0 \\ 0 & 0 & 0 & 0 & 0 & 0 \end{bmatrix} \qquad b13 = \begin{bmatrix} 0 & 0 & 0 & 0 & 0 & 0 \\ 0 & -0.05173 & 0 & 0.32419 & 0 & -0.07135 \\ 0 & 0 & 0 & 0 & 0 & 0 \\ 0 & 0.0079 & 0 & -0.04203 & 0 & 0.01056 \\ 0 & 0 & 0 & 0 & 0 & 0 \\ 0 & 0.00199 & 0 & -0.01161 & 0 & 0.00264 \\ 0 & 0 & 0 & 0 & 0 & 0 \\ 0 & 0 & 0 & 0 & 0 & 0 \\ 0 & 0 & 0 & 0 & 0 & 0 \end{bmatrix}$$

$$b14 = \begin{bmatrix} 0 & 0 & 0 & 0 & 0 & 0 \\ 0 & 0 & -0.06498 & 0 & 0.31782 & 0 \\ 0 & 0 & 0 & 0 & 0 & 0 \\ 0 & 0 & 0.00988 & 0 & -0.04134 & 0 \\ 0 & 0 & 0 & 0 & 0 & 0 \\ 0 & 0 & 0.00245 & 0 & -0.01142 & 0 \\ 0 & 0 & 0 & 0 & 0 & 0 \\ 0 & 0 & 0 & 0 & 0 & 0 \\ 0 & 0 & 0 & 0 & 0 & 0 \end{bmatrix} \qquad b15 = \begin{bmatrix} 0 & 0 & 0 & 0 & 0 & 0 \\ 0 & -0.01325 & 0 & -0.08323 & 0 & 0.36255 \\ 0 & 0 & 0 & 0 & 0 & 0 \\ 0 & 0.00198 & 0 & 0.01306 & 0 & -0.05037 \\ 0 & 0 & 0 & 0 & 0 & 0 \\ 0 & 4.625\cdot10^{-4} & 0 & 0.00264 & 0 & -0.01134 \\ 0 & 0 & 0 & 0 & 0 & 0 \\ 0 & 0 & 0 & 0 & 0 & 0 \\ 0 & 0 & 0 & 0 & 0 & 0 \end{bmatrix}$$

$$b21 = \begin{bmatrix} 0 & 0 & 0 & 0 & 0 & 0 \\ 0 & 0 & 0 & 0 & 0 & 0 \\ 0 & 0.33726 & 0 & -0.04383 & 0 & -0.01127 \\ 0 & 0 & 0 & 0 & 0 & 0 \\ 0 & -0.06596 & 0 & 0.00989 & 0 & 0.00244 \\ 0 & 0 & 0 & 0 & 0 & 0 \\ 0 & 0 & 0 & 0 & 0 & 0 \\ 0 & 0 & 0 & 0 & 0 & 0 \\ 0 & 0 & 0 & 0 & 0 & 0 \end{bmatrix} \quad b22 = \begin{bmatrix} 0 & 0 & 0 & 0 & 0 & 0 \\ 0 & 0 & 0 & 0 & 0 & 0 \\ 0 & 0 & 0.29343 & 0 & -0.0551 & 0 \\ 0 & 0 & 0 & 0 & 0 & 0 \\ 0 & 0 & -0.05608 & 0 & 0.01233 & 0 \\ 0 & 0 & 0 & 0 & 0 & 0 \\ 0 & 0 & 0 & 0 & 0 & 0 \\ 0 & 0 & 0 & 0 & 0 & 0 \\ 0 & 0 & 0 & 0 & 0 & 0 \end{bmatrix}$$

$$b23 = \begin{bmatrix} 0 & 0 & 0 & 0 & 0 & 0 \\ 0 & 0 & 0 & 0 & 0 & 0 \\ 0 & -0.04383 & 0 & 0.28216 & 0 & -0.06079 \\ 0 & 0 & 0 & 0 & 0 & 0 \\ 0 & 0.00989 & 0 & -0.05363 & 0 & 0.0132 \\ 0 & 0 & 0 & 0 & 0 & 0 \\ 0 & 0 & 0 & 0 & 0 & 0 \\ 0 & 0 & 0 & 0 & 0 & 0 \\ 0 & 0 & 0 & 0 & 0 & 0 \end{bmatrix} \quad b24 = \begin{bmatrix} 0 & 0 & 0 & 0 & 0 & 0 \\ 0 & 0 & 0 & 0 & 0 & 0 \\ 0 & 0 & -0.0551 & 0 & 0.27647 & 0 \\ 0 & 0 & 0 & 0 & 0 & 0 \\ 0 & 0 & 0.01233 & 0 & -0.05277 & 0 \\ 0 & 0 & 0 & 0 & 0 & 0 \\ 0 & 0 & 0 & 0 & 0 & 0 \\ 0 & 0 & 0 & 0 & 0 & 0 \\ 0 & 0 & 0 & 0 & 0 & 0 \end{bmatrix}$$

$$b25 = \begin{bmatrix} 0 & 0 & 0 & 0 & 0 & 0 \\ 0 & 0 & 0 & 0 & 0 & 0 \\ 0 & -0.01127 & 0 & -0.06079 & 0 & 0.27422 \\ 0 & 0 & 0 & 0 & 0 & 0 \\ 0 & 0.00244 & 0 & 0.0132 & 0 & -0.05239 \\ 0 & 0 & 0 & 0 & 0 & 0 \\ 0 & 0 & 0 & 0 & 0 & 0 \\ 0 & 0 & 0 & 0 & 0 & 0 \\ 0 & 0 & 0 & 0 & 0 & 0 \end{bmatrix} \quad b31 = \begin{bmatrix} 0 & 0 & 0 & 0 & 0 & 0 \\ 0 & -0.05191 & 0 & 0.0079 & 0 & 0.00198 \\ 0 & 0 & 0 & 0 & 0 & 0 \\ 0 & 0.32321 & 0 & -0.04184 & 0 & -0.01081 \\ 0 & 0 & 0 & 0 & 0 & 0 \\ 0 & -0.07107 & 0 & 0.01055 & 0 & 0.0026 \\ 0 & 0 & 0 & 0 & 0 & 0 \\ 0 & 0 & 0 & 0 & 0 & 0 \\ 0 & 0 & 0 & 0 & 0 & 0 \end{bmatrix}$$

$$b32 = \begin{bmatrix} 0 & 0 & 0 & 0 & 0 & 0 \\ 0 & 0 & -0.04401 & 0 & 0.00988 & 0 \\ 0 & 0 & 0 & 0 & 0 & 0 \\ 0 & 0 & 0.28136 & 0 & -0.05265 & 0 \\ 0 & 0 & 0 & 0 & 0 & 0 \\ 0 & 0 & -0.06052 & 0 & 0.01316 & 0 \\ 0 & 0 & 0 & 0 & 0 & 0 \\ 0 & 0 & 0 & 0 & 0 & 0 \\ 0 & 0 & 0 & 0 & 0 & 0 \end{bmatrix} \quad b33 = \begin{bmatrix} 0 & 0 & 0 & 0 & 0 & 0 \\ 0 & 0.0079 & 0 & -0.04203 & 0 & 0.01056 \\ 0 & 0 & 0 & 0 & 0 & 0 \\ 0 & -0.04184 & 0 & 0.27055 & 0 & -0.05815 \\ 0 & 0 & 0 & 0 & 0 & 0 \\ 0 & 0.01055 & 0 & -0.05792 & 0 & 0.0141 \\ 0 & 0 & 0 & 0 & 0 & 0 \\ 0 & 0 & 0 & 0 & 0 & 0 \\ 0 & 0 & 0 & 0 & 0 & 0 \end{bmatrix}$$

$$b34 = \begin{bmatrix} 0 & 0 & 0 & 0 & 0 & 0 \\ 0 & 0 & 0.00988 & 0 & -0.04134 & 0 \\ 0 & 0 & 0 & 0 & 0 & 0 \\ 0 & 0 & -0.05265 & 0 & 0.26505 & 0 \\ 0 & 0 & 0 & 0 & 0 & 0 \\ 0 & 0 & 0.01316 & 0 & -0.05697 & 0 \\ 0 & 0 & 0 & 0 & 0 & 0 \\ 0 & 0 & 0 & 0 & 0 & 0 \\ 0 & 0 & 0 & 0 & 0 & 0 \end{bmatrix} \quad b35 = \begin{bmatrix} 0 & 0 & 0 & 0 & 0 & 0 \\ 0 & 0.00198 & 0 & 0.01056 & 0 & -0.04105 \\ 0 & 0 & 0 & 0 & 0 & 0 \\ 0 & -0.01081 & 0 & -0.05815 & 0 & 0.26288 \\ 0 & 0 & 0 & 0 & 0 & 0 \\ 0 & 0.0026 & 0 & 0.0141 & 0 & -0.05657 \\ 0 & 0 & 0 & 0 & 0 & 0 \\ 0 & 0 & 0 & 0 & 0 & 0 \\ 0 & 0 & 0 & 0 & 0 & 0 \end{bmatrix}$$

$i = 0,1..10 \quad j = 0,1..10$

$$d_{i,j} := \int_0^{l1} \int_0^{l2} \frac{w(x,y)}{w0} \cdot \cos\left(i \cdot \pi \cdot \frac{x}{l1}\right) \cdot \cos\left(j \cdot \pi \cdot \frac{y}{l2}\right) dy\, dx$$

interrupted

$$d = \begin{bmatrix}
0.99883 & 0 & -0.24674 & 0 & -0.08526 & 0 & -0.04342 & 0 & -0.0222 & 0 & -0.01381 \\
0 & 0 & 0 & 0 & 0 & 0 & 0 & 0 & 0 & 0 & 0 \\
-0.24538 & 0 & 0.06573 & 0 & 0.02028 & 0 & 0.00912 & 0 & 0.00486 & 0 & 0.00306 \\
0 & 0 & 0 & 0 & 0 & 0 & 0 & 0 & 0 & 0 & 0 \\
-0.08324 & 0 & 0.02024 & 0 & 0.00639 & 0 & 0.00315 & 0 & 0.00162 & 0 & 0.00101 \\
0 & 0 & 0 & 0 & 0 & 0 & 0 & 0 & 0 & 0 & 0 \\
-0.03838 & 0 & 0.00887 & 0 & 0.00297 & 0 & 0.00158 & 0 & 7.94552\cdot10^{-4} & 0 & 4.91934\cdot10^{-4} \\
0 & 0 & 0 & 0 & 0 & 0 & 0 & 0 & 0 & 0 & 0 \\
-0.02189 & 0 & 0.00493 & 0 & 0.00169 & 0 & 9.45238\cdot10^{-4} & 0 & 4.68553\cdot10^{-4} & 0 & 2.89189\cdot10^{-4} \\
0 & 0 & 0 & 0 & 0 & 0 & 0 & 0 & 0 & 0 & 0 \\
-0.01411 & 0 & 0.00313 & 0 & 0.00108 & 0 & 6.24868\cdot10^{-4} & 0 & 3.15992\cdot10^{-4} & 0 & 1.94737\cdot10^{-4}
\end{bmatrix}$$

$m = 0 \quad n = 0$

$p = 0,1..5 \quad q = 0,1..5$

$b_{6,0} = 0 \quad b_{7,0} = 0 \quad b_{8,0} = 0$

$$b_{p,q} = \frac{1}{4} \cdot \left(d_{|m-p|,|n-q|} - d_{|m-p|,n+q} - d_{m+p,n-q} - d_{m+p,|n-q|}\right)$$

$$b = \begin{bmatrix}
0 & 0 & 0 & 0 & 0 & 0 \\
0 & 0 & 0 & 0 & 0 & 0 \\
0 & 0 & 0 & 0 & 0 & 0 \\
0 & 0 & 0 & 0 & 0 & 0 \\
0 & 0 & 0 & 0 & 0 & 0 \\
0 & 0 & 0 & 0 & 0 & 0 \\
0 & 0 & 0 & 0 & 0 & 0 \\
0 & 0 & 0 & 0 & 0 & 0 \\
0 & 0 & 0 & 0 & 0 & 0
\end{bmatrix} \qquad b00 = \begin{bmatrix}
0 & 0 & 0 & 0 & 0 & 0 \\
0 & 0 & 0 & 0 & 0 & 0 \\
0 & 0 & 0 & 0 & 0 & 0 \\
0 & 0 & 0 & 0 & 0 & 0 \\
0 & 0 & 0 & 0 & 0 & 0 \\
0 & 0 & 0 & 0 & 0 & 0 \\
0 & 0 & 0 & 0 & 0 & 0 \\
0 & 0 & 0 & 0 & 0 & 0 \\
0 & 0 & 0 & 0 & 0 & 0
\end{bmatrix}$$

APPENDIX C

THE FIRST THREE EIGENVALUES FOR Kn = 0.00

BY DENNIS ET AL.

THE FIRST THREE EIGENVALUES FOR Kn = 0.00 (DENNIS ET AL.)

α	1.000	0.667	0.500	0.250	0.125
λ_1	11.91	12.49	13.57	17.76	22.38
λ_2	71.09	51.58	41.17	28.17	25.61
λ_3	157.9	99.71	94.93	47.82	31.81
$\mathcal{B}_1$	0.804	0.802	0.789	0.756	0.737
$\mathcal{B}_2$	0.104	0.064	0.071	0.107	0.091
$\mathcal{B}_3$	0.014	0.043	0.020	0.028	0.034

APPENDIX D

DATA OF ROUGHNESS AND DIMENSION OF MICROCHANNEL

DATA OF ROUGHNESS AND DIMENSION OF MICROCHANNEL

Test #	Ra: nm	Rq: nm	Rt: micro
1	143.31	179.43	2.6
2	140.81	169.44	2.74
3	102.9	129.28	1.77
4	141.38	176.5	3.39
5	116.37	154.2	2.36
6	113.79	144.95	2.05
7	108.68	141.12	2.81
8	91.45	121.73	2.16
9	97.62	131.5	3.06
10	149.83	187.22	2.25
11	90	117.61	1.86
12	98.37	122.61	2.05
13	118.83	155.26	2.26
14	82.42	111.46	3.39
15	98.07	124.16	1.81
16	79.71	100.51	1.81
17	75.25	95.66	2.05
18	100.62	129.55	2.89
19	91.26	117.22	3.02
20	127.49	160.78	1.71
21	128.89	157.93	2.12
22	115.02	146.06	2.02
23	93.57	118.38	2.37
24	115.21	149.07	2.15
25	142.57	181.83	2.28
26	149.95	184.24	1.97
27	88.13	119.18	1.86
28	128.61	162.84	1.99
29	105.2	133.64	1.69
30	93.32	122.5	1.92
Mean			2.280333
Standard Error			0.089209
Median			2.135
Mode			2.05
Standard Deviation			0.488619
Variance			0.238748
Kurtosis			-0.00615
Skewness			0.973331
Range			1.7
Minimum			1.69
Maximum			3.39
Sum			68.41
Count			30

Test #		Width			Depth	
	Top		Bottom			
1	115.56		112		20.97	
2	133.11		114.12		20.58	
3	133.97		114.23		22.32	
4	131.56		113.19		20.87	
5	128.01		114.97		21.51	
6	118.52		114.37		21.96	
7	117.34		113.19		22.29	
8	117.82		114.23		23.67	
9	118.52		112.6		22.71	
10	117.93		110.82		21.55	
11	119.17		113.21		22.85	
12	122.6		113.03		24.61	
13	128		112.61		22.65	
14	126.12		113.63		25.18	
15	123.2		113.04		25.83	
16	118.89		112.35		25.51	
17	117.22		111.24		24.86	
18	117.2		112.44		24.41	
19	118.42		114.83		23.27	
20	119.71		112.6		24.62	
21	118.41		112.44		25.34	
22	118.52		113.18		26.81	
23	116.74		112.01		24.84	
24	114.35		110.01		25.94	
25	120.02		113.63		27.81	
26	117.15		112.41		27.22	
27	116.84		112.02		23.92	
28	116.59		112		26.25	
29	116.61		111.89		26.66	
30	114.69		110.58		24.21	
Mean	120.4263		112.7623		24.04067	
Standard E	0.991225		0.22057		0.368448	
Median	118.47		112.605		24.31	
Mode	118.52		112		#N/A	
Standard D	5.429164		1.20811		2.018072	
Variance	29.47582		1.459529		4.072613	
Kurtosis	0.910125		-0.0658		-0.96811	
Skewness	1.396207		-0.21856		-0.01815	
Range	19.62		4.96		7.23	
Minimum	114.35		110.01		20.58	
Maximum	133.97		114.97		27.81	
Sum	3612.79		3382.87		721.22	
Count	30		30		30	

APPENDIX E

EXPERIMENTAL HEAT TRANSFER DATA

Inlet, outlet and wall temperatures

Experiment date: June 3, 1996

Flow media: Helium gas

Size of microchannel: 117 μm x 24 μm

Length of microchannel: 63.5 mm

Operation temperature: 24^0C

Run number	G_v ml/min	T_{inlet} °C	T_{outlet} °C	T_{w1} °C	T_{w2} °C
1	343.3	29.90	37.47	78.41	78.56
2	300.9	29.62	33.56	74.89	74.96
3	246.7	29.84	32.15	69.83	69.88
4	198.6	29.77	31.69	74.81	74.89
5	173.3	29.42	30.54	70.65	70.69
6	149.2	29.31	30.12	72.13	72.22
7	125.9	29.21	29.67	71.07	71.12
8	101.8	29.11	29.18	68.69	68.74
9	47.3	29.33	28.79	70.65	70.71

Inlet, outlet and wall temperatures

Experiment date: June 18, 1996

Flow media: Helium gas

Size of microtube: 52.1 μm

Length of microchannel: 70 mm

Operation temperature: 25^0C

Run no.	G_v ml/min	T_{inlet} °C	T_{outlet} °C	T_{w1} °C	T_{w2} °C
1	0.11	29.50	25.11	88.41	82.56
2	0.11	30.05	25.58	91.35	85.43
3	0.11	30.28	25.87	89.50	84.12
4	0.11	30.29	25.92	87.73	82.93

APPENDIX F

REDUCED HEAT TRANSFER DATA

Data reduction of heat transfer

Experiment date: June 3, 1996

Flow media: Helium gas

Size of microchannel: 117 μm x 24 μm

Length of microchannel: 63.5 mm

Operation temperature: 24^0C

Table F.1

Run number	G_v ml/min	T_{inlet} °C	T_{outlet} °C	T_{w1} °C	T_{w2} °C	Nu	Re
1	343.3	29.90	37.47	78.41	78.56	80.96	720
2	300.9	29.62	33.56	74.89	74.96	43.18	618
3	246.7	29.84	32.15	69.83	69.88	20.43	507
4	198.6	29.77	31.69	74.81	74.89	11.78	408
5	173.3	29.42	30.54	70.65	70.69	6.59	356
6	149.2	29.31	30.12	72.13	72.22	3.59	307
7	125.9	29.21	29.67	71.07	71.12	1.76	259
8	101.8	29.11	29.18	68.69	68.74	0.11	208
9	47.3	29.33	28.79	70.65	70.71	–0.52	97

Experiment date: June 18, 1996

Flow media: Helium gas

Size of microtube: 52.1 μm

Length of microchannel: 70 mm

Operation temperature: 25^0C

Table F.2

Run no.	G_v ml/min	T_{inlet} °C	T_{outlet} °C	T_{w1} °C	T_{w2} °C	Nu	Re
1	0.11	29.50	25.11	88.41	82.56		0.27
2	0.11	30.05	25.58	91.35	85.43		0.27
3	0.11	30.28	25.87	89.50	84.12		0.27
4	0.11	30.29	25.92	87.73	82.93	-0.015	0.27

APPENDIX G

PROPERTIES OF THE MICROCHANNEL AND MICROTUBE

PROPERTIES OF HELIUM GAS

Table G.1. Physical properties of the microchannel

Channel material	Aluminum	Polymide
Mechanical Properties		
Density, kg/m^3	2707	1042
(lbm/ft^3)	(169)	(65)
Tensile Strength (MPa)	120.7	103
(psi)	(17500)	(15,000)
Thermal Properties		
Thermal Conductivity		
W/m–K	204	0.155
(Btu/hr–ft–^{0}F)	(118)	(0.090)
Specific Heat		
KJ/kg–K	0.896	1.088
(Btu/lbm –^{0}F)	(0.214)	(0.260)

Source of Data: J.P. Holman, Heat Transfer, McGraw–Hill Book Co., New York, 1986

Table G.2. Properties of helium gas at atmospheric pressure

Values of μ, k, and C_p are not strongly pressure–dependent for He and may be used over a fairly wide range of pressures.

T,K	ϱ kg/m^3	C_p $kJ/kg\ ^0C$	μ kg/m s	ν m^2/s	k $W/m\ ^0C$
200	0.2435	5.200	15.66×10^{-6}	64.38×10^{-6}	0.1177
255	0.1906	5.200	18.17	95.50	0.1357
366	0.13280	5.200	23.05	173.6	0.1691
477	0.08282	5.200	27.50	269.3	0.197

BIBLIOGRAPHY

Ameel, T. A., R. F. Barron, X. M. Wang and R. O. Warrington, Laminar Forced Convection in a Circular Tube with Constant Heat Flux and Slip Flow *2nd U.S. – Japan Seminar on "Molecular and Microscale Transport Phenomena,"* Santa Barbara, California (1996)

Arkilic, E. B., K. S. Breuer and M. A. Schmidt, Gaseous Flow in Microchannels, *Application of Microfabrication to Fluid Mechanics*, ASME FED–vol. 197, pp. 57–66 (1994)

Barron, R. F., X. M. Wang, R. O. Warrington and T. A. Ameel, Evaluation of the Eigenvalues for the Graetz Problem in Slip–Flow, *International Communications in Heat and Mass Transfer,* vol. 23, No. 4, 563–574 (1996)

Barron, R. F., X. M. Wang, T. A. Ameel and R. O. Warrington, The Graetz Problem Extended to Slip–Flow, *International Journal of Heat and Mass Transfer* (in print)

Beskok, A. and G. E. Karniadakis, Simulation of Slip–Flows in Complex Micro–Geometries, *ASME Proceedings* DSC vol. 40, pp. 355–370 (1992)

Choi, S. B., R. F. Barron and R. O. Warrington, Fluid Flow and Heat Transfer in Microtubes, *Micromechanical Sensors, Actuators and Systems*, ASME, New York, NY, DSC–vol. 32, pp. 123–134 (1991)

Dennis, S. C. R., A. McD. Mercer and G. Poots, Forced Heat Convection in Laminar Flow through Rectangular Ducts, *Quarterly of Applied Mathematics*, pp. 285–297 (1959)

Dittus, F. W. and C. E. Boelter, Univ. Calif. (Berkeley) Pub. Eng., vol. 2 p.443 (1930)

Ebert, W. A. and E. M. Sparrow, Slip Flow in Rectangular and Annular Ducts, *Transactions of the ASME D: Journal of Basic Engineering* (1965)

Eckert, E. R. G. and R. M. Drake, *Analysis of Heat and Mass Transfer*, McGraw–Hill Book Company, New York, pp. 486 (1972)

Flik, M. I., B. I. Choi and K. E. Goodson, Heat Transfer Regimes in Microstructures, *Journal of Heat Transfer*, vol. 114, pp. 666–674 (1992)

Graetz, L., Uber die Warmeleitungsfahigheit von Flussingkeiten, part 1, *Annalen der Physik und Chemie*, vol. 18, pp. 79–94 (1883); part 2, vol. 25, pp. 337–357 (1885)

Holman, J. P., Heat transfer, 6th edition, McGraw–Hill Company, New York (1986)

Holman, J. P., *Experimental Methods for Engineers*, 4th edition, McGraw–Hill Book Company, New York (1984)

Kays, W. M. and M. E. Crawford, *Convective Heat and Mass Transfer*, McGraw–Hill Book Company, New York (1993)

Kline, S. J. and F. A. McClintock, "Describing Uncertainties in Single–Sample Experiments," *Mechanical Engineering*, pp. 3 (1953)

Liu, J. Q., Y. C. Tai and C. M. Ho, MEMS for Pressure Distribution Studies of Gaseous Flows in Microchannels, *Proceedings of IEEE Micro Electromechanical Systems*, pp. 209–215 (1995)

Mann, D. B., The Thermodynamic Properties of Helium from 3 to 300 K between 0.5 and 100 Atmospheres, *National Bureau of Standards Technical Note* #154 (1962)

Peterson, G. P., A. B. Duncan and M. H. Weichold, Experimental Investigation on Micro Heat Pipes Fabricated in Silicon Wafer, *ASME Journal of Heat Transfer*, vol. 115, pp. 751–758 (1993)

Pfahler, J., J. Harley, H. H. Bau and J. Zemel, Liquid and gas transport in Small Channels, *Proceedings of ASME WAM Micro Structures, Sensors and Actuators*, DSC Vol. 19, pp. 149–157 (1990).

Sellars, J. R., M. Tribus and J. S. Klein, Heat Transfer to Laminar Flow in a Round Tube or Flat Conduit–The Graetz Problem Extended, *Trans. ASME*, vol. 78, pp. 441–448 (1956)

Shah, R. K. and A. L. London, *Laminar Flow Forced Convection in Ducts*, Academic Press (1978)

Shapiro, A. H., *The Dynamics and Thermodynamics of Compressible Fluid Flow*, vol. 1 and vol. 2, John Wiley (1953)

Sreekanth, A. K., Slip Flow through Long Circular Tubes, *Rarefied Gas Dynamics*, New York, Academic Press, pp. 667–680 (1968)

Tribus, M. and J. Klein, Forced Convection from Nonisothermal Surfaces, *Heat Transfer: A Symposium*, pp. 211–235 (1953)

Wang, B. X. and X. F. Peng, Experimental Investigation on Liquid Forced Convection Heat Transfer through Microchannels, *International Journal of Heat and Mass Transfer*, Vol. 37, Supplement 1, pp.73–82 (1994)

Wang, X. M., Evaluation of the Eigenvalues for the Graetz Problem in Slip Flow, *MS thesis*, Louisiana Tech University (1995)

White, F. M., *Viscous Fluid Flow*, McGraw–Hill, Inc., New York (1991)

Yu, D. L., The Effects on the Prandtl Number in Micro Heat Transfer, *DE dissertation*, Louisiana Tech University (1994)

VITA

Xianming Wang was born on April 15, 1954, in Chongqing, Sichuan, China. He graduated from Chongqing University, China, in July 1983 with a Master of Science in Mechanical Engineering. Following graduation, he worked in Chongqing Jiaotong Institute. In December 1992, he joined the Department of Mechanical and Industrial Engineering, Louisiana Tech University, and entered the Doctor of Engineering program at Louisiana Tech University in the following quarter.